MICROSCOPE's view at gravitation

Joel Bergé

Review Article

MICROSCOPE's view at gravitation

Joel Bergé

DPHY, ONERA, Université Paris Saclay, F-92322 Châtillon, France

E-mail: joel.berge@onera.fr

September 2022

Abstract. The weak equivalence principle (WEP) is the cornerstone of General Relativity (GR). Testing it is thus a natural way to confront GR to experiments, which has been pursued for four centuries with increasing precision. MICROSCOPE is a space mission designed to test the WEP with a precision of 1 in 10^{15} parts, two orders of magnitude better than previous experimental constraints. After completing its two-year mission, from 2016 to 2018, MICROSCOPE delivered unprecedented precise constraints $\eta(\mathrm{Ti},\mathrm{Pt}) = [-1.5 \pm 2.3\ (\mathrm{stat}) \pm 1.5\ (\mathrm{syst})] \times 10^{-15}$ (at 1σ in statistical errors) on the Eötvös parameter between one proof mass made of titanium and another made of platinum. This bound allowed for improved constraints on alternative theories of gravitation. This review discusses the science beyond MICROSCOPE – GR and its alternatives, with an emphasis on scalar-tensor theories – before presenting the experimental concept and apparatus. The mission's science returns are then discussed before future tests of the WEP are introduced.

Keywords: Experimental Gravitation; Space Experiments; Equivalence Principle

Submitted to: *Rep. Prog. Phys.*

Contents

1. Introduction

What is gravity? To the layman, it is the simple fact that everything falls with a well-known and predictable way. To the space engineer, it is written in the simple yet powerful Newton's laws that undoubtedly allow us to safely send probes to distant planets. To the physicist, it is the least understood of the four known interactions, the black sheep that does not want to unite with the others. And yet, the theory that describes it (General Relativity) is so well tested that it leaves us with very few freedom to improve our understanding.

Just over one century ago, Einstein closed the debate about the Mercury perihelion puzzle when he published his theory of General Relativity (GR) [1, 2]. The well-known Newtonian gravity, which culminated with the prediction of the existence of Neptune, was surpassed and embedded in a new paradigm. Einstein's gravity was quickly accepted after the measurement of the gravitational deflection of stars' light passing near the Sun by Eddington. It allowed for the quick development of physical cosmology, with the prediction of the expansion of the Universe and of the Big Bang. Other predictions of the theory seemed more far-fetched: the fabric of spacetime can vibrate and even be torn apart. And yet, up to now, GR has passed all experimental tests, from gravitational lensing [3, 4] to gravitational redshift [5, 6] to, perhaps more striking, the direct detection of gravitational waves [7] and the subsequent confirmation of the existence of black holes (spacetime is indeed pricked with singularities and can thus be torn apart) and the eventual imaging of a black hole [8]. In particular, the detection of an electromagnetic counterpart to the gravitational-wave signal emitted by a binary neutron star merger [9] put severe constraints on a whole class of alternatives to GR [10–16].

GR seems unassailable [17]. Yet, breaches in the theory may have appeared as early as the 1930s, when Zwicky noticed missing mass in the Coma cluster [18]. Decades later, Rubin found the same problem at galactic scales [19]. Finally, 28 years later, the entire Big Bang model, constructed on GR, might have swayed with the discovery of the acceleration of the expansion of the Universe [20, 21]. Nevertheless, those problems can be efficiently circumvented by the introduction of dark matter and dark energy (however mysterious they remain), leaving GR unchanged.

Alas, the story is not complete, as all attempts to unite gravity with the other interactions have still remained unsuccessful. And yet, the standard model looks as a construction at least as solid as GR itself, with the later discovery of the long-awaited Brout-Englert-Higgs boson, with a mass of 125 GeV [22, 23]. The question is then: what theoretical building should we modify? Gravitation or/and the standard model?

Theories beyond the standard model [24, 25] propose the existence of new particles. For instance, string-inspired theories introduce a spin-0 dilaton-like particle (e.g. Refs. [26, 27]), and scalar-tensor models modify GR's equations via the introduction of a new scalar field (see e.g. Refs. [28–31]), the existence of which can be made compatible with current solar system tests with the inclusion of a screening mechanism that makes the field's mass environment-dependent [32]. Although they mimic GR because of their screening mechanism, those models can nevertheless have measurable effects, such as an apparent violation of the equivalence principle (e.g. Refs. [33–35]) and a variation of the fundamental constants [36–38]. Then there is still hope. GR may not be unassailable after all.

Several tests of gravitation have been proposed and put forward in the last few years, from laboratory [39–62] to Solar System [5, 6, 34, 63–87] to astrophysical [88–103] to cosmological [30, 104–130] scales. They mostly aim to better understand the "dark sector" (dark matter and dark energy) from the two complementary points of view: should we add dark components or modify GR [131]? All those tests, spanning orders of magnitude in scale, share the same concept, while probing complementary regimes [132]: infer (or at least constrain) the laws of gravity from the dynamics of "test" masses, which are as diverse as atoms, torsion pendulums, artificial satellites orbiting the Earth, Solar System planets, binary stars, galaxies, or the Universe itself. This diversity of experiments come with a diversity of environments, which must be taken into account in order not to "blur" constraints on gravity. For instance, cosmological and galactic searches for dark matter and dark energy are hampered by baryonic physics [103, 133–138], outer solar systems tests by the Kuiper belt [81, 139], and tests in Earth orbit can be affected by the shape of the Earth [140].

Dedicated laboratory tests are better focused on one special aspect and may offer a clearer glimpse on the roots of gravity. Examples are provided by tests of the gravitational redshift with Global Navigation Satellite System (GNSS) satellites [5,6] and the Cassini spacecraft [67], of the Lense-Thirring effect [79, 141, 142], of the pericentre anomaly [143–147], and of course, of GR's cornerstone and main focus of this review, the universality of free fall (UFF [50, 54, 58, 85, 148]) recently tested with an unprecedented precision by the MICROSCOPE mission [148–160].

The UFF was first noticed by Galileo while rolling objects made of different compositions down a ramp. Newton tested it more thoroughly with a pendulum. With the introduction of the inertial and gravitational masses (see below) by Newton, it was realised that

the UFF entails the equivalence of those two masses: their ratio is a fundamental constant (that can be set to 1 through the definition of Newton's constant G). Einstein raised it to the level of a principle, on which its general theory of Relativity is built. When simply stating the equality of the inertial and gravitational masses, or similarly the UFF, this principle is refered to as the Weak Equivalence Principle (WEP). As we discuss below, stronger formulations of the Equivalence Principle exist.

Ref. [161] gives a recent and comprehensive review of the background theory and of experimental tests of the Equivalence Principle. Therefore, we content ourselves with a didactic introduction of the subject in Sect. 2, with as few equations as possible. Sect. 3 gives an enlarged introduction of theoretical modifications to GR that can be investigated experimentally by testing the WEP; though it gives an as much detailed view as possible of those few specific models actually investigated and/or constrained by MICROSCOPE, it is far from exhaustive and does not provide a comprehensive view of modern gravitation theories. We then outline the main milestones in experimental tests of the WEP in Sect. 4. We refer the reader to Refs. [17, 161] for more details. The MICROSCOPE experiment is presented in Sect. 5 and its main results discussed in Sect. 6. The future of space tests of the WEP is then discussed in Sect. 7, before closing this review in Sect. 8.

Note that although this review is limited to gravity models that have been central to MICROSCOPE investigations and data analysis (a fifth force behaving as a Yukawa interaction, a dilaton-like field that can act as an ultra-light bosonic dark matter candidate, a chameleon field and a U(1) boson), the enlarged scientific community has already benefited from MICROSCOPE, e.g. in the search for vector dark matter [162, 163], including a dark photon [164–166], for relic neutrinos [167], and in constraining dark energy models (such as Bekenstein models [168], dynamical dark energy [169, 170] or dark forces [171], for which local tests are complementary to cosmology and astrophysics observations), string theory [172–174], topological defects [175, 176], and the possibility that the muon $g-2$ anomaly arises from the existence of a new field [177]. The wealth of those analyses shows the powerful versatility of testing the WEP with ever increasing precision.

2. The equivalence principle and General Relativity

2.1. The weak equivalence principle

The central role of the universality of free-fall (UFF) has been recognised since Galileo rolled objects down inclined planes four centuries ago, paving the way for modern physics. He measured that the total traveled distance by rolling bodies is proportional to the square of the time of fall, independently of their mass and composition. This means that they all undergo the same acceleration provided that they are in a small enough region of space (e.g. in the same room on Earth). In other words, all objects within the same gravitational field fall at the same rate, independently of their mass and composition.

Newton's second law applied to a freely-falling test mass on Earth reads $m_I\vec{a} = m_G\vec{g}$, where $\vec{a}$ is the body's acceleration and $\vec{g}$ the Earth's gravitational acceleration, and where the masses m_I and m_G play two different roles and should have no reason to be identical. The former is the inertial mass, which opposes motion and plays in all kinds of interaction; the latter is the gravitational mass, which defines how a body responds to gravity, and plays a role only in the gravitational interaction. Considering two test bodies A and B freely-falling in the same gravity field $\vec{g}$, it is easy to show that the ratio of their inertial mass to their gravitational mass are equal as soon as they undergo the same acceleration and vice-versa:

$$\vec{a}_A = \vec{a}_B \iff \frac{m_{I,A}}{m_{G,A}} = \frac{m_{I,B}}{m_{G,B}}. \qquad (1)$$

Together with the observed UFF ($\vec{a}_A = \vec{a}_B$), this allows us to state the Weak Equivalence Principle (WEP) as the equality between the inertial mass and the gravitational mass.

Incidentally, the WEP suggests the existence of inertial reference frames, in which free objects move in a rectilinear way at a constant speed and of a preferred class of trajectories (called inertial, or freely-falling) through spacetime, on which unaccelerated particles travel. Here, "unaccelerated" means "subject to gravity only". In other words, all particles have the same gravitational charge, which can be defined as the ratio between the gravitational mass and the inertial mass. Therefore, if the WEP holds, then gravitation is universal, felt in the same way by every kind of particle.

Before turning to how the WEP is the starting point for GR, let us consider an observer in a small sealed capsule at rest, unable to see the outside world, doing experiments on planet A. For example, she aims to measure the gravity field of the planet through the observation of freely-falling bodies. She will obviously find different results on a different planet B, but also if the capsule is accelerating at a constant rate, even in the interstellar space, far from any gravitational source. The WEP can therefore be stated as follows: in small enough regions of spacetime, the motion of freely-falling bodies are the same in a gravitational field and a uniformly accelerated frame.

2.2. The Equivalence Principle and General Relativity

At the turn of the 20th century, with the theory of special relativity, Einstein showed that mass is just a form of energy. He therefore generalised the WEP to include other interactions, stating that in small enough regions of spacetime, the non-gravitational laws of physics reduce to those of special relativity. In particular, it is impossible to detect the existence of a gravitational field by means of local experiments. This is known as the Einstein Equivalence Principle (EEP). A subsequent version, the Strong Equivalence Principle, generalises the EEP to gravitation.

A direct consequence of the EEP is that gravity is inescapable: it is impossible to define the acceleration due to gravity. Instead, we can only define "unaccelerated" as "freely-falling". In other words, gravity cannot be seen as a force, i.e. as something leading to an acceleration. An object feeling zero acceleration is moving freely in the presence of whatever surrounding gravitational field.

This has a very profound implication, that leads to the basis of General Relativity (for more details, see classical textbooks, e.g. Refs. [178–181]): it is not possible to define universal inertial frames, but only locally-inertial frames. Let us describe an inertial frame as made of rigid rods (Fig. 1). Freely-falling objects have a rectilinear motion, for instance parallel to one set of rods. Let us try to set up such a frame around the Earth, such as a freely-falling object in Paris follows a preferred direction. In this frame, all freely-falling objects must follow the same direction. But this is clearly not possible, since the direction of the Earth's gravitational field varies from place to place. An object attracted by the Earth in New York will obviously move in a direction different from the one falling in Paris: therefore, it is not freely falling in the inertial frame that we have just constructed. If we want to abide by the Equivalence Principle, the frame that we defined must be inertial only in Paris, and we must define another inertial frame in New York. In fact, we must define a locally inertial frame at every point of the spacetime, and the entire frame is therefore constructed by sewing locally inertial frames. This realisation is the bounding rock of General Relativity, and directly implies that spacetime must be curved, and that gravity is not a force but a manifestation of curvature, curvature itself being defined by the local matter and energy distribution.

Through the definition of an appropriate metric $g_{\mu\nu}$ tensor, Einstein's field equations

$$G_{\mu\nu} = 8\pi G T_{\mu\nu} \tag{2}$$

tell nothing more than that. In this equation, the Einstein tensor $G_{\mu\nu} = R_{\mu\nu} - Rg_{\mu\nu}/2$ describes the spacetime's geometry (the Ricci tensor $R_{\mu\nu}$ and its trace R characterising curvature) and the stress-energy tensor $T_{\mu\nu}$ describes matter and energy, G being the gravitational constant. For completeness, we note that Eq. (2) is obtained by varying the Einstein-Hilbert action

$$S = \frac{\mathrm{M}_{\mathrm{Pl}}^2}{2}\int \mathrm{d}^4x\sqrt{-g}R + \int \mathrm{d}^4x\sqrt{-g}\mathcal{L}_{\mathrm{m}}\left(g_{\mu\nu}, \psi_{\mathrm{m}}^{(i)}\right) \tag{3}$$

with respect to the metric, where $\mathrm{M}_{\mathrm{Pl}}^2$ is Planck mass, g is the metric's determinant and $\mathcal{L}_{\mathrm{m}}\left(g_{\mu\nu}, \psi_{\mathrm{m}}^{(i)}\right)$ is the Lagrangian density of the ith matter field.

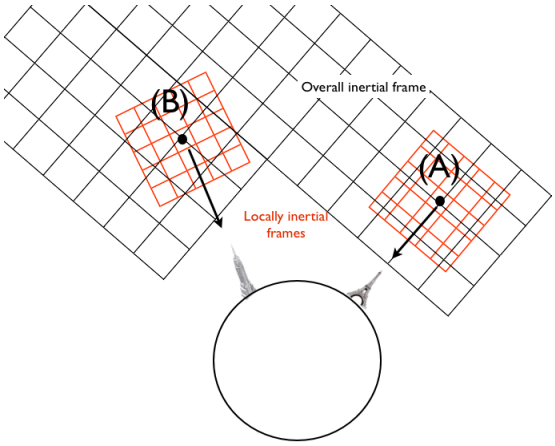

Figure 1. Locally-inertial frames. An inertial frame in Paris (black) is not inertial in New York. Instead, locally-inertial frames (red) must be defined at each location.

The Equivalence Principle has other direct implications, that do not require the full General Relativity: gravitational redshift (the wavelength of an electromagnetic wave emitted in a gravitational field is not the same in a different gravitational field) and time dilation (if we place clocks at the vertices of our locally inertial frame, time passes more or less quickly depending on the value of the gravitational field). They provide fancy tests of the Equivalence Principle, that we will not discuss here [5, 6, 67].

As GR's founding idea, the equivalence principle is a key concept to test gravity, all the more that many alternative theories of gravitation predict that it should be violated.

3. Beyond GR

Einstein's field equations (2) are the starting point to calculate the rate of expansion of the Universe. Faced with its unexplained acceleration, we can thus go back to these equations, modify them and see if the modifications account for the observations. Two possibilities are available: either we modify their l.h.s, or their r.h.s. In the former case ("modified gravity"), this is akin to modifying the geometry of the Universe

(or gravitation itself), whereas in the latter case ("dark energy"), it comes down to modifying the content of the Universe [131]. In this section, we start with a short presentation of dark energy, before digging more deeply in modified gravity. Countless modified gravity theories exist, which will not be reviewed here (see e.g. [24, 25, 30, 31] for reviews). Instead, we review a limited number models that have actually benefited from MICROSCOPE results.

3.1. Cosmological constant and dark energy

Einstein himself might have explained the accelerated expansion of the Universe when he introduced his famous cosmological constant Λ, modifying Eq. (2) as

$$G_{\mu\nu} + \Lambda g_{\mu\nu} = 8\pi G T_{\mu\nu}, \tag{4}$$

noting that Λ could as well be set on the r.h.s of the equation. The cosmological constant is usually related to the vacuum energy. Its effect on the evolution of the Universe and its large scale structures have been intensively studied. However, the cosmological constant hypothesis poses insurmontable problems and other explanations must be looked for [182–187].

Adding an invisible "dark" component to the Universe content (thereby changing its stress-energy tensor $T_{\mu\nu}$ –the r.h.s of Eq. 2) allows for the preservation of GR and of the cosmological model built upon it. This dark energy hypothesis states that a repulsive fluid with a possibly evolving equation of state w pervades the Universe and opposes gravity. The goal of upcoming ambitious surveys [109] is to measure w with a sub-percent precision. For models and reviews about dark energy, see e.g. Refs. [184, 187–193].

3.2. Phenomenological modifications to gravity

In the 1980s, the reanalysis of the Eötvös experiment [194] revived interests on the existence of a putative fifth force with gravitational characteristics [44]. Phenomenologically, a fifth force can emerge from a parametric deviation from Newton's inverse square law, with specific details depending on the underlying theory (see e.g. Ref. [48] for a review).

The most common parameterisation for a deviation from Newtonian gravity is the Yukawa potential, which is simply added to the Newtonian potential. Thence, the total gravitational potential created by a point-mass of mass M at distance r is

$$U(r) = -\frac{GM}{r}\left[1 + \alpha \exp\left(-\frac{r}{\lambda}\right)\right], \tag{5}$$

where α is the strength of the deviation compared to Newtonian gravity (which may depend on the composition of the interacting masses) and λ is the range of the corresponding fifth force. As mentioned below in the case of MICROSCOPE, Eq. (5) is modified by a shape factor for extended bodies.

For instance, a simple analysis consists in assuming a composition-dependent coupling α_{ij} that depends on a scalar dimensionless "Yukawa charge" q, characteristic of each material as [54, 58]

$$\alpha_{ij} = \alpha \left(\frac{q}{\mu}\right)_i \left(\frac{q}{\mu}\right)_j, \tag{6}$$

where α is a universal dimensionless coupling constant which quantifies the strength of the interaction with respect to gravity and μ is the atomic mass in atomic units (e.g. $\mu = 12$ for carbon-12, or $\mu = 47.948$ for titanium). Different definitions of the charge q are possible depending on the detailed microscopic coupling of the scalar field to the standard model fields. At the atomic levels, taking into account the electromagnetic and nuclear binding energies, the charge are usually reduced to the materials's baryon and/or lepton numbers (B and L) (see e.g. Refs. [195, 196]).

Note that α is a phenomenological parameter and is not by itself a constant of nature but depends on the coupling constant of the underlying fifth force theory. See Ref. [44] for a detailed account and Eq. (58) for an example with a spin-1 induced force.

Many constraints on the range and the amplitude of a Yukawa potential have been obtained so far, from sub-millimeter to solar system scales (e.g. Refs. [44, 48] and references therein, and Refs. [52, 56, 57, 59, 197] for more recent works).

Finally, despite its simplicity, the Yukawa parameterisation is useful as it describes the fifth force created by a massive scalar field (discussed below) in the Newtonian regime (see also e.g. the Supplemental material of Ref. [197] and references therein).

3.3. Scalar-tensor theories

Scalar-tensor theories add a new scalar field ϕ of potential V to GR's metric tensor. In this subsection, we provide a brief summary of their main formalism, with an emphasis on the particular chameleon model in the next subsection, which was considered as the archetypical scalar-tensor model in MICROSCOPE works so far. For more details about scalar-tensor theories, see Ref. [28].

3.3.1. Field equations In their simplest form, scalar tensor theories are obtained by modifying the Einstein-

Hilbert action (3) as (with a (-+++) signature)

$$S_{\phi,E} = \int \mathrm{d}^4x\sqrt{-g}\left[\frac{\mathrm{M}_{\mathrm{Pl}}^2}{2}R - \frac{1}{2}g^{\mu\nu}\partial_\mu\phi\partial_\nu\phi - V(\phi)\right] + \int \mathrm{d}^4x\sqrt{-\tilde{g}}\mathcal{L}_{\mathrm{m}}\left(\tilde{g}_{\mu\nu}, \psi_{\mathrm{m}}^{(i)}\right), \quad (7)$$

where R, $g_{\mu\nu}$ and g are the Einstein frame's Ricci scalar, metric tensor and its determinant, and $\tilde{g}_{\mu\nu}$ is the Jordan frame metric, related to $g_{\mu\nu}$ via the conformal transformation

$$\tilde{g}_{\mu\nu}(\phi) = \Omega^2(\phi)g_{\mu\nu}, \quad (8)$$

with $\Omega(\phi)$ the conformal factor function. Note that a large class of scalar-tensor theories exists [198], and that the conformal rescaling is not the only possible choice, as one can choose a disformal one. Also note that in general, in the model (7), unless the conformal factor depends on the matter field, the weak equivalence principle holds.

In the Jordan frame, the action reads

$$S_{\phi,J} = \int \mathrm{d}^4x\sqrt{-\tilde{g}}\left[\frac{\mathrm{M}_{\mathrm{Pl}}^2}{2}F(\tilde{\phi})\tilde{R} - \frac{1}{2}Z(\tilde{\phi})\tilde{g}^{\mu\nu}\partial_\mu\tilde{\phi}\partial_\nu\tilde{\phi} - U(\tilde{\phi})\right] + \int \mathrm{d}^4x\sqrt{-\tilde{g}}\mathcal{L}_{\mathrm{m}}\left(\tilde{g}_{\mu\nu}, \psi_{\mathrm{m}}^{(i)}\right), \quad (9)$$

where the functions F and Z and the potential U are defined via a scalar field rescaling $\phi \to \tilde{\phi}$

$$F(\tilde{\phi}) = \Omega^{-2}(\phi) \quad (10)$$

$$\left(\frac{\partial\phi}{\partial\tilde{\phi}}\right)^2 = \frac{Z(\tilde{\phi})}{F(\tilde{\phi})} + 3\frac{\mathrm{M}_{\mathrm{Pl}}^2}{2}\left(\frac{\partial \ln F(\tilde{\phi})}{\partial\tilde{\phi}}\right)^2 \quad (11)$$

$$U(\tilde{\phi}) = V(\phi)F^2(\tilde{\phi}). \quad (12)$$

The modified Einstein's field equation is obtained by varying the action in the Einstein frame with respect to the metric:

$$G_{\mu\nu} = \frac{1}{\mathrm{M}_{\mathrm{Pl}}^2}\left[\Omega^2(\phi)\tilde{T}_{\mu\nu} - 2g_{\mu\nu}\partial^\rho\phi\partial_\rho\phi + \partial_\mu\phi\partial_\nu\phi - V(\phi)g_{\mu\nu}\right], \quad (13)$$

where

$$\tilde{T}_{\mu\nu} = \frac{2}{\sqrt{-\tilde{g}}}\frac{\partial(\sqrt{-\tilde{g}}\mathcal{L}_{\mathrm{m}})}{\partial\tilde{g}^{\mu\nu}} \quad (14)$$

is the Jordan frame stress-energy tensor, which corresponds to that of the observable matter of the standard model [29]. Comparing Eq. (13) with Eq. (2), it is clear that the scalar field introduces an extra term of curvature and modifies the way matter curves spacetime via the conformal factor in front of the stress-energy tensor.

The Klein-Gordon equation describing the dynamics of the scalar field is obtained by variation of the action with respect to ϕ:

$$\nabla^\mu\phi = \frac{\mathrm{d}V}{\mathrm{d}\phi} - \frac{\mathrm{d}\ln\Omega}{\mathrm{d}\phi}T^{\mu\nu}g_{\mu\nu}, \quad (15)$$

where the Einstein frame stress-energy tensor is related to that of the Jordan frame by $T^{\mu\nu}g_{\mu\nu} = \Omega^4(\phi)\tilde{T}^{\mu\nu}\tilde{g}_{\mu\nu}$. As the scalar field couples to the Einstein frame stress-energy tensor, it feels ordinary matter affected by the factor Ω^4. It should be noted that the field is not sourced by traceless stress-energy tensor fields (like the electromagnetic field).

A note is in order about the differences between the Einstein and the Jordan frames. Although they are physically equivalent, it is usually said that the Jordan frame is the one that is observable, in the sense that it is in this frame that matter respects energy conservation. On the contrary, in the Einstein frame, matter fields are affected by the scalar field, leading to a modification of the energy conservation with an extra term accounting for the coupling with the scalar field. This coupling leads to an apparent modification of the matter fields' masses. In the Jordan frame, masses are constant, but the gravitational constant is modified as an effective gravitational constant $G_{\mathrm{eff}} = \Omega^2(\phi)G$. However, gravitational experiments give access only to products of the gravitational constant and masses (e.g. Gm_1m_2 when considering the gravitational interaction between two bodies of mass m_1 and m_2), thereby making both frames experimentally equivalent (either we modify masses, or we modify the gravitational constant).

As long as no additional coupling terms are added, matter fields are minimally coupled to the metric in the Jordan frame. Consequently, matter particles follow geodesics in that frame. Note however that this does not mean that they follow geodesics predicted by GR: the non-minimal coupling between the scalar field and the tensor field affects the gravity field such that the trajectory of matter particles is modified compared to pure GR. On the contrary, matter particles do not follow geodesics in the Einstein frame, but are affected an extra term depending on the gradient of the scalar field. Transforming the Jordan frame geodesics equation into the Einstein frame, we can show that this "fifth force" is [62]

$$F_\phi^\rho = -\frac{\partial\ln\Omega}{\partial\phi}\perp^{\mu\rho}\partial_\mu\phi, \quad (16)$$

where $\perp^{\mu\nu} \equiv u^\mu u^\nu - g^{\mu\nu}$ is the projector on the 3-space normal to the 4-velocity u^μ. This force leads to a WEP violation if the scalar field does not couple universally with all matter fields.

3.3.2. Newtonian limit Linearising the modified Einstein's field equation (13) in the weak-field and non-relativistic limit ($g_{\mu\nu} = \eta_{\mu\nu} + h_{\mu\nu}$, with $h_{\mu\nu}$ a perturbation from Minkowski metric $\eta_{\mu\nu}$), it becomes

$$\partial^\rho\partial_\rho\Phi = \frac{1}{2}\frac{1}{\mathrm{M}_{\mathrm{Pl}}^2}\left[\Omega^2(\phi)\tilde{\rho} + \partial_t\phi\partial_t\phi + 2\partial^\rho\phi\partial_\rho\phi + V(\phi)\right], \tag{17}$$

where, noting $h = h^\mu_\mu$, $\Phi = -(h_{00} - \frac{1}{2}h\eta_{00})$ is the equivalent of the Newtonian potential and $\tilde{\rho}$ is the local density matter distribution function. For static configurations, we obtain a modified Poisson equation

$$\Delta\Phi = 4\pi G\left[\Omega^2(\phi)\tilde{\rho} + 2(\nabla\phi)^2 + V(\phi)\right], \tag{18}$$

where Δ is the spatial Laplacian. It is clear that the energy density of the scalar field affects the gravitational potential, which is not any more the classic Newtonian potential $\Phi_N = -GM/r$.

Similarly, the scalar field's Klein-Gordon equation becomes

$$\Box\phi = \frac{\mathrm{d}V}{\mathrm{d}\phi} + \frac{\mathrm{d}\ln\Omega}{\mathrm{d}\phi}\Omega^4(\phi)\tilde{\rho}, \tag{19}$$

where $\Box$ is the d'Alembertian.

Finally, the equation of motion of a test mass m can be shown to be

$$\frac{\mathrm{d}^2x^i}{\mathrm{d}t^2} = -\partial_{x^i}\Phi - \frac{\partial\ln\Omega}{\partial\phi}\partial_{x^i}\phi, \tag{20}$$

where x^i are the three spatial components of the 4-position vector. Thus, the fifth force created by the scalar field on this test mass reduces to

$$\mathbf{F}_\phi = -m\frac{\partial\ln\Omega}{\partial\phi}\boldsymbol{\nabla}\phi. \tag{21}$$

If the scalar field couples non-universally to matter (i.e. to each matter field i corresponds the conformal factor $\Omega_i(\phi)$), it is clear that the force $\mathbf{F}^{(i)}_\phi = -m\partial_\phi\ln\Omega_i\boldsymbol{\nabla}\phi$ created on (pure, point-like) test masses will depend on their composition, thereby inducing a WEP violating. In real experiments, test masses are usually made of compounds and spatially extended – in the remainder of this article, we talk about "proof" masses –, so that Eq. (21) must be integrated on all matter fields. Note also that for a non-universally coupled scalar field, the Jordan frame metric (8) explicitely depends on the matter field, so that different matter particles follow their own (different) geodesics.

3.3.3. Light scalar field: dilaton-like field and ultra-light dark matter To see the effect of a universally coupled massless ($V(\phi) = 0$) scalar field, it is convenient to Taylor-expand the coupling function Ω around the background finite value ϕ_0 of the field far from any massive source [29]:

$$\ln\Omega(\phi) = \ln\Omega(\phi_0) + k_1(\phi-\phi_0) + k_2(\phi-\phi_0)^2 + o[(\phi-\phi_0)^3], \tag{22}$$

where k_1 and k_2 are constants parametrising the exchange of one, resp. two, scalar field particles. Constraints have been provided from various pulsar observations and solar system experiments, with k_1 and k_2 consistent with 0 [67]. In particular, the prototypical Brans-Dicke theory [199, 200] is based on this expansion (with $k_2 = 0$).

It is convenient to consider the coupling functions

$$\Omega_i(\phi) = \exp\left(\frac{\beta_i}{\mathrm{M}_{\mathrm{Pl}}}\phi\right), \tag{23}$$

where β_i is the coupling constant between the scalar field and the ith matter field. It can then be shown that the gravitational force created by a source of mass M and coupling constant β_i on a test mass m of coupling constant β_j, at the distance r, derives from the potential

$$U(r) = -\frac{GM}{r}(1 + 2\beta_i\beta_j). \tag{24}$$

Given their resemblance with string theory's dilaton (the scalar partner of the graviton, see e.g. Refs. [26, 201, 202]), such fields are generically referred to "dilaton-like" fields. In the remainder of this paper, we call them simply dilaton fields and follow the conventions of Refs. [26, 203, 204].

Following Refs. [203, 204], dilatons ϕ interact with the Standard Model fields following the Lagrangian $\mathcal{L} = \mathcal{L}_{\mathrm{SM}} + \mathcal{L}_{\mathrm{int}}$. The interaction Lagrangian is

$$\mathcal{L}_{\mathrm{int}} = \frac{\phi}{\mathrm{M}_{\mathrm{Pl}}^2}\left[\frac{d_e}{4e^2}F_{\mu\nu}F^{\mu\nu} - \frac{d_g\beta_3}{2g_3}F^A_{\mu\nu}F^{A\mu\nu} - \sum_{i=e,u,d}(d_{m_i} + \gamma_{m_i}d_g)m_i\bar{\psi}_i\psi_i\right], \tag{25}$$

where $F_{\mu\nu}$ and $F^A_{\mu\nu}$ are the electromagnetic and gluonic tensors, e is the electron's charge, g_3 is the QCD gauge coupling, β_3 is the β-function for g_3 (it should not be confused with the coupling defined in Eq. 23), γ_{m_i} is the anomalous dimension due to the renormalisation-group running of the quark masses, and ψ_i are the fermion spinors. The constants d_e and d_g parametrise the dilaton coupling with the electromagnetic and gluonic fields, while d_{m_e}, d_{m_u} and d_{m_d} are its coupling to the electron, u and d quarks mass terms. The latter two can be replaced by the couplings $d_{\delta m}$ and $d_{\tilde{m}}$ to the symmetric and antisymmetric linear combination of u and d,

$$\hat{m} = \frac{1}{2}(m_d + m_u) \tag{26}$$

$$\delta m = m_d - m_u. \tag{27}$$

Refs. [203, 204] show that in the presence of the dilaton, the fine structure constant α and masses m_i of the Standard Model's fields are modified such as

$$\alpha(\phi) = (1 + d_e M_{\rm Pl}^{-1}\phi)\alpha \tag{28}$$

and

$$m_i(\phi) = (1 + d_{m_i} M_{\rm Pl}^{-1}\phi)m_i, \quad i = u, d, e. \tag{29}$$

Noting that the mass of an atom A of atomic number Z and mass number A can be decomposed as

$$m_A(A, Z) = Zm_{\rm p} + (A-Z)m_{\rm n} + Zm_{\rm e} + E_1 + E_3, \tag{30}$$

where $m_{\rm n,p}$ is the mass of the neutron or proton, $m_{\rm e}$ is the electron mass and E_1 and E_3 are the electromagnetic and strong interaction binding energies, it follows that the dilaton does not couple universally to atoms. Rather, the coupling of the dilaton with the atom A,

$$\beta_A = \frac{M_{\rm Pl}}{m_A}\frac{\partial m_A(\phi)}{\partial\phi}, \tag{31}$$

is given by a combination of the dilaton coupling constants and of "dilaton charges",

$$\beta_A = d_g + \left[(d_{\hat{m}} - d_g)Q_{\hat{m}} + (d_{\delta m} - d_g)Q_{\delta m} + (d_{m_e} - d_g)Q_{m_e} + d_e Q_e\right]_A, \tag{32}$$

with

$$Q_{\hat{m}} = F_A\left[0.093 - \frac{0.036}{A^{1/3}} - 0.020\frac{(A-2Z)^2}{A^2} - 1.4\times10^{-4}\frac{Z(Z-1)}{A^{4/3}}\right], \tag{33}$$

$$Q_{\delta m} = F_A\left[0.0017\frac{A-2Z}{A}\right], \tag{34}$$

$$Q_{m_e} = F_A\left[5.5\times10^{-4}\frac{Z}{A}\right] \tag{35}$$

and

$$Q_e = F_A\left[-1.4 + 8.2\frac{Z}{A} + 7.7\frac{Z(Z-1)}{A^{4/3}}\right]\times10^{-4}, \tag{36}$$

where

$$F_A = \frac{Am_{\rm amu}}{m_A}, \tag{37}$$

with $m_{\rm amu} = 931$ MeV the nucleon mass with the average binding energy, 8 MeV, substracted.

A direct consequence of this non-universal coupling is an apparent violation of the equivalence principle, as discussed with MICROSCOPE data in Sect. 6.3.

Furthermore, the above formalism is prototypical of several ultra-light dark matter scenarios, which can be constrained from tests of the WEP and are routinely tested via atomic spectroscopy to search for variations in the fundamental constants. Sensitive atomic observables arise primarily due to possible changes in the fine-structure constant or the electron mass. See e.g. Refs. [205–209] for recent works. Their results are discussed and compared with MICROSCOPE in Sect. 6.3.

3.3.4. Massive scalar field Let us assume that the potential of the scalar field has a minimum at which the field reaches the value $\phi_{\rm min}$. The mass of the field is defined as the curvature of the potential at $\phi_{\rm min}$,

$$m_\phi^2 = \frac{{\rm d}^2V}{{\rm d}\phi^2}(\phi_{\rm min}). \tag{38}$$

The Klein-Gordon equation of a massive scalar field coupled non-universally to matter with coupling functions given by Eq. (23) and characterised by a quadratic potential $V(\phi) = m_\phi^2\phi^2/2$ is, in the Newtonian limit,

$$\Delta\phi = m_\phi^2\phi + \frac{1}{\rm M_{Pl}}\sum_i \beta_i\tilde{\rho}_i, \tag{39}$$

where, as before, ρ_i is the density distribution function of the ith matter field and β_i its coupling constant with the scalar field.

The profile of the field is thus given as an integral over the volume V_s of the source

$$\phi(\mathbf{r}) = \frac{1}{\rm M_{Pl}}\int_{V_s}{\rm d}^3\mathbf{r}'\frac{{\rm e}^{-m_\phi|\mathbf{r}-\mathbf{r}'|}}{4\pi|\mathbf{r}-\mathbf{r}'|}\sum_i\beta_i\tilde{\rho}_i(\mathbf{r}'), \tag{40}$$

which reduces, for a point source of mass M and homogeneous composition, to

$$\phi(r) = \frac{\beta_i M}{4\pi{\rm M_{Pl}}}\frac{{\rm e}^{-m_\phi r}}{r}. \tag{41}$$

The total gravitational force $F = m\partial_r U(r)$ undergone by a test mass m and coupling constant β_j in the field of the source M thus derives from the potential

$$U(r) = -\frac{GM}{r}(1 + 2\beta_i\beta_j{\rm e}^{-m_\phi r}), \tag{42}$$

which is shown by substituting Eq. (41) in Eq. (20).

Introducing the field's Compton wavelength

$$\lambda_\phi = \frac{\hbar}{cm_\phi}, \tag{43}$$

where $\hbar$ is the reduced Planck constant and c the speed of light, it is clear that the total gravitational potential (42) is formally identical to the sum of the Newtonian and Yukawa potentials (5), the range of which is thus inversally proportional to the mass of the scalar field.

3.3.5. Screening mechanisms Solar system tests of gravity tightly constraint the existence of the putative long-range fifth force associated to light scalar fields. However, scalar fields can evade detection from local experiments through screening mechanisms. A handful of them have been proposed:

- the chameleon mechanism [32–34, 68, 210–212] operates when the effective mass of a scalar field depends on the local matter density. In deep space, where the density is low, the field is light enough to mediate a fifth force; on the contrary, it is massive on Earth where the density is high, and its associated fifth force is exponentially suppressed.
- the symmetron mechanism [32, 213, 214] operates when the vacuum expectation value (vev) of a scalar field depends on the local mass density, becoming large in low-density regions and small in high-density regions. Since the coupling of the scalar to matter is proportional to the vev, the scalar couples with gravitational strength in low-density regions, but is screened in high-density regions.
- in the Vainshtein mechanism [215–219], also known as k-mouflage, non linear effects –typically for source distances smaller than a so-called Vainshtein radius which depends on the source and on the theory considered– allow for the suppression of degrees of freedom whose effects are then only left important at large distances.
- in the least coupling principle [26], string-loop modifications of the low-energy matter couplings of the dilaton may provide a mechanism for fixing the vev of a massless dilaton in a way which is naturally compatible with existing experimental data, the dilaton's cosmological evolution driving it to values where it decouples from matter.
- in the runaway-dilaton scenario [27, 220], the dilaton dependence of the low-energy effective action is extremised for infinitely large values of the bare string coupling (instead of finite values in the least coupling principle, of which the runaway-dilaton is a generalisation); the dilaton runs away to its fixed point during the Universe's inflationary epoch, with the current dilaton couplings to matter related to the amplitude of the density fluctuations during inflation.

In the remainder of this review, we focus on the chameleon as the prototypical screening mechanism for scalar-tensor models used in MICROSCOPE data analysis.

3.4. Chameleon mechanism

The chameleon mechanism relies on the scalar field acquiring a density-dependent mass that controls the range of the associated fifth force (from small-range in high-density regions to long-range in low-density regions). This behaviour made the chameleon not only a promising candidate to explain the accelerated expansion of the universe, but also a potentially easily testable model. Indeed, as shown by Refs. [34, 68], space tests of the WEP were expected to measure violations stronger than allowed by experiments on the ground. Alas, as we show in Sect. 6.4, this conclusion was too optimistic. In this section, we summarise the main characteristics of the chameleon field.

The chameleon mechanism is given by the action (7) in the Einstein frame and (9) in the Jordan frame, with a coupling constant associated to the ith matter field

$$\beta_i = \mathrm{M_{Pl}} \frac{\mathrm{d}\ln\Omega_i(\phi)}{\mathrm{d}\phi}, \tag{44}$$

defined from the coupling function (23). Although the chameleon can couple differently to each component of matter, in which case it causes an apparent WEP violation, we assume below that it couples universally to matter and drop the i subscript. In this case, the WEP is respected for point-like particles, but it may be violated for macroscopic objects (see below).

For static configurations of non relativistic matter, the field dynamics derive from the Klein-Gordon equation

$$\nabla^2\phi = V_{\mathrm{eff},\phi}, \tag{45}$$

where the effective potential

$$V_{\mathrm{eff}}(\phi) = V(\phi)\frac{\beta\tilde{\rho}}{M_{\mathrm{Pl}}}\phi \tag{46}$$

depends on the mass density function $\tilde{\rho}$. For the chameleon mechanism to occur, the potential $V(\phi)$ of the field must be monotonically decreasing, tending to 0 at infinity with a null derivative. A prototypical potential is given by the Ratra-Peebles inverse power-law potential of energy scale Λ and exponent n [212, 221]

$$V(\phi) = \Lambda^4\left(1 + \frac{\Lambda^n}{\phi^n}\right). \tag{47}$$

The minimum of the effective potential V_{eff} explicitly depends on the density environment density:

$$\phi_{\min}(\tilde{\rho}) = \left(\mathrm{M_{Pl}}\frac{n\Lambda^{n+4}}{\beta\tilde{\rho}}\right)^{\frac{1}{n+1}}. \tag{48}$$

In a medium of constant density, the field is expected to relax exponentially to the minimum of its potential.

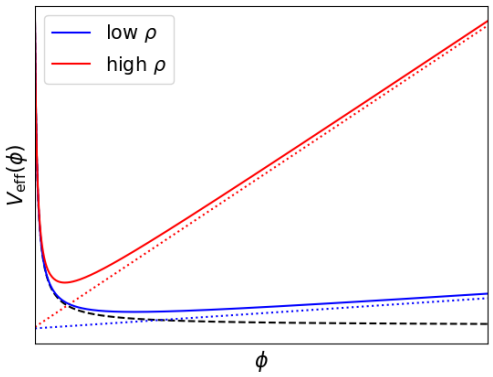

Figure 2. Chameleon effective potential (solid lines), in high (red) and low (blue) density regions. The dashed line shows the chameleon potential $V(\phi)$ and the dotted lines the local-matter-density-dependent term.

It varies on a typical scale of the order of its local Compton wavelength

$$\lambda_{\rm c}(\tilde{\rho}) \equiv m^{-1}(\tilde{\rho}) = \frac{1}{\sqrt{V''_{\rm eff}(\phi_{\rm min})}}. \tag{49}$$

As shown in Fig. 2, adding a local matter density dependent term to this potential (Eq. 45) affects its mass and the value $\phi_{\rm min}$ that minimises the potential: the higher the local matter density, the lower $\phi_{\rm min}$, the higher the chameleon's mass and the shorter its Compton wavelength λ_c.

Two related effects follow from this environmental dependence, allowing for the field to hide from local experiments. To see them, we consider a spherically symmetric object of density $\rho_{\rm in}$, radius r_c and mass M_c. We assume that the density outside the body is $\rho_{\rm out}$, and we denote by $\phi_{\rm in}$ and $\phi_{\rm out}$ the minima of the effective potential of the field inside and outside the body, respectively. Inside the object, the value of field will decrease from $\phi_{\rm surf}$ to ϕ_c from the surface to the center of the object, with $\phi_c = \phi_{\rm in}$ only if the object is massive enough for the field's Compton wavelength to be much smaller than r_c. Let us start by assuming that this condition is met. In this case, the field reaches $\phi_{\rm min}$ within a depth

$$\Delta r_c = \frac{\phi_{\rm out} - \phi_{\rm in}}{6\beta\Phi_c} r_c, \tag{50}$$

where $\Phi_c = M_c/8\pi r_c$. The exterior profile of the chameleon field is then

$$\phi(r) = -\frac{\beta}{4\pi}\frac{3\Delta r_c}{r_c}\frac{M_c {\rm e}^{-(r-r_c)/\lambda_{\rm out}}}{r} + \phi_{\rm out}, \tag{51}$$

where $\lambda_{\rm out}$ is the field's Compton wavelength in the external environment.

The Yukawa suppression in Eq. (51) causes the chameleon's environmental screening. If a test mass is placed farther than $\lambda_{\rm out}$ from the body, then the chameleon interaction is canceled. Given that the Compton wavelength depends on the local density, the interaction between two bodies may be Yukawa-suppressed in a high-density environment (such as the Earth atmosphere) but may still be significant in a low-density region (such as deep space).

The second effect comes when the chameleon reaches its minimum inside the source near the surface, such that the thin-shell parameter

$$Q_c \equiv 3\frac{\Delta r_c}{r_c} \ll 1. \tag{52}$$

If this thin-shell condition is met, then only a thin portion of the body contributes to the exterior profile. The chameleon contribution to the gravity field is then marginal compared to that of the Newtonian gravity, so that it is effectively hidden to experiments and the source is screened. This screening obviously also occurs to a mass interacting with a source. This is why planets orbits do not show deviations from Newtonian gravity: even if the chameleon's Compton wavelength in space is greater than typical distances between planets, the chameleon is hidden as soon as planets are screened (i.e. meet the thin-shell condition).

On the opposite, the chameleon field does not reach its minimum in objects that do not meet the thin-shell condition (because they are not massive enough); those objects just act as perturbations on the chameleon field, and are subject to a chameleon-induced force. The fifth force induced by the coupling to the chameleon field on a point test mass is proportional to the gradient of the scalar field and given by

$$\vec{F} = -\frac{\beta}{{\rm M_{Pl}}} m_{\rm test}\vec{\nabla}\phi. \tag{53}$$

It is clear that if the coupling is not universal, this force depends on the composition (since two test masses of different composition have their own coupling constant β), and a violation of the WEP is expected.

On the opposite, if the coupling is universal, no WEP violation is to be expected when considering point-like test masses. Nevertheless an extended body of mass m cannot, a priori, be considered as a test body and is subject to the thin-shell condition (with thin-shell parameter Q_m). Substituting for $\nabla\phi$ from Eq. (51) in Eq. (53), the norm of the force at a distance r of a symmetrical body on such an object is

$$F(r) = 2\beta^2 Q_c Q_m \frac{M_c m}{8\pi {\rm M_{Pl}}^2 r^2}, \tag{54}$$

such that two bodies of different thin-shell parameters (e.g. because of different mass, even if the same

composition) will then undergo different forces, thence an apparent violation of the WEP when placed in the right conditions of low-density region (so that the chameleon's Compton wavelength is large enough). From this observation, Ref. [34] predicted a possibly significant violation in space-based tests of the WEP. This motivated the works presented in Sect. 6.4.

3.5. Standard model extensions and spin-1 particles

At the quantum level, the Standard Model describes the strong, weak and electromagnetic interactions with the $SU(3) \times SU(2) \times U(1)$ gauge group, but still excludes gravity. Approaches towards a consistent theory of quantum gravity, and most notably string theories, usually involve new symmetries, fields and particles. One of the simplest possibilities is to add an extra $U(1)$ symmetry within a $SU(3) \times SU(2) \times U(1) \times$ extra$-U(1)$ gauge group. Although the resulting boson may be very heavy ($\gtrsim$ a few TeV), in some unconventional instances it may be very light and have a very small coupling g'', potentially leading to an extremely weak new long-range force [195, 196, 222–224]. Given the measured solar system dynamics, this force should of course be much weaker than gravitation.

As an example, we follow Refs. [223, 224] and we denote the corresponding new spin-1 particle as the U boson. It can be viewed as a generalised dark photon coupled to standard model particles through the linear combination [195, 225]

$$(\epsilon_Q Q + \epsilon_B B + \epsilon_L L)e \tag{55}$$

where ϵ_Q, ϵ_B and ϵ_L are coupling constants (with the electric charges, baryon and lepton number respectively) depending in particular on the mixing between the new gauge boson, the Z and the photon, which need to be determined experimentally.

The corresponding new force acts additively on ordinary neutral matter, proportionally to a linear combination of baryon and lepton numbers. This is equivalent to considering a force acting effectively on a linear combination of the numbers of protons and neutrons, $Z = L$ and $N = B - L$. Such a new force is thus generally expected to be repulsive (except if $\epsilon_B B + \epsilon_L L$ has different signs for the Earth and the test mass considered). This is in contrast with a spin-0 induced force, normally expected to be attractive, and not expected to have such an additivity property, making its couplings more difficult to evaluate (as illustrated with the chameleon field above).

Its mass may vanish if its gauge symmetry is conserved, or be naturally small, especially if the corresponding gauge coupling is very small. If the new symmetry associated with the U is spontaneously broken, e.g. through the vev of an extra singlet field, the U acquires a mass m_U, vanishing with g'', mediating a new force of range [223]

$$\lambda_U = \frac{\hbar}{m_U c} \approx 1973 \text{ km } \left(\frac{m_U}{10^{-13} \text{ eV}/c^2} \right)^{-1}. \tag{56}$$

When the U boson couples to the baryon number only, this force derives from a composition-dependent Yukawa-like potential with strength [224]

$$\alpha_{ij} = \alpha_{gB} \left(\frac{B}{A_r} \right)_i \left(\frac{B}{A_r} \right)_j \tag{57}$$

when the masses are expressed in atomic mass units as $m = A_r \mu$ and

$$\alpha_{gB} = -\alpha \left(\frac{\mathrm{M_{Pl}}}{m_p} \right)^2 \left(\frac{m_p}{\mu} \right)^2 \epsilon_B^2 \tag{58}$$

where m_p is the mass of the proton and α is the fine-structure constant (not to be confused with the Yukawa amplitude of Eq. 5). As shown in Sect. 6.5, this composition-dependent force can induce a WEP violation and may be measurable with MICROSCOPE.

4. Experimental tests of the WEP

4.1. Historical overview

Experimental tests of the WEP rely on the comparison between the acceleration undergone by two proof masses A and B in the same gravitational field [17,161]. They are quantified in terms of the Eötvös parameter

$$\eta = 2\frac{a_A - a_B}{a_A + a_B} = 2\frac{m_{G,A}/m_{I,A} - m_{G,B}/m_{I,B}}{m_{G,A}/m_{I,A} + m_{G,B}/m_{I,B}}, \tag{59}$$

named after Loránd Eötvös, who used a torsion balance to perform the first modern test of the WEP in the late 19th century, reaching a precision of 5×10^{-8} [226], which he eventually improved it to 3×10^{-9} [227]. In those experiments, two masses made of different composition are positioned at the end of a suspended rod. The centrifugal forces on the masses due to the Earth rotation are balanced against a component of the Earth's gravity field. If the ratio of the inertial to gravitational mass was different for both proof masses, a torque would twist the torsion balance, highlighting a WEP violation. Spinning torsion balances based on an ever improving technology allowed for a continuous increase in the experiment precision [228–233]. The best constraints from a torsion balance experiment currently come the Eöt-Wash group, with an upper bound of the WEP at the level of 2×10^{-13} [54, 58]. Although they can be mitigated with clever experimental tricks [231,234], systematic errors such as environmental gravity gradients, thermal fluctuations

and magnetic fields are currently the main limitations of torsion balance tests. See Refs. [48, 55] for reviews of tests of gravity (including the WEP) with torsion pendulums.

Free-fall tests consist in dropping proof masses made of different compositions and monitoring their fall in the same gravitational field. Precise experiments emerged in the 1980s. Since the driving force in free-fall experiments (the Earth gravity, $g \approx 9.8\text{ms}^{-2}$ on the ground) is much higher that that of rotating balances (of order 10^{-2}ms^{-2}), the former were expected to easily outperform the latter. Several experiments were designed, to eventually reached a precision of order 10^{-10} [235–240]. Free-fall experiments are limited by errors in initial conditions at release coupling to the gravity gradient of the Earth, which entail a differential acceleration mimicking a WEP violation. High drop towers may allow for an increased time of free-fall, thereby increasing the precision of the test (since the effect of a violation increases quadratically with time). For instance, the ZARM tower of the University of Bremen allows for free-fall times up to 9.3 seconds. Experiments on balloons [241] and sounding rockets [242] have been proposed, with free-fall times that could reach tens of seconds.

The natural next step is then to perform free-fall experiments in space, where the free fall can a priori be unlimited in time as proof masses follow their geodesics in the Earth orbit [243]. The proposed Satellite Test of the Equivalence Principle (STEP [244–246]) and Galileo Galilei (GG [247, 248]) missions, as well as the completed MICROSCOPE mission, exploit this principle. Given that MICROSCOPE is the focus of this review, we discuss the pros and cons for free-fall experiments in space below, after closing the general panorama on experimental tests of the WEP.

Using microscopic bodies (e.g. atoms, neutrons, charged particles) as proof masses is now possible thanks to the advent of atom interferometry [249], and should allow for a much better control of systematic effects in free-fall experiments: atoms have well-known and reproducible properties, it is possible to make a very small atomic probe, the position of which is very precisely controlled, and the possibility to use different atomic states and isotopes allow for the rejection of systematic errors. Recent atom interferometry tests of the WEP reach a precision of the order of 10^{-12} [250–256]. This precision is expected to improve in the near future, especially thanks to proposed space experiments [257–259]. Additionally, proposals and proof-of-concept have been made to test the WEP with anti-matter [260–268].

Beside laboratory-scale proof masses and atoms, celestial bodies can be used as free-falling probes. For instance, the Earth and the Moon both fall in the Sun gravitational field. If the WEP is violated, their accelerations towards the Sun are different, leading to a modulation of the Earth-Moon distance along the Earth-Sun direction at the synodic period (29.53 days) [269]. This distance can be routinely measured at high precision by shooting lasers at the Moon, which is possible thanks to reflectors positioned on the Moon during the Apollo missions. This Lunar Laser Ranging (LLR) has been on since the 1970s, providing exquisite measurements and allowing for an ever-increasing test of the WEP down to 5×10^{-14} [50,270]. See [271] for a review of the LLR; note that since the bodies of interest are massive, LLR tests not only the WEP, but a combination of the WEP and of the Strong Equivalence Principle. A similar effect can be looked for in Satellite Laser Ranging (SLR), whereby the distance of satellites to the Earth is measured, e.g. LAGEOS and LARES [272]. However, artificial satellites are much more subject to tidal effects and non-gravitational forces (such as solar radiation pressure) than the Moon, and tests based on SLR are not competitive with LLR [273].

4.2. Free-fall experiments in space

Space allows for much longer free falls than allowed by on-ground experiments, but with a similar driving acceleration (in low-earth orbit, $g \approx 8\text{ ms}^{-2}$), giving such experiments the potential to surpass torsion balance experiments (which can have long integration times but are driven by small accelerations). As importantly, weightlessness, coupled to the now well-established drag-free technology (which allows for the cancellation of non-gravitational external accelerations) provides a quiet gravitational environment, ideal for minute acceleration and forces measurement: LISA Pathfinder showed that residual differential accelerations can be reduced down to $10^{-15}\text{ ms}^{-2}\text{Hz}^{-1/2}$ [274, 275]. MICROSCOPE is not as precise, for reasons that will be made clear below, but still achieves residual accelerations below $10^{-11}\text{ ms}^{-2}\text{Hz}^{-1/2}$.

Free-fall experiments in space can be performed in small boxes (they do not require 100 meter high drop towers), which allows for a better control over external perturbations. Proof masses in STEP, GG and MICROSCOPE are concentric, allowing for a fine control of their differential accelerations, requiring small forces. Another advantage is the possibility to spin the entire experiment to modulate the frequency of a potential WEP violation. For instance, the MICROSCOPE satellite spun to look for a WEP violation at the frequency where the noise is minimum. Finally, the orbit followed by the experiment can be defined to allow for very stable thermal conditions, thereby reducing related systematic errors.

Nonetheless, space tests are not exempt from systematic errors. Gravity gradients due to test-

masses not being perfectly concentric, nor having exactly the same multipole moments, are significant systematics. However, since they couple with the well-known Earth gravity field, it is easy to correct for gravity gradients due to proof-masses offcentering; furthermore, their couplings with the proof masses shape can be reduced by designing them to be as close as possible to monopoles. Moreover, those tests are so sensitive that tiny effects such as the radiometer effect and the radiation pressure must be taken into account (see below for MICROSCOPE).

A final significant systematic error (and MICROSCOPE's main limitation) is linked to test-masses being hit by cosmic radiation, thereby accumulating electric charges that eventually introduce noise in the measurement. Controlling the test-masses' electric potential is thus essential. MICROSCOPE uses a gold wire to physically link the proof masses with the satellite and control their charge. LISA Pathfinder demonstrated that illuminating the proof masses with an ultra-violet lamp allows for an efficient charge control [276]. Being contactless, LISA Pathfinder's charge control management introduces significantly less noise into the measurement than MICROSCOPE's wire. This explains the different residual differential acceleration levels mentioned above.

Selected for a phase A study in 1990, STEP was expected to test the WEP down to the 10^{-18} level, with a drag-free satellite. The payload consisted in four pairs of accelerometers, each consisting of a pair of proof masses made of either Be, Pt:Ir or Nb, set in a cryogenic environment allowing for exquisite control of thermal systematics and for a high-precision SQUID-technology-based measurement of the proof masses motion.

GG is a proposed mission based on the principle of a beam balance. The experimental design is expected to significantly reduce the requirement on the satellite's drag control compared to STEP and MICROSCOPE, and to reduce gas damping and the radiometer effect, allowing for a test of the WEP down to 10^{-17}. A laboratory demonstrator has been built and is currently under tests [277].

Proposed by ONERA and the Observatoire de la Côte d'Azur (OCA), the MICROSCOPE mission was selected by CNES in 1998, to test the WEP with a 10^{-15} precision. Its payload, developed by ONERA, was based on ONERA's long experience on ultra-sensitive space accelerometers [278], generations of which had already flown on the CASTOR D5B satellite [279], on the International Space Station [280] and on the CHAMP mission [281,282], then eventually flew on GRACE [283] and GOCE [284, 285], and are currently flying on GRACE-Follow On [286]. The mission underwent several external (modification of the satellite's micro-thrusters, development of the Vega launcher) and internal (weakness of the wire used to control the proof masses' charge) delays, postponing the launch initially planned in 2004. MICROSCOPE was eventually launched on April 25, 2016.

5. The MICROSCOPE experiment

5.1. Experimental concept

In essence, MICROSCOPE is a test of the UFF with an easy recipe: drop two test bodies and compare their fall. Performing the experiment in space allows for a very long fall (MICROSCOPE's longest falls lasted one week), since test bodies freely-fall as they orbit the Earth, which helps to outperform on-ground experiments (in which free fall is limited to a few seconds). Actually, instead of letting two test bodies freely orbit the Earth and monitoring the differences in their orbits, MICROSCOPE forced two test masses to stay centered with respect to each other by means of electrostatic forces. This was done with a differential ultrasensitive electrostatic accelerometer, consisting of two coaxial and concentric cylinders made of different materials. The difference of electric potentials applied to keep the cylinders in equilibrium is a direct measure of the difference in their motion. Hence, a non-zero difference of applied potentials is a measure of a non-zero difference of the accelerations felt by the two masses: in other words, it is a measure of a violation of the WEP.

The gravity that pulls MICROSCOPE's proof masses is sourced by the Earth. Therefore, a possible violation of the WEP can be expected to be proportional to the Earth gravity acceleration. More precisely, when measured along the main axis of the cylindrical masses (as done by MICROSCOPE), the signal we are looking for is the projection of the Earth's gravity acceleration on this axis. It is therefore proportional to the modulation of the Earth's gravity field, depending on the motion of the satellite around the Earth and of its attitude, resulting in a periodic signal with a well predictable frequency. This is illustrated by Fig. 3 .

The frequency of the potential WEP violation signal can be tuned by spinning the satellite about its axis orthogonal to the orbital plane at frequency $f_{\rm spin}$:

$$f_{\rm EP} = f_{\rm orb} + f_{\rm spin}, \tag{60}$$

where $f_{\rm orb}$ is the satellite's orbital frequency. Several spinning configurations (corresponding to different $f_{\rm spin}$) were envisioned to confirm a possible WEP violation at different frequencies.

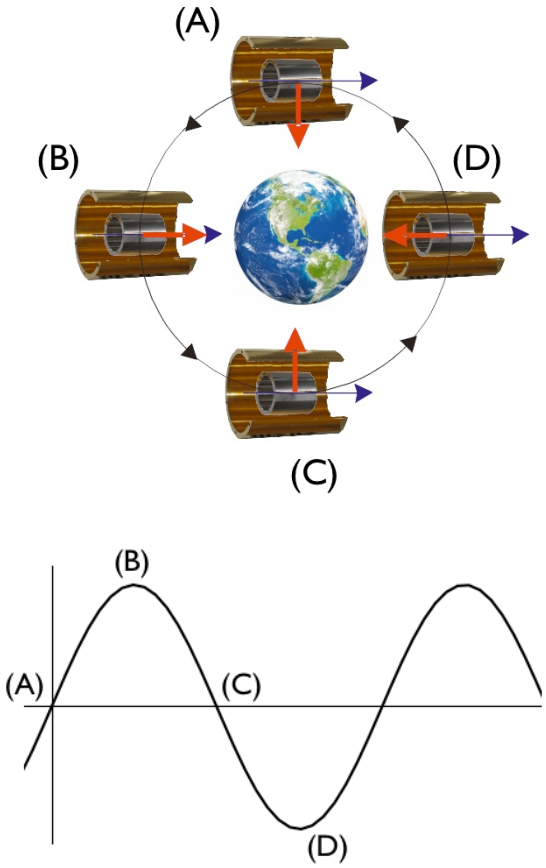

Figure 3. MICROSCOPE's measurement principle. A WEP violation is detected if the two cylindrical test-masses experience different accelerations (red arrows) as the satellite orbits the Earth; the difference in those accelerations is measured by the difference in the voltages applied to the test-masses to keep them in equilibrium. On the upper panel, black arrows show the sensitive axis along which a WEP violation is looked for. At point (A), the Earth gravitational field is orthogonal to the test axis, resulting in a null signal; at point (B), the axis is aligned with, and in the same direction as, the test axis, resulting in a maximal signal; point (A) is similar to point (B), resulting in a null signal; point (D) is similar to point (B), but the signal is the opposite direction. The resulting signal for a possible violation of the WEP is thus periodic.

5.2. Experimental apparatus

The electrostatic control of the proof masses relies on two nested control loops (Fig. 4). The first one is inside the payload (lower right box of the figure): each proof mass is placed between pairs of electrodes and its motion with respect to its cage fixed to the satellite is monitored by capacitive sensors. It can be kept motionless by applying the electrostatic force required to compensate all other forces. In that way, the knowledge of the applied electrostatic potential provides a measurement of the acceleration which would affect the test-mass with respect to the satellite without the electrostatic force. The second control loop in the MICROSCOPE experiment is included in the satellite's Drag Free and Attitude Control System (DFACS). This system cancels (or at least considerably reduces) the level of external disturbances with very performant cold gas thrusters. External disturbing forces and torques are sensed by the instrument's accelerometers and the satellite's star trackers. Those measurements are combined to control the cold gas thrusters and counteract disturbing forces. This system also ensures a very accurate control of the pointing and of the attitude of the satellite from the measurements of angular position delivered by the stellar sensors and of the angular acceleration delivered by T-SAGE.

The next subsections provide details about the satellite, the payload and the measurement technique.

5.2.1. Satellite MICROSCOPE's spacecraft is derived from the CNES's Myriad series of microsatellites. With a mass of 325 kg and dimensions of about one cubic-meter, it has been designed to be as symmetric as possible, with the payload sitting near its center-of-mass, embedded in a magnetic and thermal shield. No moving mechanical parts can contaminate the Equivalence Principle measurement.

The thermal and mechanical architecture design was driven by the centering of the instrument as close as possible to the satellite center of mass and by the high thermal stability requirement around $f_{\rm EP}$ (better than 1 mK at the sensor unit interface and 10 mK at the associated analog electronics interface). These most thermally sensitive payload units were integrated in a particular cocoon at the core of the satellite.

But the main driver of the satellite design was the reduction of the mean level of accelerations applied on the instrument through an efficient drag-free control [287]. The drag-free control uses the payload as an inertial sensor to measure the external forces and is performed by the cold gas micro propulsion system provided by ESA, which counteracts the perturbations (atmospheric drag, radiation pressure, electromagnetic forces) at a evel of tens of μN. Combining the six degrees of freedom (angular and linear acceleration) allows for the control of torques and forces in only one subsystem, the DFACS, which was shown to exceed its expected performances [154].

5.2.2. Payload The core of MICROSCOPE's instrument (T-SAGE – Twin Space Accelerometer for Gravitation Experiment [153]) consists of two differential accelerometers (called Sensor Units – SU), the proof masses of which are co-axial cylinders kept in equilibrium with electrostatic actuation.

Fig. 5 shows an exploded view of the mechanical parts of one SU, with its:

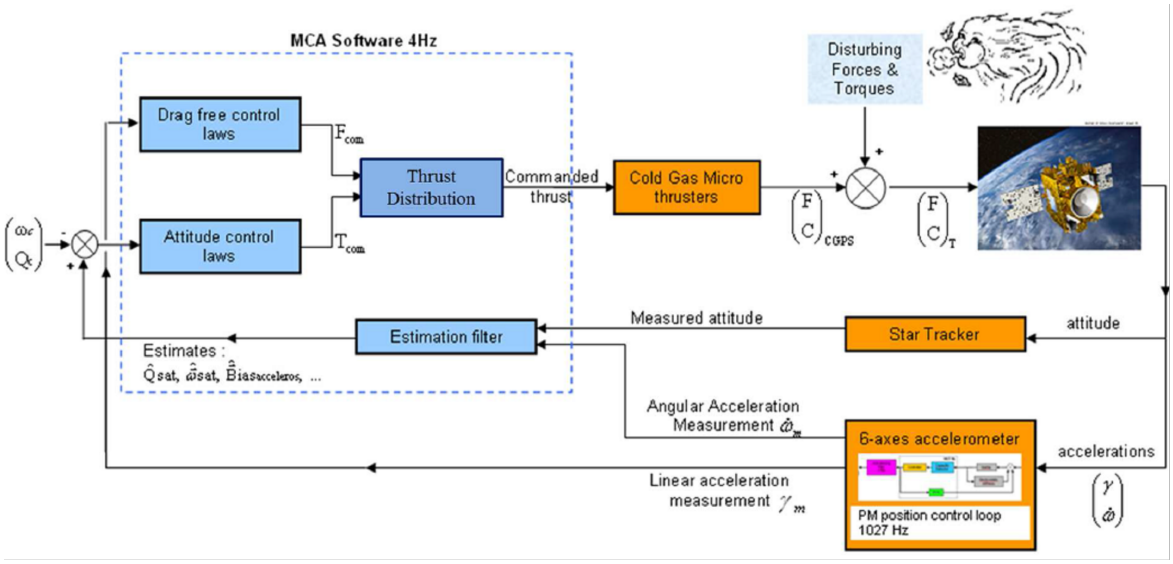

Figure 4. Nested loops to optimise the experiment's environment: satellite's DFACS and instrument's control-loop. External disturbing forces and torques are sensed by the instrument's accelerometers and the satellite's star trackers. Those measurements are combined to counteract disturbing forces by acting cold gas thrusters. Figure from Ref. [154].

- two test-masses
- electrode-bearing gold-coated silica cylinders (two surrounding each proof mass)
- gold coated silica mounting base plate for a precise positioning of the electrode sets; electrodes are used to probe the proof masses and to control them test with electrostatic forces
- Invar sole plate for the positioning of the mounting base plate; supports the titanium inner housing and the vacuum tight housing
- mechanical stops to prevent any electric contact between the test-mass and the electrodes
- 7 μm gold wires connecting each test-mass to the satellite, allowing for a very stable voltage of the test-masses; it is the only mechanical contact between the proof masses and their cage
- test-mass blocking mechanism preventing any damage from the heavy test-masses (0.4 kg to 1.4 kg) during the launch. The test-masses were unlocked before the first in-orbit switch on.
- vacuum system used to maintain a sufficient low vacuum and cleanliness of the electrode set
- vacuum Invar tight housing to hermetically close the SU
- hermetic electrical connectors.

The electrostatic control of the proof masses is performed via a detection/action electronic control loop depicted by Fig. 6. The proof mass position in its cage is performed by a capacitive sensor: its motion induces a capacity difference between the electrodes

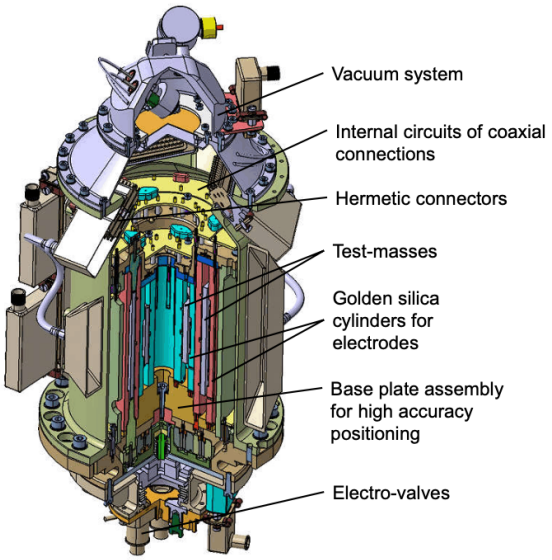

Figure 5. Exploded view of a MICROSCOPE sensor unit, with its two proof masses, their surrounding electrodes bearing cylinders, cylindrical invar shield, base plate, upper clamp and vacuum system. The reference system is shown on the left of the figure. Figure from Ref. [288].

(1) converted into an output voltage by the capacitive detector electronics (3). A digital PID (Proportional Integral Derivative) servo-control loop calculates the control signal from the detector's ouput (4). This signal is amplified (5) before being applied to the electrodes in order to recentre the test-mass in its cage,

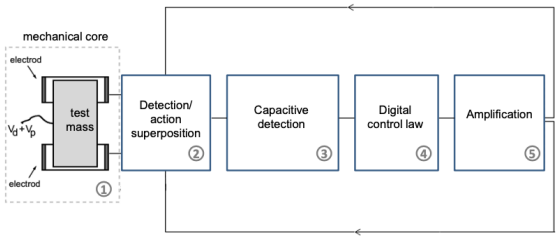

Figure 6. T-SAGE control loop. See main text. Figure from Ref. [288].

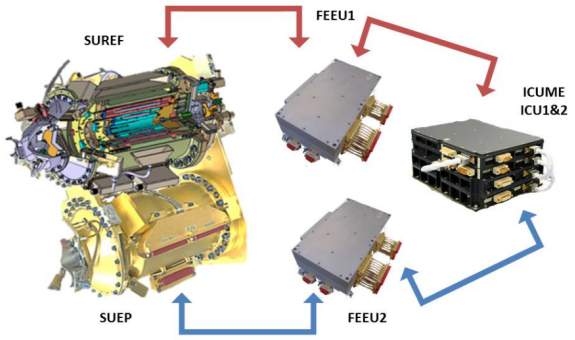

Figure 7. T-SAGE payload: SUEP and SUREF sensor units (SU), Front-End Electronics (FEEU) and Interface Control Unit (ICU). Figure from Ref. [153].

by asymmetrically applying an electrostatic potential to it (1). The same electrodes are used for both detection and action, through the same electronic interface (2). Additionally, as aforementioned, the same electronics' output is used by the satellite's drag-free system.

Details about this control loop can be found in Refs. [153, 288]. Nevertheless, to enlighten the discussion of the proof masses' dynamics below, we provide some elements about the detection and action processes (block (2) of Fig. 6). A proof mass surrounded by two opposite electrodes can be considered as a double capacitor, with capacitances C_1 and C_2. The motion of the proof mass induces a variation in the capacitances, sensed by the detector, which outputs a voltage

$$V_{\rm det} = G_{\rm det}(C_1 - C_2), \tag{61}$$

where $G_{\rm det} = 2V_d/C_{\rm eq}$ is the gain of the detector, with V_d the potential of the proof mass and $C_{\rm eq}$ the capacitance of the capacitor formed by the proof mass and the electrodes when the proof mass is at the centre of the cage. The capacitances C_i depend on the geometry, and therefore their form differ along the longitudinal and radial axes of T-SAGE; nevertheless, it can be shown that along each axis, at first order in the displacement δ of the proof mass about the center of the cage $V_{\rm det} \propto \delta$ [153, 288],

The control loop digitises the detector output voltage $V_{\rm det}$ and computes the actuation voltage to apply to the electrodes in order to compensate for the displacement of the proof mass, and recentre it in the cage. The (restoring) electrostatic force applied by an electrode i is then

$$\vec{F}_{{\rm el},i} = \frac{1}{2}(V_i - V_p)^2 \vec{\nabla} C, \tag{62}$$

where $\vec{\nabla} C$ is the spatial gradient of the capacitance. The (polarisation) potential of the test-mass V_p is maintained constant and the potential V_i of the electrode is tuned by the servo-control loop. This "action" takes the general form

$$F_{{\rm el},i} \approx -m_I \left\{ G_{\rm act} V_e + \omega_p^2 \left[1 + \left(\frac{V_e}{V_p} \right)^2 \right] \delta \right\}, \tag{63}$$

where the sensitivity factor $G_{\rm act}$ and the stiffness coefficient ω_p^2 depend on the geometry of the sensor, V_e is the voltage output from the control loop and applied to the electrodes, and m_I is the inertial mass of the proof mass.

If $G_{\rm act}$ is known well enough, the acceleration of the test-mass can be measured through the voltage V_e required to apply the restoring force. This measurement is perturbed by the electrostatic stiffness, which introduces a bias if the test-mass is not servo-controlled to the equilibrium point. Nevertheless, the asymmetry in the design of the electrostatic configuration and the displacement are sufficiently small to ignore it during nominal WEP test operations.

All in all, as shown in Fig. 7, T-SAGE is made of two sensor units controlled by two Front End Electronics Unit (FEEU) boxes (one per SU) and an Interface Control Unit (ICU). The FEEU include the capacitive sensing of masses, the reference voltage sources and the analog electronics to generate the electrical voltages applied to the electrodes and the ICU includes the digital electronics associated with the servo-loop digital control laws, as well as the interfaces to the satellite's data bus.

The two SU, side by side, share the same geometry. However, they have different proof masses, to fulfil complementary purposes. The primary SU is used to measure the WEP (hence it is called SUEP), and the second one (SUREF) is used as a reference instrument. The materials of SUEP's proof masses were chosen carefully to maximise a potential violation of the WEP from a light dilaton [26, 203, 204] and to optimise their industrial machining: they are made of alloys of Platinum-Rhodium (PtRh10 – 90% Pt, 10% Rh)

and Titanium-Aluminium-Vanadium (TA6V – 90% Ti, 6% Al, 4% V). To act as a reference, with which no violation of the WEP should be measured (at least in models with no environmental screening), the proof masses of SUREF share the same composition, a PtRh10 alloy.

A final note about SUREF is necessary. In order to maximise the performance of the SUEP when testing the WEP, the acceleration measured by one of its proof mass is used as the command of the DFACS (we say that the drag-free point is set on this proof mass). SUREF is then far enough from the drag-free point to have competitive performances. As a consequence, measurements performed by SUREF (were they synchronous with those performed by SUEP), which could be considered as systematics, cannot be directly subtracted from those made with SUEP. In that sense, SUREF really is a "reference instrument", but does not provide "reference measurements". As a SUEP's twin (up to its proof masses), it can hint towards systematic errors, but cannot be used to simply correct for them.

5.3. Proof mass dynamics and measurement equation

5.3.1. Measured acceleration The electrostatic (control) force applied by the electronics servo-control to maintain the jth proof mass motionless ($j = 1, 2$ for the internal and external proof masses of a given SU) was introduced above (Eq. 63). It takes into account all forces acting on the proof mass, and the corresponding acceleration is thus [289]

$$\vec{\Gamma}_{\mathrm{cont},j} = \frac{\vec{F}_{\mathrm{el},j}}{m_{I_j}} = \vec{\Gamma}_{\oplus,j} - \frac{\vec{F}_{\mathrm{loc},j}}{m_{I_j}} - \frac{\vec{F}_{\mathrm{pa},j}}{m_{I_j}} + \frac{\vec{F}_{\mathrm{ext}}}{M_{I_{\mathrm{sat}}}} + \frac{\vec{F}_{\mathrm{th}}}{M_{I_{\mathrm{sat}}}} \tag{64}$$

where $\vec{F}_{\mathrm{ext}}$ are non-gravitational forces affecting the satellite (drag, solar radiation pressure), $\vec{F}_{\mathrm{th}}$ are forces applied by the thrusters (to compensate for external forces) and $\vec{F}_{\mathrm{loc},j}$ and $\vec{F}_{\mathrm{pa},j}$ are local forces (inside the sensor) that we can consider explicitly (e.g. electrostatic stiffness, gold wire stiffness, self-gravity) or implicitly (e.g. electrostatic parasitic), respectively. Finally, the Earth gravitational acceleration, modulated by the rotation of the satellite (hence the contribution of Coriolis acceleration),

$$\vec{\Gamma}_{\oplus,j} = \frac{M_{G_{\mathrm{sat}}}}{M_{I_{\mathrm{sat}}}} \vec{g}(O_{\mathrm{sat}}) - \frac{m_{G_j}}{m_{I_j}} \vec{g}(O_j) + [\mathrm{In}]\overrightarrow{O_{\mathrm{sat}}O_j} + 2[\Omega]\dot{\overrightarrow{O_{\mathrm{sat}}O_j}} + \ddot{\overrightarrow{O_{\mathrm{sat}}O_j}} \tag{65}$$

where $\vec{g}(O_{\mathrm{sat}})$ (resp. $\vec{g}(O_j)$) is the Earth gravity acceleration at the center of mass of the satellite (resp. proof mass), $[\mathrm{In}] = \left[\dot{\Omega}\right] + [\Omega]\,[\Omega]$ is the gradient of inertia matrix of the satellite and $[\Omega]$ its angular velocity. To derive Eq. (65), we assumed that the proof masses are homogeneous and that the Earth's gravity field does not vary significantly within the satellite.

Eq. (64) is an idealised version of what really happens [289]. First, the sensor is not perfectly aligned with the satellite's frame; this is described by the $[\theta_j]$ matrix

$$\vec{\Gamma}_{\mathrm{cont,j|instr}} = [\theta_j]\left(\vec{\Gamma}_{\oplus,j|\mathrm{sat}} + \frac{\vec{F}_{\mathrm{ext|sat}}}{M_{I_{\mathrm{sat}}}} + \frac{\vec{F}_{\mathrm{th|sat}}}{M_{I_{\mathrm{sat}}}}\right) - \frac{\vec{F}_{\mathrm{loc},j|\mathrm{instr}}}{m_{I_j}} - \frac{\vec{F}_{\mathrm{pa},j|\mathrm{instr}}}{m_{I_j}}, \tag{66}$$

where the subscripts "|instr" and "|sat" mean that forces and accelerations are expressed in the instrument or satellite frame, respectively.

Moreover, the measured acceleration is given by the control acceleration (66) affected by the sensitivity matrix $[A_j]$ ‡, by electrostatic parasitic forces (since the applied electrostatic forces are the sum of the measured and parasitic electrostatic forces $m_{I_j}\vec{\Gamma}_{\mathrm{cont},j|\mathrm{instr}} = \vec{F}_{\mathrm{el},j} = \vec{F}_{\mathrm{el,meas},j} + \vec{F}_{\mathrm{elec,par},j}$), by the measurement bias $\vec{b}_{0,\mathrm{j}}$ due to the electronics read-out circuit and by noise n_j. It is therefore given by

$$\vec{\Gamma}_{\mathrm{meas,j|instr}} = \vec{b}_{0,\mathrm{j}} + [A_j]\left(\vec{\Gamma}_{\mathrm{cont},j|\mathrm{instr}} - \frac{\vec{F}_{\mathrm{elec,par},j|\mathrm{instr}}}{m_{I_j}}\right) + K_{2,j}\left[\vec{\Gamma}_{\mathrm{cont},j|\mathrm{sat}}\right]^2 + n_j, \tag{67}$$

where $K_{2,j}$ is the sensor's quadratic factor.

We can then wrap up and write the acceleration measured measured by the jth sensor explicitly in terms of external and local forces:

$$\vec{\Gamma}_{\mathrm{meas,j|instr}} = \vec{B}_{0,j} + [A_j][\theta_j]\left(\vec{\Gamma}_{\oplus,j|\mathrm{sat}} + \frac{\vec{F}_{\mathrm{ext|sat}}}{M_{I_{\mathrm{sat}}}} + \frac{\vec{F}_{\mathrm{th|sat}}}{M_{I_{\mathrm{sat}}}}\right) - [A_j]\frac{\vec{F}_{\mathrm{loc},j|\mathrm{instr}}}{m_{I_j}} + K_{2,j}\left[\vec{\Gamma}_{\mathrm{cont},j|\mathrm{sat}}\right]^2 + n_j, \tag{68}$$

where

$$\vec{B}_{0,j} \equiv \vec{b}_{0,j} - [A_j]\left(\frac{\vec{F}_{\mathrm{pa},j|\mathrm{instr}}}{m_{I_j}} + \frac{\vec{F}_{\mathrm{elec,par},j|\mathrm{instr}}}{m_{I_j}}\right) \tag{69}$$

‡ The diagonal elements of the sensitivity matrix are the instrument's scale factors – one by degree of freedom, which are constants converting between the measured voltage and acceleration –; its off-diagonal elements characterize the roughly constant couplings between degrees of freedom due to slight geometrical defects of the proof mass and to electrostatic defects. The sensitivy matrix can be measured in-flight, see Sect. 5.5.1.

is the scale-factor dependent bias.

A WEP violation signal would hide in the difference between the acceleration measured by the internal sensor and that measured by the external sensor, called the differential acceleration,

$$\vec{\Gamma}^{(d)} \equiv \vec{\Gamma}_{\rm meas,1} - \vec{\Gamma}_{\rm meas,2}. \tag{70}$$

Incidentally, we also define the common-mode acceleration

$$\vec{\Gamma}^{(c)} \equiv \frac{1}{2}\left(\vec{\Gamma}_{\rm meas,1} + \vec{\Gamma}_{\rm meas,2}\right). \tag{71}$$

The difference of gravitational accelerations (Eq. 65)

$$\begin{aligned}\vec{\Gamma}^{(d)}_{\oplus} = (1+\delta_2)\vec{g}(O_2) - (1+\delta_1)\vec{g}(O_1) \\ + [\mathrm{In}]\overrightarrow{O_2O_1} + 2[\Omega]\dot{\overrightarrow{O_2O_1}} + \ddot{\overrightarrow{O_2O_1}}.\end{aligned} \tag{72}$$

where δ_j are defined such that

$$\frac{m_{G_j}}{m_{I_j}} = 1 + \delta_j \tag{73}$$

Taylor expanding the gravitational acceleration about the satellite's center of mass as

$$\vec{g}(O_k) = \vec{g}(O_{\rm sat}) + [\mathrm{T}]\overrightarrow{O_{\rm sat}O_k} + \ldots, \tag{74}$$

where [T] is the Earth gravity gradient (GGT), and assuming that $\delta_i \ll 1$, we get

$$(1+\delta_2)\vec{g}(O_2) - (1+\delta_1)\vec{g}(O_1) = \delta\vec{g}(O_{\rm sat}) + [T]\overrightarrow{O_1O_2}, \tag{75}$$

where $\delta \equiv \delta_1 - \delta_2$ approximates the Eötvös parameter.

Finally, we define the proof masses offcentering as $\vec{\Delta} \equiv \overrightarrow{O_1O_2}$, and the gravity differential acceleration is

$$\vec{\Gamma}^{(d)}_{\oplus} = \delta\vec{g}(O_{\rm sat}) + ([\mathrm{T}] - [\mathrm{In}])\vec{\Delta} - 2[\Omega]\dot{\vec{\Delta}} - \ddot{\vec{\Delta}}. \tag{76}$$

Injecting it in Eqs. (68)-(70), the measured differential acceleration is [289]

$$\begin{aligned}\vec{\Gamma}^{(d)}_{\rm meas} = [A_c]\left(\delta\vec{g} + ([\mathrm{T}] - [\mathrm{In}])\vec{\Delta} - 2[\Omega]\dot{\vec{\Delta}} - \ddot{\vec{\Delta}}\right) \\ + \vec{B}^{(d)}_0 + [A_d]\vec{\Gamma}^{(c)}_{\rm cont} + [C_d]\dot{\vec{\Omega}} + n^{(d)}\end{aligned} \tag{77}$$

where $[A_d]$ and $[A_c]$ are the differential-mode and common-mode sensitivity matrices (defined as combinations of the individual sensors' $[A_j]$ and $[\theta_j]$ matrices), $[C_d]$ is the differential-mode sensitivity matrix to the angular acceleration, $\vec{B}^{(d)}_0$ is the differential bias and we ignored the quadratic terms since they are estimated to be negligible in the actual MICROSCOPE data [289]. The common-mode control acceleration $\vec{\Gamma}^{(c)}_{\rm cont}$ contains all external accelerations (atmospheric drag, thrusters) and is canceled by the satellite's DFACS. Note that if the sensors' electronics were perfectly identical, we would have $[A_d] = 0$, and no drag-free would be required.

Per Eq. (77), it is clear that a WEP violation signal would multiply the Earth gravity acceleration; since it is modulated by the motion and attitude of the satellite, this signal would be at the $f_{\rm EP}$ frequency defined above. The fact that proof masses are not perfectly concentric ($\vec{\Delta} \neq \vec{0}$) implies a systematic error related to the Earth gravity gradient. As shown below, this signal can be efficiently estimated and subtracted, and the main limitation of the experiment lies in the instrumental noise.

5.3.2. Projected measurement equation MICROSCOPE sensors are most sensitive along their longitudinal (x-coordinate in the instrument's frame, see Fig. 5) axes. Consequently, the WEP is tested along this axis, and the primary measurement equation is the differential acceleration projected on it,

$$\begin{aligned}\Gamma^{(d)}_x = 2\tilde{b}^{(d)}_x + a_{c11}g_x\delta + a_{c12}g_y\delta + a_{c13}g_z\delta \\ + \Delta'_xS_{xx} + \Delta'_yS_{xy} + \Delta'_zS_{xz} \\ + \left(a_{c13}\Delta'_y + a_{c12}\Delta'_z\right)S_{yz} \\ + a_{c12}\Delta'_yS_{yy} + a_{c13}\Delta'_zS_{zz} \\ + \left(-a_{c13}\Delta'_y + a_{c12}\Delta'_z + 2c_{d11}\right)\dot{\Omega}_x \\ - \left(\Delta'_z - 2a_{c13}\Delta'_x - 2c_{d12}\right)\dot{\Omega}_y \\ + \left(\Delta'_y - 2a_{c12}\Delta'_x + 2c_{d13}\right)\dot{\Omega}_z \\ + 2\left(a_{d11}\tilde{\Gamma}^{(c)}_x + a_{d12}\tilde{\Gamma}^{(c)}_y + a_{d13}\tilde{\Gamma}^{(c)}_z\right) \\ + 2\dot{\Delta}'_x\Omega_x - 2\dot{\Delta}'_z\Omega_y + 2\dot{\Delta}'_y\Omega_z \\ - a_{c11}\ddot{\Delta}_x - a_{c12}\ddot{\Delta}_y - a_{c13}\ddot{\Delta}_z + 2n^{(d)}_x,\end{aligned} \tag{78}$$

where, as before, we neglected the quadratic factors, and where [T] is the Earth gravity gradient tensor (GGT) in the instrument's frame, [S] the symmetric part of the [T] − [In] matrix, and [Ω] the angular velocity tensor of the satellite. In Eq. (78), $\tilde{\vec{\Gamma}}^{(c)} = \vec{\Gamma}^{(c)} - \vec{n}^{(c)}$ is the noise-free common-mode measured acceleration, $[a_{d11}, a_{d12}, a_{d13}]$ and $[a_{c11}, a_{c12}, a_{c13}]$ are the first row of the differential-mode $[A_d]$ and common-mode sensitivity $[A_c]$ matrices, $[c_{d11}, c_{d12}, c_{d13}]$ is the first row of the differential-mode sensitivity matrix to the angular acceleration, $\tilde{b}^{(d)}_x = b^d_{0x} + a_{c11}b^{(d)}_{1x} + a_{c12}b^{(d)}_{1y} + a_{c13}b^{(d)}_{1z}$ (with $\vec{b_0}^{(d)}$ the differential electrostatic bias and $\vec{b_1}^{(d)}$ the difference of mechanical perturbations acting on the two proof masses).

Finally, note that the measurement is not directly sensitive to the actual offcenterings $\vec{\Delta}$, but to the

following combinations of instrumental parameters:

$$\Delta'_x \approx a_{c11}\Delta_x - a_{c12}\Delta_y - a_{c13}\Delta_z \quad (79)$$

$$\Delta'_y \approx a_{c11}\Delta_y + 2a_{c12}\Delta_x - a_{c23}\Delta_z \quad (80)$$

$$\Delta'_z \approx a_{c11}\Delta_z + 2a_{c13}\Delta_x + a_{c23}\Delta_y. \quad (81)$$

Only those "derived" offcenterings $\Delta_{x,y,z}$ can be estimated.

Most terms in the measurement equation can be controlled, either by design of the instrument, by model or by in-flight measurement (see below and Ref. [158]). Upon correcting for them, considering that proof masses are kept motionless during WEP measurements (so that the velocities $\dot{\Delta}_x$, $\dot{\Delta}_y$, $\dot{\Delta}_z$ and the accelerations $\ddot{\Delta}_x$, $\ddot{\Delta}_y$, $\ddot{\Delta}_z$ vanish), and considering that the spin rate of the satellite is constant ($\dot{\Omega}_i = 0$) the measurement equation (78) simplifies to

$$\Gamma^{(d)}_{x,\mathrm{corr}} = 2\tilde{b}'^{(d)}_x + a_{c11}g_x\delta + a_{c13}g_z\delta + \Delta'_x S_{xx} + \Delta'_z S_{xz} + 2n^{(d)}_x, \quad (82)$$

which is the core model fitted to the data after applying the calibration parameters: in addition to the Eötvös parameter, we also estimate the components Δ'_x and Δ'_z of the apparent offcentering.

5.3.3. Force budgets and systematic errors

Earth gravity The Earth gravity and its gradient tensor projected on the instrument frame are computed following Ref. [290], using the ITSG-Grace2014 gravity potential model [291] expanded up to spherical harmonic degree and order 50. This computation requires the position of the satellite along its orbit (in the J2000 frame) and its attitude; CNES provides them as shown in [154]. The strong line at $2f_{\mathrm{EP}}$ visible on Fig. 9 is due to the coupling of the proof masses' off-centering $\vec{\Delta}$ with the Earth gravity gradient. Measuring this line allows for an estimation of $\vec{\Delta}$, given the gravity field model [291].

Electrostatic force The electrostatic force is discussed at length in Ref. [153] and given by Eq. (63) above.

The sensitivity and stiffness coefficients depend on the geometry of the proof mass and of the electrodes, and on the electric configuration (voltages applied to the different parts of the sensor). In particular, the electrostatic stiffness along the x-axis is expected to be zero for all sensors.

Gold wire The electric charge on proof masses is controlled via a gold wire linking them to the satellite. The wire can be modelled as a spring acting on the proof mass with the force

$$\overrightarrow{F_w} = -k_w[1 + \mathrm{i}\phi(f)]\vec{x} - \lambda_w\dot{\vec{x}}, \quad (83)$$

where k_w is the wire's stiffness and $\phi(f)$ describes the internal damping; note that ϕ can depend on the frequency. The wire's quality factor $Q = 1/\phi$.

Radiation pressure The electrode-bearing cylinders, being at temperature T, emit thermal radiation through photons that eventually hit the proof mass and transfer their impulsion to it, thus creating a pressure. A difference of temperature ΔT between the electrodes surrounding the proof mass will therefore cause a force directed from the hottest to the coldest region [292, 293]:

$$\vec{F}_p = \frac{16}{3c}S\sigma\Delta T T^3\vec{e}, \quad (84)$$

where T is the average temperature, c the speed of light, σ the Stefan-Boltzmann constant, S the surface of the proof mass, and $\vec{e}$ is the vector directed from the hottest to the coldest region.

Radiometer effect Taking its name from Crookes' radiometer, originally thought to prove the photon pressure, the radiometer effect is actually a residual gas effect affecting proof masses in rarefied atmospheres whose mean free path exceed the size of the container. In this case, equilibrium conditions do not happen when the pressure is uniform, but when the ratios of pressure to square root of temperature equal one another [292, 293].

This entails a force on the proof mass proportional to the temperature gradient about its faces ΔT,

$$\vec{F}_r = \frac{1}{2}PS\frac{\Delta T}{T}\vec{e}, \quad (85)$$

where P is the pressure in the container, S the surface of the proof mass orthogonal to the temperature gradient, T the average temperature in the container, and $\vec{e}$ is still the vector directed from the hottest to the coldest region.

Lorentz force and eddy currents Using numerical models of the satellite structure (including its magnetic shield) and of the Earth magnetic field, it was shown that magnetic effects due to the interaction of the proof masses with the Earth magnetic field were well below the requirements [157].

Overall expected performance All the forces introduced above can affect the test of the WEP. The slight offcentering of the proof masses induces a non-zero gravity gradient which, although dominant at $2f_{\mathrm{EP}}$, has a small contribution at f_{EP}. However, it is easily subtracted by measuring the $2f_{\mathrm{EP}}$ line as aforementioned.

Of primary importance are those linked to thermal fluctuations. For instance, from Eqs. (84)-(85), in presence of stochastic temperature fluctuations, the radiation pressure and radiometer effect impart acceleration noises with spectral density

$$\sqrt{S_p} = \frac{16}{3c}\frac{S\sigma}{m}T^3\sqrt{S_{\Delta T}} \quad (86)$$

$$\sqrt{S_r} = \frac{1}{2}\frac{PS}{mT}\sqrt{S_{\Delta T}}, \quad (87)$$

where m is the mass of the proof mass and $S_{\Delta T}$ is the power spectral density of temperature fluctuations. Controlling those noises is made possible by protecting the instrument in a thermal shield and by stabilising the external temperature with a Sun-synchronous orbit (see below).

The thermal dissipation of the gold wire is the dominant source of noise at low frequency. According to the dissipation-fluctuation theorem [294], because of thermal fluctuation, the internal damping of the wire is at the origin of the f^{-1} low-frequency noise that limits MICROSCOPE's test of the WEP [148], as shown in Fig. 8. This acceleration noise reads [294, 295]

$$\Gamma_{n,w}(f) = \frac{1}{m}\sqrt{\frac{4k_BT}{2\pi}\frac{k_w}{Q(f)}}f^{-1/2}\ \mathrm{ms}^{-2}/\sqrt{\mathrm{Hz}}, \quad (88)$$

where k_B is the Boltzmann constant.

Finally, the detector read-out electronics causes a noise in position specified to $S_{\mathrm{det}} = 10^{-11}\ \mathrm{mHz}^{-1/2}$. By double integration, this noise corresponds to an acceleration noise

$$\sqrt{S_{\mathrm{ro}}} \propto (2\pi f)^2\sqrt{S_{\mathrm{det}}}. \quad (89)$$

Although largely dominant at high frequency, this noise marginally affects the f_{EP} frequency.

Fig. 8 shows the performance of the four MICROSCOPE sensors expected before launch [296].

5.4. Mission

This section briefly introduces the mission scenario drivers and the typology of measurement sessions (a session being defined by an uninterrupted period focused on a well-defined task). A detailed discussion of the mission scenario and its drivers can be found in Ref. [155].

5.4.1. Mission scenario drivers The MICROSCOPE mission was designed for a nominal year of operation, with an optional second year, with the amount of gas as the main driver of the mission's duration (which eventually lasted 2.5 years).

The 7090 km semi-major axis of MICROSCOPE's orbit was chosen as a trade-off to maximise the Earth gravitation signal and minimise the atmospheric drag. Furthermore, the requirements on thermal stability imposed a Sun-synchronous (nearly polar) orbit, in which the satellite-Sun angle remains constant. However, such an orbit inevitably entails eclipse periods, when the satellite crosses the umbra of the Earth when flying over the night pole. MICROSCOPE's eclipse periods lasted three months about the summer solstice, making the satellite unavailable for science measurements.

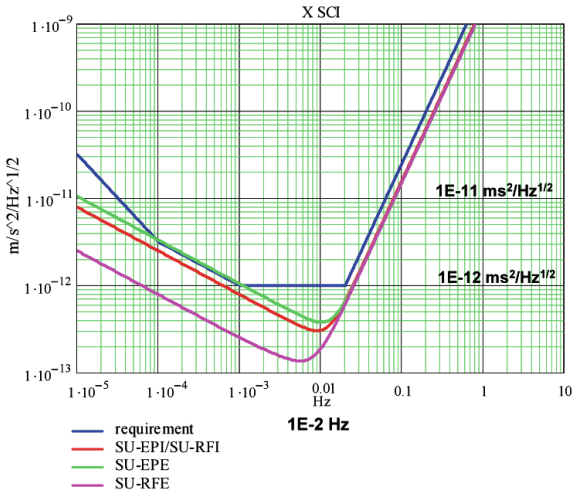

Figure 8. Performance expected before launch, for the four sensors. Also shown is the requirement for a 10^{-15} precision on the test of the WEP. Figure from Ref. [296].

Out of eclipse periods, MICROSCOPE had to stop science operations during 4 days at every lunar cycle in order to avoid Moon flares in the star trackers by depointing the satellite such that they look at outer space. This operation induced thermal variations impinging on the science performances.

The duration of each session was set according to its goal: five orbits for calibration sessions and at least 20 orbits for WEP measurement sessions. However, due to operational reasons, the duration of sessions was limited to 120 orbits.

The scenario was managed by the ground segment and was built on the basis of successive elementary sessions. They were programmed on board for a 15-day period and updated every week.

5.4.2. Measurement sessions WEP-measurement sessions were designed to each allow for a 10^{-15} precision on the Eötvös parameter. Spinning the satellite at different frequencies f_{spin} allowed for the modulation of the WEP signal frequency $f_{\mathrm{EP}} = f_{\mathrm{orb}} + f_{\mathrm{spin}}$. Given the frequency-dependent PSD of the expected noise (Fig. 8), we could modulate the duration of measurement sessions based on f_{spin}: the higher f_{spin} (up to $f_{\mathrm{EP}} \approx 8$ mHz), the lower the noise, so the shorter the required session duration. From that point of view, inertial ses-

Table 1. Spinning science sessions. The orbital frequency $f_{\rm orb} = 1.6818 \times 10^{-4}$Hz.

	Spinning rate $f_{\rm spin}$ [mHz]	WEP frequency $f_{\rm EP}$ [mHz]	Duration [orbits]
$\rm EPR_{V1}$	$\frac{7}{2}f_{\rm orb}$=0.58863	0.75681	20
$\rm EPR_{V2}$	$\frac{9}{2}f_{\rm orb}$=0.75681	0.92499	20–120
$\rm EPR_{V3}$	$\frac{35}{2}f_{\rm orb}$=2.94315	3.11133	20–120

sions ($f_{\rm spin} = 0$ Hz) needed to last 120 orbit, whereas spinning sessions had to last at least 20 orbits. Table 1 defines the three spinning configurations used during the mission. The first one ($\rm EPR_{V1}$) was used only during the commissioning phase. The second one was the nominal spinning frequency, but was replaced by the faster spinning third one ($\rm EPR_{V3}$) after the measurement noise was found higher than expected during commissioning. Those spinning rates were chosen as non-integer rational fractions of the orbital frequency to minimise the projection of systematic effects on the $f_{\rm EP}$ frequency [297].

Short, 5-orbit calibration sessions were used to estimate those parameters of Eq. (78) that could be measured in-flight. Each of these sessions was dedicated to estimating one (or two) parameters and designed so that the signals sourced by those parameters have a favourable signal-to-noise ratio [298]. In particular, we could shake either the proof masses or the satellite, as well as oscillate the satellite, at specific frequencies to excite a signal at a given frequency. Measuring the corresponding spectral line allowed for an estimate of the concerned parameter.

5.4.3. Technical sessions Technical sessions were performed mainly when the satellite could not be used for science (i.e. in eclipse periods) and at the end of the mission. They consisted in characterising the instrument [156, 157] and the satellite [154], and to maintenance operations. The last six months of the mission were used for aeronomy experiments.

5.4.4. Mission history The MICROSCOPE satellite was launched on April 25, 2016, just before an eclipse period during which the commissioning of the satellite and of the payload were performed [149, 156, 299].

A capacitance failure on SUREF impacted the mission in May 2016. This failure was linked to a voltage housekeeping and had no visible impact on the measurement. Nevertheless, it increased the power consumption by 2W in the FEEU, and thus also the operating temperature. It quickly appeared that this capacitance reference had a defect and that other electronic components could be potentially affected. Therefore, in order to minimise the risk of another failure, the mission scenario was constrained (i) to reduce the temperature of operation, by switching on only one SU at a time, as the risk increases with temperature, (ii) to switch off both SU when acceleration measurement were not needed for science, as the risk of new failures increased with time of operation and (iii) to put a high-priority on SUEP's WEP measurement. Fortunately, SUEP was much more robust than SUREF. Therefore, this failure had no impact on the test of the WEP; nevertheless, they prevented gradiometry measurements, which were planed as a secondary goal of the mission [300].

The commissioning phase ended in November 2016, followed by a first phase of WEP measurement until May 2017, when the next eclipse period started. The payload was switched off from May 2017 to August 2017. Then a second phase of WEP tests lasted from September 2017 to February 2018, when technical sessions started. In particular, data was collected for aeronomy studies [301].

The satellite was finally decommissioned on October 16, 2018, after 13,193 orbits around the Earth, 21% of which were actually used to perform the science experiment (others were occupied either by technical and satellite maintenance sessions, or were not usable because during eclipses and Moon flare periods). The Innovative DEorbiting Aerobrake System (IDEAS) was deployed, and MICROSCOPE's altitude is now slowly decreasing for its final plunge in the Earth atmosphere expected within 25 years.

5.5. Data analysis

MICROSCOPE's science data consist in proof masses' accelerations and positions time series, accompanied with house-keeping data (temperatures, voltages, electronics flags). The primary data is the acceleration measured along the x-axis of the proof masses (Eq. 78). The data analysis then consists in correcting it from –calibrated– instrumental defects and from the deterministic signals due to the imperfect shape of the Earth, before seeking a signal (collinear with the Earth gravity acceleration) amounting to a violation of the WEP.

5.5.1. Iterative least-square estimation Each in-flight calibration session is dedicated to estimating one (or two) parameters and designed to maximising their corresponding signals. Although it is theoretically possible to estimate all parameters simultaneously from all calibration sessions using Eq. (78) – as showed by an unpublished study, based on Ref. [302], which used a Markov Chain Monte Carlo (MCMC) technique on nine sessions of the data of Ref. [148] –, we use the fact that they are almost independent from each

other to simplify and better control the estimation process via an alternative method: we estimate each parameter iteratively, refining and updating the estimation of a given parameter using the estimation of the other parameters until some convergence criterium is reached.

The measurement equation (78) is of the form $\Gamma_x^{(d)} = f(p_k, t) + n_x^{(d)}$, where p_k are parameters and the time dependence is linked to measured or modeled signals $s_i(t)$. For each session, the data provides us with $\Gamma_x^{(d)}$ and all $s_i(t)$. It is then possible to perform a least-square (or similar) fit to estimate the parameters p_k from a given model.

Moreover, for a given calibration session, we have a priori values $p_{k,0}$ for the parameters p_k, as some of them have been measured on ground, and others have been estimated during previous in-flight calibration sessions. It is then possible to subtract the corresponding signals from the measurement, and use an updated version of the measurement equation,

$$\Gamma_{x,\mathrm{corr}}^{(d)}(t) = \Gamma_x^{(d)}(t) - f(p_{k,0}, t). \tag{90}$$

This equation can finally be used to refine the estimation of some parameters p_{ke}, with a least-square method using the model

$$\Gamma_{x,\mathrm{corr}}^{(d)}(t) = \Sigma_{ke} \frac{\partial f(p_k, t)}{\partial p_{ke}} \left(p_{ke} - p_{ke,0}\right). \tag{91}$$

We use ADAM, an iterative least-square technique, to estimate parameters in the frequency domain [158]. Once this iterative process has converged (typically in two to three iterations), we use Eq. (82) to measure the Eötvös parameter δ on calibrated data.

This method has been shown to provide precise and accurate on intensive numerical simulations [158].

5.5.2. Missing and invalid data Data gaps come in two flavours: (i) telemetry losses, where data is missing during some time intervals, and (ii) glitches, where data is available but contaminated by physical (e.g. impact with a micrometeorite or a satellite crack) or measurement (e.g. an internal saturation in the instrument's servo-loop command) processes uncorrelated with testing the WEP.

Glitches have been shown to be periodic and create a spurious signal at the f_{EP} frequency, potentially biasing the WEP measurement [159]. To counteract their effect, we can model and subtract them as discussed in Ref. [303]; nevertheless, we choose to remove them, hence giving them the same status as telemetry losses ("missing" data). We use a standard recursive σ-clipping technique to detect glitches [159]. We then mask a specific time interval (a dozen seconds) after each detected outlier to make sure that the transient regime is always removed.

Additional data points are flagged by the instrument's electronics, if an internal saturation has been detected by the accelerometer digital electronics (and eventually smoothed out, thereby invisible in the acceleration data [153]): we reject those points.

Missing data break the even sampling of data in time, thereby preventing us from using a standard ordinary least-squares technique in the frequency domain and, most critically, creating an important spectral leakage due to noise colour, potentially burrying the WEP signal in MICROSCOPE data [304, 305]. We can nevertheless reach the required accuracy on the measurement thanks to one of the following methods: (i) the Kalman Auto-Regressive Model Analysis (KARMA [304]) is a generalised least-square technique based on an autoregressive model of the (unknown) instrumental noise, whitened with a Kalman filter; (ii) M-ECM (Modified-Expectation-Conditional-Maximization [306]) allows us to maximise the likelihood of available data through the estimation of missing data by their conditional expectation, based on the circulant approximation of the complete data covariance; (iii) the *inpainting* [305, 307] technique, originally developed for 2D observational cosmology [308] and 1D asteroseismology [309], uses a sparsity prior to estimate the most probable value of missing data, therefore allowing us to use an ordinary least-squares fit. Those techniques were successfully tested on numerical simulations, either idealised [304–307] or realistic [158], and used on real data [149, 159].

Beside glitches, a handful of jumps can be spotted in the differential acceleration, mostly on SUREF [151]. They are not simple discontinuities, but appear as unsteady transitions between two stable states. Although hidden in the noise, they perturb the data analysis and must be discarded. Since this amounts to creating gaps of several hundred seconds, we decided, in the presence of jumps, to extract "segments" between them (or between them and any extremity of the session). Segments are as long as possible and consist of an even number of orbital periods to ensure that potential contamination by signals at frequencies $mf_{\mathrm{orb}} + nf_{\mathrm{spin}}$ $(m, n \in \mathbb{N})$ are cancelled [151].

6. MICROSCOPE science results and return

6.1. A new upper bound on the WEP

Fig. 9 shows the spectral density of the differential acceleration measured by SUEP during a 120-orbit session. Arrows highlight the absence of line at the f_{EP} frequency and the strong line at $2f_{\mathrm{EP}}$ caused by the coupling of the Earth gravity gradient with the proof masses off-centering. The red line is a power law fit to the spectral density, showing that the noise varies as f^2 at high frequency and as $f^{-1/2}$ at low frequency,

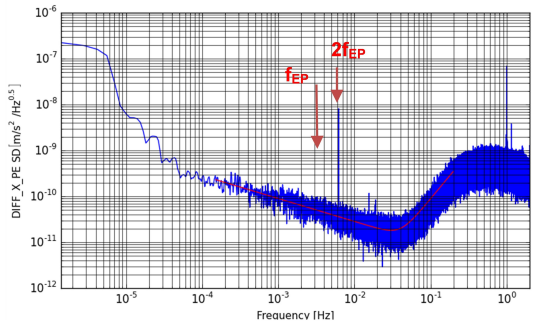

Figure 9. Square root of SUEP's measured PSD of the differential acceleration along the X axis during a 120-orbit scientific session 218 with SUEP, where $f_{\rm EP} = 3.1113 \times 10{-}3$ Hz. The red line is a power law fit to the spectral density. Figure from Ref. [148].

as expected.

Fig. 10 shows the estimates of the Eötvös parameter for each segment, obtained with M-ECM (blue circles) and ADAM (gaps being filled beforehand – orange diamonds). The two methods are perfectly consistent. Error bars vary in accordance with the duration of segments and with the spin rate: the higher the spin rate, the lower the error bars, since the noise is minimal for the highest spin rate, see Ref. [151]. The black lines and grey areas show the combined constraints and their 68% confidence region [151,158]. Those uncertainties contain statistical errors only. Systematic errors are discussed below.

The overall systematics upper bound, of 2.3×10^{-15} for SUREF and 1.5×10^{-15} for SUEP (compared to specifications of 0.2×10^{-15} [157]), is dominated by thermal effects. Indeed, we found that all other contributors (except non-linearity [156]) have effects lower than required. For instance, the contribution of the Earth gravity gradient could be cancelled by the precise estimation of the proof masses offcenterings, while local gravity effects were mitigated by a careful design of the satellite and of the instrument [157]. Similarly, thanks to magnetic shield around the payload, magnetic effects due to the interaction of the proof masses with the Earth magnetic field were well below the requirements [157]. The DFACS performance allowed for a residual linear accelerations at $f_{\rm EP}$ smaller than 2×10^{-13} ms^{-2} (resp. 6×10^{-14} ms^{-2}) in (resp. out of) the orbital plane, and for residual angular accelerations smaller than 2.5×10^{-11} rad s^{-2}, much better than expected, with related systematic errors well below specifications.

Temperature variations are the main source of systematic errors. They induce a differential acceleration through a thermal sensitivity of the SU and of the FEEU (Front End Electronics Unit). Specific sessions were designed to characterize the thermal sensitivity through a periodic stimulus by on-

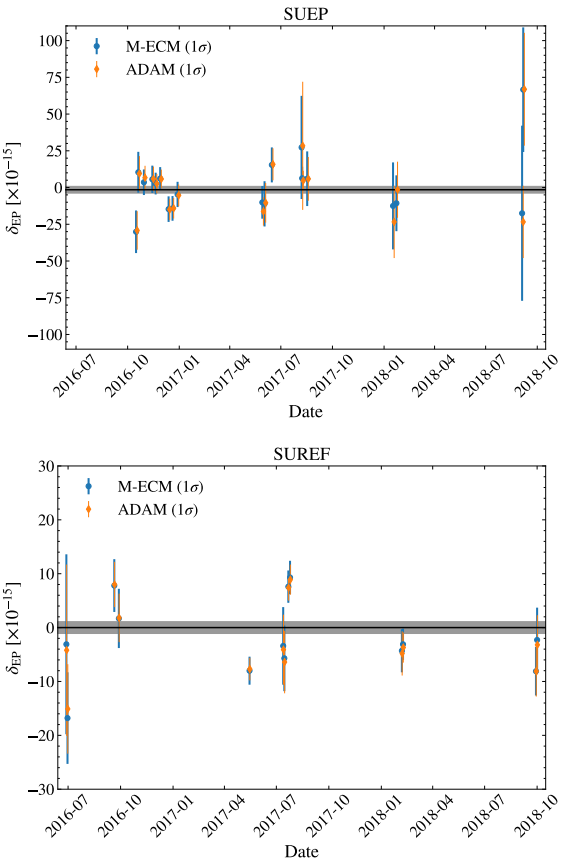

Figure 10. Eötvös parameter estimates for each segment and overall estimate and its 68% confidence region (black line and grey area). Blue circles show M-ECM's estimates and orange ones ADAM's. Upper panel: SUEP. Lower panel: SUREF. Panels span the same time.

board heaters; a fine monitoring of temperature and differential accelerations provided good estimates of the thermal sensitivities at different frequencies [157, 310]. We noticed a linear frequency-dependence for SUEP's thermal sensitivities, but none for SUREF's.

On the other hand, the temperature data during EP sessions only allowed for a pessimistic upper bound since the temperature variations were smaller than the temperature probe's noise at $f_{\rm EP}$. In response to this limitation, additional sessions were devoted to confirm the thermal design of the satellite. It was possible to show that temperature variations are driven by the Earth's albedo coming through the FEEU radiator's baffle (Fig. 15 of Ref. [157]), inducing a modulation of the temperature at $f_{\rm EP}$ [157]. A first session, based on heating the FEEU panel with local heaters, showed that the impact of the Earth's albedo on the satellite walls is negligible. In a second session, the satellite was tilted by 30° about its spin axis in inertial mode during 465 orbits (32.3 days) in order to maximize the albedo light entering the FEEU radiator. Temperature

variations were found to be attenuated by a factor 500 between the FEEU and the SU. Based on the data available (at frequencies lower than 10^{-3} Hz), this factor 500 was taken as the lowest limit to compute an upper bound of temperature fluctuations at frequencies higher than 10^{-3} Hz, in particular at $f_{\rm EP}$, where temperature probes allow for a measurement of the FEEU temperature variations but not of the SU's, since it is below the probe's noise [157].

All in all, MICROSCOPE's new constraint on the validity of the WEP is

$$\eta(\mathrm{Ti},\mathrm{Pt}) = [-1.5 \pm 2.3\ (\mathrm{stat}) \pm 1.5\ (\mathrm{syst})] \times 10^{-15}, \tag{92}$$

where the statistical error is given at 1σ, and the measured, approximated Eötvös ratio δ is identified with the exact one η. This result is close to the 10^{-15} precision for which the mission was designed.

The reference instrument provided a null result, $\eta(\mathrm{Pt},\mathrm{Pt}) = [0.0 \pm 1.1\ (\mathrm{stat}) \pm 2.3\ (\mathrm{syst})] \times 10^{-15}$, showing no sign of unaccounted systematic errors in Eq. (92). As expected from its higher sensitivity, SUREF's result has a smaller statistical error than SUEP's. On the opposite, its systematic errors, as dominated by thermal effects, are higher since they were estimated with less optimal sessions than SUEP's ones [157].

6.2. Modified gravity: Yukawa potential

For two proof masses in the field of the Earth E, the Eötvös parameter reduces to (Sect. 3.2)

$$\eta = \frac{(\alpha_i - \alpha_j)\alpha_E}{1 + \frac{1}{2}(\alpha_i + \alpha_j)\alpha_E} \simeq (\alpha_i - \alpha_j)\alpha_E, \tag{93}$$

where α_i and α_j are the proof masses' coupling constants, and α_E is that of the Earth.

6.2.1. Light Yukawa field We first consider constraints on composition-dependent Yukawa interactions available from MICROSCOPE's test of the WEP. As we show below, only light enough Yukawa potentials can be probed via this test (their range must be larger than the radius of the Earth). Here, we assume that the Yukawa charge $q = B$ (the baryon number). This section updates the constraints of Ref. [197] (a similar improvement between the upper limits shown here and in Ref. [197] exists when the charge is taken to be the lepton number).

For MICROSCOPE, the Eötvös parameter due to a Yukawa potential is

$$\eta = \alpha \left[\left(\frac{q}{\mu}\right)_{\rm Pt} - \left(\frac{q}{\mu}\right)_{\rm Ti} \right] \left(\frac{q}{\mu}\right)_E \left(1 + \frac{r}{\lambda}\right) \mathrm{e}^{-\frac{r}{\lambda}} \tag{94}$$

where $r = R_E + h$ is the mean distance from the satellite to the center of the Earth, with $h \approx 710$ km its mean altitude and R_E is the Earth mean radius. The Earth charge takes into account the Earth differentiation between core and mantle as well as the spherical shape of the Earth through the function [48]

$$\Phi(x) \equiv 3(x\cosh x - \sinh x)/x^3 \tag{95}$$

which describes the fact that all Earth elements do not contribute similarly to the Yukawa interaction at the satellite's altitude. This function has the form (95) only for perfect spheres: the Earth's asphericity is ignored in this analysis, but should be accounted for (see Ref. [140] for more general shape functions). Furthermore, since the size of the proof masses is much smaller than the ranges λ that can be probed in orbit, they are considered point-like, so that their $\Phi = 1$. Finally, it is assumed that the core of the Earth is composed of iron and that the mantle is composed of silica (SiO_2) [203]. The baryonic charge for the MICROSCOPE experiment is summarised in Table 2.

Table 2. Baryonic and dilaton charges for MICROSCOPE's proof masses.

Material	B/μ	$Q'_{\tilde{m}}$	Q'_e
Pt/Rh	1.00026	0.0859	0.0038
Ti/Al/V	1.00105	0.0826	0.0019

By adding statistical and systematic errors, MICROSCOPE's 2σ level constraints on the Eötvös parameter derive trivially from Eq. (92), and can readily be transformed into constraints on Yukawa's (α, λ). Fig 11 shows the corresponding exclusion regions for $q = B$. MICROSCOPE's constraints are compared to the bounds from Eöt-Wash's torsion pendulum experiments [54, 58, 311] and to the constraints from the Lunar-Laser Ranging experiment [50, 312]. This shows that MICROSCOPE allows for almost a two-orders-of-magnitude improvement compared to previous analyses for $\lambda >$ a few 10^5m.

As MICROSCOPE orbits Earth at about 7000 km from its center, one would naively expect that it can only probe interactions with $\lambda >$ a few 10^6m; smaller ranges could not be probed as they imply too much of a damping at MICROSCOPE's altitude. However, would a fifth force with $\lambda \approx$ a few 10^5m be strong enough to affect MICROSCOPE, the contribution from the nearest point to the Earth (as seen from MICROSCOPE) would be higher than that of the farthest point of the Earth, implying an asymmetric behavior that can be probed by MICROSCOPE (as captured by the function $\Phi(x)$ above). Hence, by testing the WEP with the Earth as the source of the gravity field, MICROSCOPE is sensitive to scalar interactions with ranges as low as a few hundreds of kilometers.

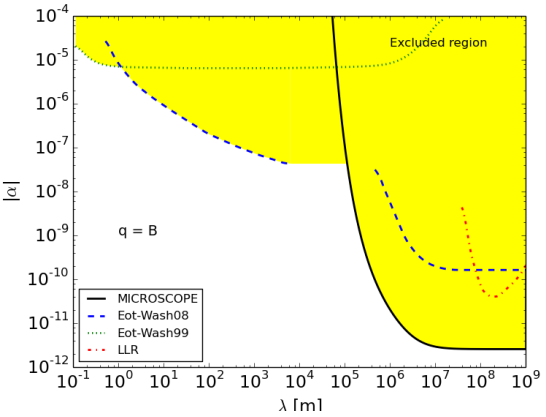

Figure 11. Constraints on the Yukawa potential parameters (α, λ) with $q = B$. The excluded region is shown in yellow and compared to earlier constraints from Ref. [311] (dotted), Ref. [54] (dashed) and Refs. [50, 312] (dot-dashed).

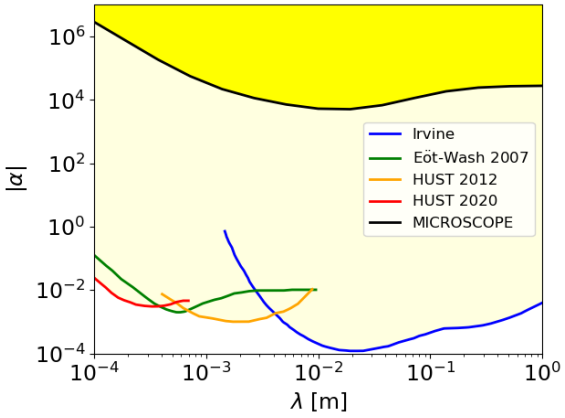

Figure 12. 95% confidence contour for a Yukawa potential. The light grey area shows the excluded region by various experiments: Irvine [39], Eöt-Wash 2007 [52], HUST 2012 [313], HUST 2020 [314], and the yellow area shows the region excluded by MICROSCOPE [160]. Figure from Ref. [160].

6.2.2. Centimetric Yukawa interaction During WEP-measurement sessions, MICROSCOPE's proof masses are controlled to be motionless. They are therefore insensitive to the local gravity from the instrument and the satellite (up to a negligible level at $f_{\rm EP}$). This is not true anymore during instrument's characterisation sessions. In particular, they are submitted to a sinusoidal excitation in position to estimate the sensors' stiffness. The stiffness is expected to be dominated by the electrostatic stiffness (2nd term of the r.h.s of Eq. 63), but other contributors exist, such as the gold wires and local gravity.

Ref. [160] used stiffness-measurement sessions to infer constraints on short-range (centimetric) composition-independent Yukawa interactions arising from the interaction between the proof masses and the electrode-carrying cylinders. They found unaccounted for patch effects, while uncertainties are largely dominated by gold wires.

Fig. 12 shows the corresponding 95% upper bound on the Yukawa potential. The curves in the lower part of the figure show the current best upper bounds on a Yukawa potential, inferred from dedicated torsion balance experiments [39, 52, 313, 314]. MICROSCOPE's constraints are clearly poor compared to the state of the art. It would have been surprising otherwise, since MICROSCOPE was not designed to look for short-range deviations from Newtonian gravity. However, those results show that thanks to its non-trivial geometry, an experiment looking like MICROSCOPE, if highly optimised, may allow for new constraints of gravity through the measurement of the short-range interaction between several bodies.

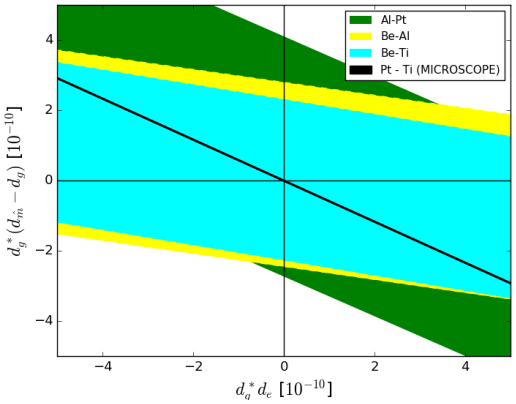

Figure 13. Constraints on the couplings of a massless dilaton $(D_{\tilde{m}}, D_e)$. The region allowed by the MICROSCOPE measurement (black band) is compared to earlier constraints by torsion pendulum experiments from Ref. [230] (green) and Ref. [58] (yellow, cyan). The difference of slopes arises from the difference of material used in these 3 experiments. MICROSCOPE allows us to shrink the allowed region by one order of magnitude.

6.3. Dilaton models

We now consider the characteristics of a generic dilaton with couplings described in Sect. 3.3.3 and update the results of Ref. [197].

6.3.1. Massless dilaton The coupling to matter of a massless dilaton ($m_\phi = 0$, whose range λ_ϕ is infinite) and hence the related fifth force, is parametrised by the five numbers $(d_g, d_e, d_{\tilde{m}}, d_{\delta m}, d_{m_e})$ and is rigourously defined by Eq. (32). Nevertheless, given the current experimental precision, it can be approximated as (note that for consistency with the previous paragraph,

we rename the coupling factor) [203, 204]

$$\alpha_i \approx d_g^* + \left[(d_{\tilde{m}} - d_g)\, Q'_{\tilde{m}} + d_e Q'_e\right]_i , \qquad (96)$$

with

$$d_g^* = d_g + 0.093(d_{\hat{m}} - d_g) + 0.00027 d_e, \qquad (97)$$

and where the "approximate" dilaton charges

$$Q'_{\hat{m}} = -\frac{0.036}{A^{1/3}} - 1.4 \times 10^{-4} \frac{Z(Z-1)}{A^{4/3}} \qquad (98)$$

and

$$Q'_e = 7.7 \times 10^{-4} \frac{Z(Z-1)}{A^{4/3}}. \qquad (99)$$

As recalled in Sect. 3.3.3, they depend on the chemical composition of the proof masses and on the local value of the dilaton. In the limit where λ_ϕ is much larger than any other spatial scales, the Eötvös parameter reduces to Eq. (93) so that (at first order in dilaton charges Q'_j –given that $|Q'_j| \ll 1$)

$$\eta_0 = D_{\tilde{m}} \left([Q'_{\tilde{m}}]_{\rm Pt} - [Q'_{\tilde{m}}]_{\rm Ti}\right) + D_e \left([Q'_e]_{\rm Pt} - [Q'_e]_{\rm Ti}\right), \qquad (100)$$

where the coefficients $D_{\tilde{m}} = d_g^*(d_{\tilde{m}} - d_g)$ and $D_e = d_g^* d_e$ are to be estimated. The charges $Q'_{\tilde{m}}$ and Q'_e corresponding to MICROSCOPE's proof masses are given in Table 2.

Fig. 13 summarises MICROSCOPE's constraints obtained from Eq. (92) and compares them to the earlier ones from the Eöt-Wash [58] and the Moscow groups [230]. The different slopes of the allowed regions are due to the different pairs of materials used by each experiment. MICROSCOPE's significant improvement is due to optimising the composition of its proof masses for the dilaton search [203, 204].

6.3.2. Massive dilaton Similarly to a Yukawa potential, the mass of the dilaton modifies the range of its interaction so that Eq. (100) is modified as

$$\eta = \eta_0 \Phi \left(\frac{R_E}{\lambda_\phi}\right)\left(1 + \frac{r}{\lambda_\phi}\right) \mathrm{e}^{-r/\lambda_\phi}. \qquad (101)$$

This equation is simpler than Eq. (94) because Eq. (100) does not depend on the Earth dilaton charge, and it is therefore independent of the exact Earth model used.

To draw constraints on the dilaton's mass, we assumed in Ref. [197] that the dilaton field couples only to the electromagnetic field, i.e. the only non-vanishing coupling is d_e. The coupling to proton and neutron is then induced from their binding energy [315]. A number of groups set constraints on the couplings of such a dilaton from the fine structure constant oscillations in atomic and molecular frequency comparisons [206, 207, 316–323] based on the time evolution of the scalar field that oscillates within its self-potential. Fig. 14 shows a summary of the current constraints on the coupling constant d_e of a dilaton-like ultra-light dark matter with photons, as a function of mass, obtained from WEP tests (Eöt-Wash [58], MICROSCOPE and the planned STE-QUEST mission [324]) and from atomic sensors [317–319,325–328]. The complementarity between experiments is obvious to probe a wide range of masses.

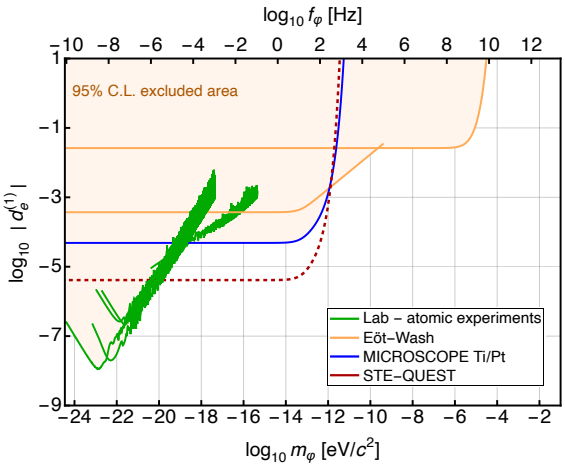

Figure 14. Constraints on the coupling constant d_e of a dilaton-like ultra-light dark matter with photons, obtained from WEP tests (Eöt-Wash [58], MICROSCOPE and the planned STE-QUEST mission [324]) and from atomic sensors [317–319, 325–328]. Figure adapted from Ref. [324] by A. Hees.

6.3.3. Runaway dilaton Ref. [173] combined the MICROSCOPE bound on the WEP with type Ia supernovae data [329], Hubble parameter measurements [330] and astrophysical measurements of the fine structure constant [331–333] to constrain the evolution and coupling constants of the runaway dilaton. They showed that the MICROSCOPE constraint (with the Eötvös parameter proportional to the coupling constant of the runaway dilaton with baryons) helps to break a critical degeneracy between model parameters, thus leading to significantly improved constraints compared to previous studies [334]. They concluded that current data already exclude couplings between the runaway dilaton and the dark sector of order unity, which would be their natural value. Consequently, any allowed runaway dilaton scenario should be, in terms of background cosmology, very similar to the standard ΛCDM model.

6.4. Modified gravity: chameleon field

6.4.1. Chameleon, WEP and MICROSCOPE We discussed in Sect. 3.4 how a chameleon field can, through the thin-shell effect, cause a WEP violation even between proof masses of the same composition. Following Eq. (54), the Eötvös parameter for a pair of spherical bodies in the field of the Earth is

$$\eta = 6\beta^2 Q_\oplus (Q_1 - Q_2), \tag{102}$$

where $Q_\oplus$ is Earth's thin-shell parameter.

Assuming first that Eq. (102) applies to MICROSCOPE's cylindrical proof masses, it is easy to see that unless they are unscreened (in which case $Q_1 = Q_2 = 1$), a WEP violation can be triggered by the chameleon in the field of the Earth. In particular, this is true for the reference sensor (SUREF), the proof masses of which have same composition but different mass, and thence different thin-shell parameter. Therefore, measuring a non-zero Eötvös parameter on SUREF would not necessarily have been the sign of an instrumental systematics, but might have been a putative chameleon-induced WEP violation.

However, given the chameleon's non-linear behaviour, it is necessary to thoroughly take into account the geometry of the experiment before drawing conclusions from the measured Eötvös parameters. Ref. [335] set up to do that. Since no analytic thin-shell parameter exists for cylindric objects, Eq. (102) is not applicable to MICROSCOPE. Thus, a numerical method was devised to compute the profile of the chameleon inside a cylindrical cavity (which can be taken to be made of MICROSCOPE's electrode-bearing cylinders), given the value of the exterior chameleon field at infinity. Computing this profile is the first step towards evaluating the force imparted by the exterior chameleon on the proof masses as it goes through the satellite. The key point is indeed that the chameleon can go through the satellite, i.e. that the satellite is not itself screened. If the satellite is screened, it acts as a cavity and protects the proof masses from the exterior field, i.e. the very field that the experiment aims to measure.

In Refs. [335], the Compton wavelength $\lambda_{c,\mathrm{shield}}(\beta, n, \Lambda)$ of the chameleon in the invar shield surrounding MICROSCOPE sensors was used as a criterion to quantify the instrument's screening: if it is less than 1% of the shield's thickness e_{shield}, the experiment is declared screened, it is partially screened if $\lambda_c < e_{\mathrm{shield}}$ and unscreened otherwise (which does not mean, however, that the value of the chameleon inside the proof masses is equal to that of the exterior environment, such that it varies, even slightly, from one proof mass to another). Using this screening criterion, Fig. 15 shows that the chameleon (Λ, β) parameter space (for $n = 1$) is divided into two regions: above the black line (which shows where $100\lambda_{c,\mathrm{shield}} < 0.5 e_{\mathrm{shield}}$) MICROSCOPE is not screened, but it is screened below the line. Thus, no violation of the weak equivalence principle can be expected below the line, while it could still be expected above it. The coloured regions in Fig. 15 correspond to regions that have already been experimentally excluded [212]. It is then clear that the constraining potential of MICROSCOPE's test of the WEP is much less than originally anticipated in Ref. [34], where the screening of the satellite was not taken into account, but proof masses were assumed to be freely-floating in space. MICROSCOPE is then expected to only improve our current knowledge about the chameleon in a small region. This is work in progress.

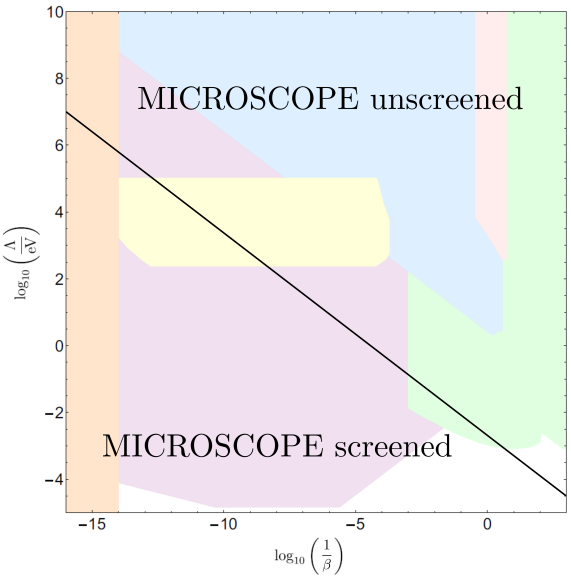

Figure 15. Chameleon's parameter space adapted from Refs. [212, 336]. The black line corresponds to parameters for which $100\,\lambda_{\mathrm{c,shield}} = 0.5 e_{\mathrm{shield}}$ and delimits two regimes whether the MICROSCOPE set-up is screened or not. Coloured regions correspond to current constraints from other experiments as atomic interferometry (purple, [337]), Eöt-Wash (green, [52, 338]), Casimir effect measurements (yellow, [51, 339]), astrophysics tests (blue, [93]) and lensing (pink, [212]), or precision atomic tests (orange, [340,341]). Figure from Ref. [335].

6.4.2. Chameleon's stiffness In Ref. [342], it was realised that MICROSCOPE's proof masses might be affected in a measurable way by a chameleon field even if the satellite is screened. This is because MICROSCOPE's instrument is made of diverse interacting parts. Indeed, as proof masses move inside their cage, they move within a chameleon field. The latter can be local, restricted to the instrument if its shield is screened, or even to the proof mass' cage if the electrode-bearing cylinders are screened. In particular, the proof masses move significantly during sessions aimed to measure the electrostatic stiffness

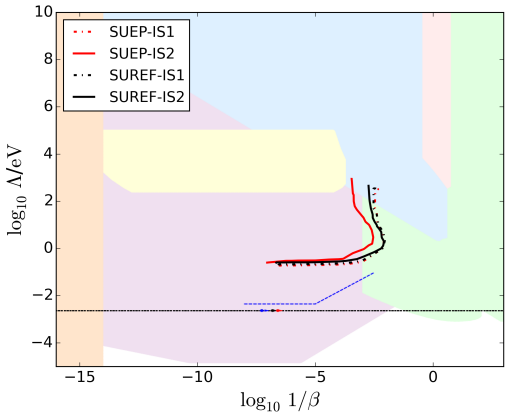

Figure 16. Constraints on the chameleon model for $n = 1$ from the MICROSCOPE experiment using stiffness measurement sessions: the region excluded at 2σ is above the four lines described in the legend. They correspond to the different proof masses: IS1 (resp. IS2) denotes the internal (resp. external) proof masses of the SUREF and SUEP sensor units. Their constraints are compared to the current constraints from other experiments denoted with the colored regions as presented in [212] and Fig. 15. The horizontal doted line denotes the energy scale of dark energy. Figure from Ref. [343].

(Sect. 6.2.2).

Ref. [342, 343] showed that when a proof mass moves radially inside its cage, the local chameleon field creates a destabilising force linear with the displacement. Therefore, the chameleon behaves like a stiffness, that may be measurable. MICROSCOPE's constraints in the chameleon's (β, Λ) plane (for $n = 1$) are summarized in Fig. 16. It shows the 2σ constraints from each proof mass and compares them to the current constrains summarized in Ref. [212]. They overlap the constraints from atom interferometry [337, 344], torsion balances [338] and Casimir effect experiments [51]. Nevertheless, they are not competitive with current constraints. As for the Yukawa potential, this is not surprising since MICROSCOPE was not designed for this test.

6.5. Spin-1 U boson

Noting that from Sect. 3.5, the Eötvös parameter related to a spin-1 U boson is

$$\eta \approx -1.2546 \times 10^{36}(\epsilon_B + 0.4866\epsilon_L) \times \left[\epsilon_B \Delta\left(\frac{B}{A_r}\right) + \epsilon_L \Delta\left(\frac{Z}{A_r}\right)\right], \quad (103)$$

Fayet uses MICROSCOPE's constraints on the Eötvös parameter for the Titanium–Platinum pair of proof masses to set new upper bounds of the coupling constants ϵ_B, ϵ_L and ϵ_{B-L} [223, 224]. At 2σ, for a force coupled to B

$$|\epsilon_B| < 2.5 \times 10^{-24} \quad (104)$$

and for a force coupled to either L or $B - L$

$$|\epsilon_{L,B-L}| < 0.4 \times 10^{-24} \quad (105)$$

after dividing the constraints of Refs. [223, 224] – based on Ref. [148] – by a factor 2 to account for the improved precision of MICROSCOPE's test of the WEP [150, 151] (Fayet, private communication).

Those results confirm that a new long-range force added to gravity must be extremely weak, typically with a gauge coupling smaller than 10^{-24}, and provide increased constraints on its possible magnitude.

6.6. Local Lorentz invariance

We mentioned in Sect. 2 that the WEP generalises to the Einstein Equivalence Principle (EEP) when other interactions are included. Formally, the EEP is obtained when adding the local position invariance (LPI) and the local Lorentz invariance (LLI) to the WEP [345]. Systematic searches for LLI violations can be carried out within the standard model extension (SME) framework, an effective field theory developed to characterise low-energy signatures of Planck-scale physics [346–350]. In that frame, the amplitude of a possible LLI violation is quantified by tensor fields call coefficients. As different combinations of coefficients can be probed by different physical systems, the SME has been used to explore LLI across a large range of experiments (see Ref. [351] for an annually updated review of experimental and observational progress and a full list of references).

As shown in Ref. [352], MICROSCOPE offers a valuable opportunity to constrain the matter-gravity sector of the SME. Indeed, WEP tests can distinguish the species-dependent coefficients associated with matter-gravity couplings from the universal gravity-sector coefficients. Moreover, relative measurements on colocated test particles offer higher-precision tests compared with other observables in which Lorentz violation in matter-gravity couplings has been sought [350, 353–356]. MICROSCOPE is sensitive to composition-dependent $(\bar{a}^w_{\rm eff})_\mu$ coefficients, and Ref. [352] provided constraints on those coefficients associated to fundamental atomic particles ($w = e, p, n$). Five measurement sessions spread from February 2017 to Septembre 2017 were used to search for an orientation-dependent differential acceleration of the Pt vs Ti proof masses while Earth was orbiting around the Sun.

Differential SME coefficients which took into account the alloys making MICROSCOPE's proof masses were estimated

$$\alpha(\bar{a}^d_{\rm eff})_\mu = A\alpha(\bar{a}^{(n-e-p)}_{\rm eff})_\mu, \quad (106)$$

where the α numerical factor depends on the specifics of the theory [350] and where $(\bar{a}^{(n-e-p)}_{\rm eff})_\mu \equiv (\bar{a}^n_{\rm eff})_\mu -$

$(\bar{a}^e_{\rm eff})_\mu - (\bar{a}^p_{\rm eff})_\mu$ and $A \approx 0.06$ GeV^{-1}. This analysis allowed for an improvement on the best previous results by one order of magnitude on $\alpha(\bar{a}^w_{\rm eff})_{X,Y,Z}$ and two orders of magnitude of $\alpha(\bar{a}^w_{\rm eff})_T$ when assuming independence of the coefficients. In particular, the results constrained Lorentz/WEP violation to well below the mass-scale of the electron (10^{-3} GeV), thus placing severe constraints on the scenario of "large" Lorentz violation [357].

7. Testing the WEP after MICROSCOPE

MICROSCOPE not only improved the precision on the WEP by two orders of magnitude, it was the first space-based laboratory dedicated to testing the WEP. Originally thought as a cheap competitor and precursor to the more ambitious STEP satellite mission [244], which aimed for a 10^{-18} precision but was eventually cancelled, it reached all its goals: setting a new reference measurement of the WEP, but also demonstrating technological advances (e.g. 6-degrees-of-freedom drag-free and attitude control) and investigating the limits of the experiment. We can now use MICROSCOPE as a benchmark to plan for improved space tests of the WEP. Several of them can be thought of, from a mission using the same rationale as MICROSCOPE but with improved technology, to a mission using a radically different technology. In this section, we first introduce the "advanced" MICROSCOPE 2, before briefly presenting experiments based on cold atoms technology.

7.1. MICROSCOPE 2

Currently under preliminary investigation at CNES and ONERA, MICROSCOPE 2 will aim to improve MICROSCOPE's measurement by two orders of magnitude, to reach a 10^{-17} precision on the Eötvös parameter. As discussed below, advanced technological choices, based on the MICROSCOPE's experience and most of them readily available, will allow for this significant jump in precision.

The goals of MICROSCOPE 2 could be augmented by adding a cold atom interferometer [249], which will allow for (i) a combined test of the WEP using macroscopic and quantum masses, (ii) a measurement of Newton's constant G with atoms [358] and (iii) an advanced Earth gradiometry experiment [359]. Moreover, adding an optical position sensor will allow for a test of the Casimir effect by using the electrostatic device to move the proof mass accurately with a particular pattern [360].

We now discuss the lessons learned with MICROSCOPE and the way forward.

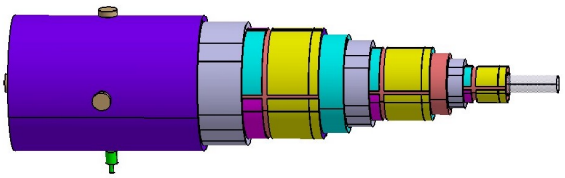

Figure 17. MICROSCOPE 2 instrument core made of three concentric test-masses (grey) surrounded by their respective electrode-bearing cylinders. Figure from Ref. [363].

Instrument core As mentioned in Sect. 5.2.2, because SUEP and SUREF are placed side by side, the SUREF instrument is a reference instrument but cannot be used to readily subtract systematic errors from SUEP's measurements. This limitation can be surpassed by gathering both instruments, and have only one triple differential accelerometer.

The core of the instrument thus comprises three concentric test-masses (Fig. 17). The choice of the materials must be established according to theoretical considerations. We could either use three different materials (allowing for testing the WEP with more than one pair of materials, as advocated in Refs. [361, 362]), or only two (having two proof masses of the same material makes up for an improved SUREF instrument).

Charge management system MICROSCOPE's main stochastic noise is attributed to the thermal dissipation of the gold wires required to control the proof masses' charge. This noise's spectral density has a $f^{-1/2}$ frequency dependence at low-frequency (Eq. 88), the amplitude of which depends on the wire's stiffness to quality factor ratio. Noting that the stiffness depends on the diameter D and length L of the wire as D^4/L^3 [295], the corresponding noise can be reduced by either shrinking the wire's radius or using a longer wire. For instance, to reduce the noise by a factor 1000, the length should be increased by a factor 100 or the diameter reduced by a factor 33. In both cases, it appears far from what is technologically feasible today. A LISA-like charge management system should suppress this limitation [275].

Position sensor Ideally, proof masses should be concentric to relieve gravity gradient systematics. By biasing its capacitive sensor, an electrostatic accelerometer like MICROSCOPE's allows for a cancellation of the offcentering between proof masses. However, this means operating the capacitive sensor out of its zero position, which induces larger sensitivity to temperature. It is possible to cope with this limitation with a LISA-like interferometer position sensing [274]. This has several advantages: (i)

improvement of the acceleration noise at frequency higher than 0.01Hz, (ii) suppression of the coupling in the loop between the electrostatic action and detection, (iii) possibility to cancel the inertial motion effects (thus relaxing the requirements on the proof masses offcentring and on the attitude motion), and (iv) possibility to perform a direct optical differential measurement between two test-masses.

Low-frequency drift Electrostatic accelerometers are known to drift in time. Added to slow thermal variations, this drift induces low-frequency noise and hampers long measurement sessions. It was corrected for with a polynomial fit in MICROSCOPE data [158].

This can be improved with a hybridisation of the electrostatic accelerometer with an atomic interferometer, the latter being used as a reference to calibrate the former. In spite of the increased complexity, cold atoms may bring absolute scale factor determination of the electrostatic accelerometer. This technology is under study and tested within the frame of an ESA gradiometer [359]. The atomic interferometer can have the same laser source as the optical readout.

In-flight calibration In MICROSCOPE, instrumental parameters were estimated in inertial pointing whereas the WEP test was performed in spinning mode. It was verified that this procedure was robust enough to reach a 10^{-15} precision in the Eötvös parameter, but in an advanced mission, the calibration should be more robust, i.e. performed in inertial pointing and in rotating mode.

Glitches MICROSCOPE data are contaminated by periodic transient events (glitches) most likely linked to crackles of the satellite's coating, which create a signal at the frequency of the WEP test [159]. In the absence of a clear understanding of their physics and of a robust model to quantify their impact, they were discarded from the data. An advanced mission should be designed to prevent them from happening. Replacing MICROSCOPE's coating with a stiffer structure like that of the GOCE satellite may be a solution [284].

Operations MICROSCOPE's science sessions were limited to 120 orbits because the flight parameters of the satellite had to be adjusted every 15 days, potentially impacting the experimental conditions, such as temperature, which varies as electronics are turned on and off. The operation of an advanced mission should rely on longer sessions of e.g. 480 orbits instead of 120 to readily gain a factor 2 in precision, by simply increasing the integration time, while easing data analysis thanks to more stable experimental conditions. Another operational limitation came from Moon glares on the star sensor border once a month, forcing to depoint the satellite, inducing thermal condition changes incompatible with the science requirements. Additional star sensors (that can be switched on and off as needed without acting on the satellite pointing) should be considered.

Mitigation of other sources of errors Patch fields and contact-potentials differences [364] should be considered in an advanced MICROSCOPE mission. In MICROSCOPE the corresponding error budget is evaluated at $2 \times 10^{-13}\mathrm{m\,s^{-2}Hz^{-1/2}}$. To reduce the effect of the contact potential over 480 orbits by a needed factor of 10, the gaps between the test-mass and the environment should be increased by a factor $10^{-1/3} \simeq 2$, since the effect is inversely proportional to the cube of the distance. This implies a reduction of control range by a factor 4 and an increase of the free-motion of the test-mass by a factor 2 as the stops limiting the free-motion should be taken away from the test-masses.

The star sensor noise or the drag-free control outperformed their requirement on MICROSCOPE. Their performance should still gain one order of magnitude in MICROSCOPE 2.

Finally, MICROSCOPE showed that increasing the spinning rate of the satellite (to perform the measurement at a higher frequency), improves the temperature stability, as was advocated by Refs. [247, 277]. A fast rotation then helps to reduce temperature-induced systematics.

7.2. Cold atoms in space tests

The report of ESA's Voyage 2050 Senior Science Committee (SSC) § noted the scientific potential of cold atoms technology, both for terrestrial and fundamental physics experiments. The SSC outlined a programme to increase technology readiness, starting with qualifying atomic clocks in space, before atom interferometry (which has the potential to test the WEP) can be fully qualified. As mentioned above, cold atom interferometers are highly accurate over the entire frequency range and do not need any external calibration, they thus have the capability to surpass electrostatic accelerometers. Following this report, the cold atom community set out a roadmap, where the main milestones are presented with the objective to test gravity with cold atoms in space in the middle of the century [365].

An STE-QUEST-like mission [258, 259, 324, 363] could allow for a test of the WEP with a 10^{-17}

§ https://www.cosmos.esa.int/documents/1866264/1866292/Voyage2050-Senior-Committee-report-public.pdf/e2b2631e-5348-5d2d-60c1-437225981b6b?t= 1623427287109

precision thanks to a double atom interferometer with rubidium and potassium "test masses" in quantum superposition. ‖

Note that additional tests of the WEP [366], as well as other uses of quantum sensing in space have been proposed, such as dark matter searches [367,368], test of fundamental constants' stability [369], measurement of the gravitational redshift [370, 371], gravitational waves detection [368, 372, 373] or inertial sensing [374]. For reviews, see e.g. Refs. [375, 376].

8. Conclusion

MICROSCOPE's success allowed for an unprecedented precision on the measurement of the WEP. In this review, we summarised the main objective of the mission and put it in perspective among the current theoretical and experimental efforts to solve some of the biggest problems in nowadays fundamental physics, namely the difficulty to unify gravitation with the other standard model's interactions and the puzzles of the dark sector. We then presented the experiment and its results related to gravitational physics, before providing hints for improvement in the next few decades.

The central part of the WEP in modern physics gives a broad range of applications to the MICROSCOPE results. For instance (the list is not exhaustive), they can be combined to laboratory, astrophysical and cosmological data to look for long range fifth forces [171], for variations of the fine structure constant [176, 377], for dark matter and new-physics particles [163, 164, 197, 206, 223, 224, 319, 320, 378–380], for relic neutrinos wind [167] or for interactions of a domain-wall-model scalar field with standard model particles [175], or to constrain primordial black holes formation [381].

Of course, while MICROSCOPE holds the state-of-the-art measurement of the WEP, its concept and technology are by no means the only way to test it. In particular, the WEP can be tested at cosmological scales with redshift-space distortion, baryon accoustic oscillations and gravitational lensing [129], but also from the measurement of the galaxy cross-power spectrum and bispectrum [382]. The WEP has also been already tested with observations of radio pulsars [383] and Ref. [384] proposes to test the WEP around black holes. Moreover, observations of the galactic center supermassive black hole can be complementary to MICROSCOPE and test of the Local Lorentz Invariance [385–388]. Finally, as mentioned in Sect. 7.2, atom interferometry-based WEP tests [389–391] are fastly improving, reaching a precision of 10^{-12} on the Eötvös parameter [256].

As central as the WEP may be, tests of gravitation and related searches for new physics are diverse and several experiments, either on the ground or in space, are developed. Among the latest ones, we can cite (beside those appearing in the main text) the measurement of the Lense-Thirring effect [79, 141, 142] – which could potentially be performed with a better-than-100% precision by MICROSCOPE via the fine monitoring of its orbit, with the drag-free system helping to cancel non-gravitational forces, as shown by Baghi and collaborators in an unpublished study –, the measurement of the gravitational constant by LISA Pathfinder's accelerometers [392], the search for ultralight scalar and vector field with gravitational wave detectors [393–395], measurements of the free fall of anti-matter [263, 264, 266], or tests of gravity's quantum limit [396, 397]. In particular, Ref. [398] states that the spreading of wave-packet and free-fall are exclusive phenomena implying a violation of the WEP of the order of 10^{-16}. This potentially ultimate quantum limit should be tested with atomic test masses. It would then be interesting to compare the results of future tests of the WEP made with atomic (STE-QUEST) and macroscopic (MICROSCOPE 2) proof masses.

Acknowledgments

I want to thank Manuel Rodrigues, Gilles Métris, Alain Robert, Martin Pernot-Borràs, Jean-Philippe Uzan, Philippe Brax, Bruno Christophe, Hugo Lévy, Sandrine Pires, Quentin Baghi, Françoise Liorzou, Bernard Foulon, Ratana Chhun, Pierre Fayet, Thibault Damour and Serge Reynaud for uncountable discussions during and after the MICROSCOPE data analysis. I also thank Aurélien Hees for providing Fig. 14. Special thanks go to Martin Pernot-Borràs, who wrote his PhD thesis at the same time as this review was being written, and whose text was a good inspiration to some sections. On behalf of the MICROSCOPE consortium, this review is dedicated to the memory of Pierre Touboul, who was the vibrant soul of the consortium for many years.

References

[1] Einstein A 1908 *Jahrbuch der Radioaktivität und Elektronik* **4**
[2] Einstein A 1916 *Annalen der Physik* **354** 769–822
[3] Bartelmann M and Schneider P 2001 *Physics Reports* **340** 291–472 (*Preprint* `astro-ph/9912508`)
[4] Hoekstra H and Jain B 2008 *Annual Review of Nuclear and Particle Science* **58** 99–123 (*Preprint* `0805.0139`)
[5] Delva P, Puchades N, Schönemann E, Dilssner F, Courde C, Bertone S, Gonzalez F, Hees A, Le Poncin-Lafitte C, Meynadier F, Prieto-Cerdeira R, Sohet B, Ventura-

‖ The proposed STE-QUEST mission was not selected by ESA during the M7 mission opportunity call in November 2022

Traveset J and Wolf P 2018 *Physical Review Letters* **121** 231101 (*Preprint* 1812.03711)

[6] Herrmann S, Finke F, Lülf M, Kichakova O, Puetzfeld D, Knickmann D, List M, Rievers B, Giorgi G, Günther C, Dittus H, Prieto-Cerdeira R, Dilssner F, Gonzalez F, Schönemann E, Ventura-Traveset J and Lämmerzahl C 2018 *Physical Review Letters* **121** 231102 (*Preprint* 1812.09161)

[7] Abbott B P *et al.* 2016 *Phys. Rev. Lett.* **116** 061102

[8] Event Horizon Telescope Collaboration, Akiyama K, Alberdi A, Alef W, Asada K, Azulay R, Baczko A K, Ball D, Baloković M, Barrett J, Bintley D, Blackburn L, Boland W, Bouman K L, Bower G C, Bremer M, Brinkerink C D, Brissenden R, Britzen S, Broderick A E, Broguiere D, Bronzwaer T, Byun D Y, Carlstrom J E, Chael A, Chan C k, Chatterjee S, Chatterjee K, Chen M T, Chen Y, Cho I, Christian P, Conway J E, Cordes J M, Crew G B, Cui Y, Davelaar J, De Laurentis M, Deane R, Dempsey J, Desvignes G, Dexter J, Doeleman S S, Eatough R P, Falcke H, Fish V L, Fomalont E, Fraga-Encinas R, Freeman W T, Friberg P, Fromm C M, Gómez J L, Galison P, Gammie C F, García R, Gentaz O, Georgiev B, Goddi C, Gold R, Gu M, Gurwell M, Hada K, Hecht M H, Hesper R, Ho L C, Ho P, Honma M, Huang C W L, Huang L, Hughes D H, Ikeda S, Inoue M, Issaoun S, James D J, Jannuzi B T, Janssen M, Jeter B, Jiang W, Johnson M D, Jorstad S, Jung T, Karami M, Karuppusamy R, Kawashima T, Keating G K, Kettenis M, Kim J Y, Kim J, Kim J, Kino M, Koay J Y, Koch P M, Koyama S, Kramer M, Kramer C, Krichbaum T P, Kuo C Y, Lauer T R, Lee S S, Li Y R, Li Z, Lindqvist M, Liu K, Liuzzo E, Lo W P, Lobanov A P, Loinard L, Lonsdale C, Lu R S, MacDonald N R, Mao J, Markoff S, Marrone D P, Marscher A P, Martí-Vidal I, Matsushita S, Matthews L D, Medeiros L, Menten K M, Mizuno Y, Mizuno I, Moran J M, Moriyama K, Moscibrodzka M, Müller C, Nagai H, Nagar N M, Nakamura M, Narayan R, Narayanan G, Natarajan I, Neri R, Ni C, Noutsos A, Okino H, Olivares H, Ortiz-León G N, Oyama T, Özel F, Palumbo D C M, Patel N, Pen U L, Pesce D W, Piétu V, Plambeck R, PopStefanija A, Porth O, Prather B, Preciado-López J A, Psaltis D, Pu H Y, Ramakrishnan V, Rao R, Rawlings M G, Raymond A W, Rezzolla L, Ripperda B, Roelofs F, Rogers A, Ros E, Rose M, Roshanineshat A, Rottmann H, Roy A L, Ruszczyk C, Ryan B R, Rygl K L J, Sánchez S, Sánchez-Arguelles D, Sasada M, Savolainen T, Schloerb F P, Schuster K F, Shao L, Shen Z, Small D, Sohn B W, SooHoo J, Tazaki F, Tiede P, Tilanus R P J, Titus M, Toma K, Torne P, Trent T, Trippe S, Tsuda S, van Bemmel I, van Langevelde H J, van Rossum D R, Wagner J, Wardle J, Weintroub J, Wex N, Wharton R, Wielgus M, Wong G N, Wu Q, Young K, Young A, Younsi Z, Yuan F, Yuan Y F, Zensus J A, Zhao G, Zhao S S, Zhu Z, Algaba J C, Allardi A, Amestica R, Anczarski J, Bach U, Baganoff F K, Beaudoin C, Benson B A, Berthold R, Blanchard J M, Blundell R, Bustamente S, Cappallo R, Castillo-Domínguez E, Chang C C, Chang S H, Chang S C, Chen C C, Chilson R, Chuter T C, Córdova Rosado R, Coulson I M, Crawford T M, Crowley J, David J, Derome M, Dexter M, Dornbusch S, Dudevoir K A, Dzib S A, Eckart A, Eckert C, Erickson N R, Everett W B, Faber A, Farah J R, Fath V, Folkers T W, Forbes D C, Freund R, Gómez-Ruiz A I, Gale D M, Gao F, Geertsema G, Graham D A, Greer C H, Grosslein R, Gueth F, Haggard D, Halverson N W, Han C C, Han K C, Hao J, Hasegawa Y, Henning J W, Hernández-Gómez A, Herrero-Illana R, Heyminck S, Hirota A, Hoge J, Huang Y D, Impellizzeri C M V, Jiang H, Kamble A, Keisler R, Kimura K, Kono Y, Kubo D, Kuroda J, Lacasse R, Laing R A, Leitch E M, Li C T, Lin L C C, Liu C T, Liu K Y, Lu L M, Marson R G, Martin-Cocher P L, Massingill K D, Matulonis C, McColl M P, McWhirter S R, Messias H, Meyer-Zhao Z, Michalik D, Montaña A, Montgomerie W, Mora-Klein M, Muders D, Nadolski A, Navarro S, Neilsen J, Nguyen C H, Nishioka H, Norton T, Nowak M A, Nystrom G, Ogawa H, Oshiro P, Oyama T, Parsons H, Paine S N, Peñalver J, Phillips N M, Poirier M, Pradel N, Primiani R A, Raffin P A, Rahlin A S, Reiland G, Risacher C, Ruiz I, Sáez-Madaín A F, Sassella R, Schellart P, Shaw P, Silva K M, Shiokawa H, Smith D R, Snow W, Souccar K, Sousa D, Sridharan T K, Srinivasan R, Stahm W, Stark A A, Story K, Timmer S T, Vertatschitsch L, Walther C, Wei T S, Whitehorn N, Whitney A R, Woody D P, Wouterloot J G A, Wright M, Yamaguchi P, Yu C Y, Zeballos M, Zhang S and Ziurys L 2019 *Astrophysical Journal Letters* **875** L1 (*Preprint* 1906.11238)

[9] Abbott B P, Abbott R, Abbott T D, Acernese F, Ackley K, Adams C, Adams T, Addesso P, Adhikari R X, Adya V B and et al 2017 *Physical Review Letters* **119** 161101 (*Preprint* 1710.05832)

[10] Brax P, Burrage C and Davis A C 2016 *Journal of Cosmology and Astroparticle Physics* **3** 004 (*Preprint* 1510.03701)

[11] Lombriser L and Taylor A 2016 *Journal of Cosmology and Astroparticle Physics* **3** 031 (*Preprint* 1509.08458)

[12] Lombriser L and Lima N A 2017 *Physics Letters B* **765** 382–385 (*Preprint* 1602.07670)

[13] Baker T, Bellini E, Ferreira P G, Lagos M, Noller J and Sawicki I 2017 *Physical Review Letters* **119** 251301 (*Preprint* 1710.06394)

[14] Creminelli P and Vernizzi F 2017 *Physical Review Letters* **119** 251302 (*Preprint* 1710.05877)

[15] Ezquiaga J M and Zumalacárregui M 2017 *Physical Review Letters* **119** 251304 (*Preprint* 1710.05901)

[16] Sakstein J and Jain B 2017 *Physical Review Letters* **119** 251303 (*Preprint* 1710.05893)

[17] Will C M 2014 *Living Reviews in Relativity* **17** 4 (*Preprint* 1403.7377)

[18] Zwicky F 1933 *Helvetica Physica Acta* **6** 110–127

[19] Rubin V C and Ford Jr W K 1970 *Astrophysical Journal* **159** 379

[20] Riess A G, Filippenko A V, Challis P, Clocchiatti A, Diercks A, Garnavich P M, Gilliland R L, Hogan C J, Jha S, Kirshner R P, Leibundgut B, Phillips M M, Reiss D, Schmidt B P, Schommer R A, Smith R C, Spyromilio J, Stubbs C, Suntzeff N B and Tonry J 1998 *Astronomical Journal* **116** 1009–1038 (*Preprint* astro-ph/9805201)

[21] Perlmutter S, Aldering G, Goldhaber G, Knop R A, Nugent P, Castro P G, Deustua S, Fabbro S, Goobar A, Groom D E, Hook I M, Kim A G, Kim M Y, Lee J C, Nunes N J, Pain R, Pennypacker C R, Quimby R, Lidman C, Ellis R S, Irwin M, McMahon R G, Ruiz-Lapuente P, Walton N, Schaefer B, Boyle B J, Filippenko A V, Matheson T, Fruchter A S, Panagia N, Newberg H J M, Couch W J and Project T S C 1999 *Astrophysical Journal* **517** 565–586 (*Preprint* astro-ph/9812133)

[22] Aad G, Abajyan T, Abbott B, Abdallah J, Abdel Khalek S, Abdelalim A A, Abdinov O, Aben R, Abi B, Abolins M and et al 2012 *Physics Letters B* **716** 1–29 (*Preprint* 1207.7214)

[23] Chatrchyan S, Khachatryan V, Sirunyan A M, Tumasyan A, Adam W, Aguilo E, Bergauer T, Dragicevic M, Erö J, Fabjan C and et al 2012 *Physics Letters B* **716** 30–61 (*Preprint* 1207.7235)

[24] De Felice A and Tsujikawa S 2010 *Living Reviews in Relativity* **13** 3 (*Preprint* 1002.4928)
[25] Sotiriou T P and Faraoni V 2010 *Reviews of Modern Physics* **82** 451–497 (*Preprint* 0805.1726)
[26] Damour T and Polyakov A M 1994 *Nucl. Phys. B* **423** 532–558 (*Preprint* hep-th/9401069)
[27] Damour T, Piazza F and Veneziano G 2002 *Physical Review Letters* **89** 081601 (*Preprint* gr-qc/0204094)
[28] Damour T and Esposito-Farese G 1992 *Classical and Quantum Gravity* **9** 2093–2176
[29] Esposito-Farèse G and Polarski D 2001 *Physical Review D* **63** 063504 (*Preprint* gr-qc/0009034)
[30] Clifton T, Ferreira P G, Padilla A and Skordis C 2012 *Physics Reports* **513** 1–189 (*Preprint* 1106.2476)
[31] Joyce A, Jain B, Khoury J and Trodden M 2015 *Physics Reports* **568** 1–98 (*Preprint* 1407.0059)
[32] Khoury J 2010 *arXiv e-prints* arXiv:1011.5909 (*Preprint* 1011.5909)
[33] Khoury J and Weltman A 2004 *Phys. Rev. D* **69** 044026 (*Preprint* astro-ph/0309411)
[34] Khoury J and Weltman A 2004 *Phys. Rev. Lett.* **93** 171104 (*Preprint* astro-ph/0309300)
[35] Damour T 2012 *Classical and Quantum Gravity* **29** 184001 (*Preprint* 1202.6311)
[36] Uzan J P 2003 *Rev. Mod. Phys.* **75** 403 (*Preprint* hep-ph/0205340)
[37] Uzan J P 2005 *AIP Conf. Proc.* **736** 3–20 [,3(2004)] (*Preprint* astro-ph/0409424)
[38] Uzan J P 2011 *Living Rev. Rel.* **14** 2 (*Preprint* 1009.5514)
[39] Hoskins J K, Newman R D, Spero R and Schultz J 1985 *Physical Review D* **32** 3084–3095
[40] Mitrofanov V P and Ponomareva O I 1988 *Zhurnal Eksperimentalnoi i Teoreticheskoi Fiziki* **94** 16–22
[41] Lamoreaux S K 1997 *Physical Review Letters* **78** 5–8
[42] Lamoreaux S K 1998 *Physical Review Letters* **81** 5475–5476
[43] Mohideen U and Roy A 1998 *Physical Review Letters* **81** 4549–4552 (*Preprint* physics/9805038)
[44] Fischbach E and Talmadge C L 1999 *The Search for Non-Newtonian Gravity*
[45] Long J C, Chan H W and Price J C 1999 *Nuclear Physics B* **539** 23–34 (*Preprint* hep-ph/9805217)
[46] Chiaverini J, Smullin S J, Geraci A A, Weld D M and Kapitulnik A 2003 *Physical Review Letters* **90** 151101 (*Preprint* hep-ph/0209325)
[47] Hoyle C D, Schmidt U, Heckel B R, Adelberger E G, Gundlach J H, Kapner D J and Swanson H E 2001 *Physical Review Letters* **86** 1418–1421 (*Preprint* hep-ph/0011014)
[48] Adelberger E G, Heckel B R and Nelson A E 2003 *Annual Review of Nuclear and Particle Science* **53** 77–121 (*Preprint* hep-ph/0307284)
[49] Hoyle C D, Kapner D J, Heckel B R, Adelberger E G, Gundlach J H, Schmidt U and Swanson H E 2004 *Physical Review D* **70** 042004 (*Preprint* hep-ph/0405262)
[50] Williams J G, Turyshev S G and Boggs D H 2004 *Phys. Rev. Lett.* **93** 261101 (*Preprint* gr-qc/0411113)
[51] Brax P, van de Bruck C, Davis A C, Mota D F and Shaw D 2007 *Physical Review D* **76** 124034 (*Preprint* 0709.2075)
[52] Kapner D J, Cook T S, Adelberger E G, Gundlach J H, Heckel B R, Hoyle C D and Swanson H E 2007 *Physical Review Letters* **98** 021101 (*Preprint* hep-ph/0611184)
[53] Geraci A A, Smullin S J, Weld D M, Chiaverini J and Kapitulnik A 2008 *Physical Review D* **78** 022002 (*Preprint* 0802.2350)
[54] Schlamminger S, Choi K Y, Wagner T A, Gundlach J H and Adelberger E G 2008 *Physical Review Letters* **100** 041101 (*Preprint* 0712.0607)
[55] Adelberger E G, Gundlach J H, Heckel B R, Hoedl S and Schlamminger S 2009 *Progress in Particle and Nuclear Physics* **62** 102–134
[56] Masuda M and Sasaki M 2009 *Physical Review Letters* **102** 171101 (*Preprint* 0904.1834)
[57] Sushkov A O, Kim W J, Dalvit D A R and Lamoreaux S K 2011 *Physical Review Letters* **107** 171101 (*Preprint* 1108.2547)
[58] Wagner T A, Schlamminger S, Gundlach J H and Adelberger E G 2012 *Classical and Quantum Gravity* **29** 184002 (*Preprint* 1207.2442)
[59] Klimchitskaya G L and Mostepanenko V M 2014 *Gravitation and Cosmology* **20** 3–9 (*Preprint* 1403.5778)
[60] Almasi A, Brax P, Iannuzzi D and Sedmik R I P 2015 *Physical Review D* **91** 102002 (*Preprint* 1505.01763)
[61] Murata J and Tanaka S 2015 *Classical and Quantum Gravity* **32** 033001 (*Preprint* 1408.3588)
[62] Uzan J P, Pernot-Borràs M and Bergé J 2020 *Physical Review D* **102** 044059 (*Preprint* 2006.03359)
[63] Anderson J D, Laing P A, Lau E L, Liu A S, Nieto M M and Turyshev S G 1998 *Physical Review Letters* **81** 2858–2861 (*Preprint* gr-qc/9808081)
[64] Anderson J D, Laing P A, Lau E L, Liu A S, Nieto M M and Turyshev S G 2002 *Physical Review D* **65** 082004 (*Preprint* gr-qc/0104064)
[65] Anderson J D, Turyshev S G, Nieto M M and Ahluwalia D V 2002 *International Journal of Modern Physics D* **11** 1545–1551 (*Preprint* gr-qc/0205059)
[66] Iorio L 2002 *Physics Letters A* **298** 315–318 (*Preprint* gr-qc/0201081)
[67] Bertotti B, Iess L and Tortora P 2003 *Nature* **425** 374–376
[68] Brax P, van de Bruck C, Davis A C, Khoury J and Weltman A 2004 *Physical Review D* **70** 123518 (*Preprint* astro-ph/0408415)
[69] Dittus H, Turyshev S G, Lämmerzahl C and et al 2005 A mission to explore the Pioneer anomaly *39TH ESLAB Symposium on Trends in Space Science and Cosmic Vision 2020* (*ESA Special Publication* vol 588) ed Favata F, Sanz-Forcada J, Giménez A and Battrick B p 3
[70] Jaekel M T and Reynaud S 2005 *Modern Physics Letters A* **20** 1047–1055 (*Preprint* gr-qc/0410148)
[71] Johann U A 2007 *International Journal of Modern Physics D* **16** 2297–2307
[72] Lämmerzahl C, Dittus H, Hackmann E, Scheithauer S, Peters A and Schiller S 2008 Optis - High Precision Test of Special and General Relativity in Space *The Eleventh Marcel Grossmann Meeting On Recent Developments in Theoretical and Experimental General Relativity, Gravitation and Relativistic Field Theories* ed Kleinert H, Jantzen R T and Ruffini R pp 905–915
[73] Reynaud S, Lamine B, Duchayne L, Wolf P and Jaekel M T 2008 *Physical Review D* **77** 122003 (*Preprint* 0801.2896)
[74] Reynaud S, Salomon C and Wolf P 2009 *Space Science Reviews* **148** 233–247 (*Preprint* 0903.1166)
[75] Christophe B, Andersen P H, Anderson J D, Asmar S, Bério P, Bertolami O, Bingham R, Bondu F, Bouyer P, Bremer S, Courty J M, Dittus H, Foulon B, Gil P, Johann U, Jordan J F, Kent B, Lämmerzahl C, Lévy A, Métris G, Olsen O, Pàramos J, Prestage J D, Progrebenko S V, Rasel E, Rathke A, Reynaud S, Rievers B, Samain E, Sumner T J, Theil S, Touboul P, Turyshev S, Vrancken P, Wolf P and Yu N 2009 *Experimental Astronomy* **23** 529–547 (*Preprint* 0711.2007)
[76] Wolf P, Bordé C J, Clairon A, Duchayne L, Landragin A, Lemonde P, Santarelli G, Ertmer W, Rasel E, Cataliotti F S, Inguscio M, Tino G M, Gill P, Klein H, Reynaud S, Salomon C, Peik E, Bertolami O, Gil P, Páramos J,

Jentsch C, Johann U, Rathke A, Bouyer P, Cacciapuoti L, Izzo D, de Natale P, Christophe B, Touboul P, Turyshev S G, Anderson J, Tobar M E, Schmidt-Kaler F, Vigué J, Madej A A, Marmet L, Angonin M C, Delva P, Tourrenc P, Metris G, Müller H, Walsworth R, Lu Z H, Wang L J, Bongs K, Toncelli A, Tonelli M, Dittus H, Lämmerzahl C, Galzerano G, Laporta P, Laskar J, Fienga A, Roques F and Sengstock K 2009 *Experimental Astronomy* **23** 651–687 (*Preprint* 0711.0304)

[77] Lucchesi D M 2011 *Advances in Space Research* **47** 1232–1237

[78] Hees A, Lamine B, Reynaud S, Jaekel M T, Le Poncin-Lafitte C, Lainey V, Füzfa A, Courty J M, Dehant V and Wolf P 2012 *Classical and Quantum Gravity* **29** 235027 (*Preprint* 1201.5041)

[79] Ciufolini I, Paolozzi A, Koenig R, Pavlis E C, Ries J, Matzner R, Gurzadyan V, Penrose R, Sindoni G and Paris C 2013 *Nuclear Physics B Proceedings Supplements* **243** 180–193 (*Preprint* 1309.1699)

[80] Murphy T W 2013 *Reports on Progress in Physics* **76** 076901 (*Preprint* 1309.6294)

[81] Buscaino B, DeBra D, Graham P W, Gratta G and Wiser T D 2015 *Physical Review D* **92** 104048 (*Preprint* 1508.06273)

[82] Fienga A, Laskar J, Manche H and Gastineau M 2016 *ArXiv e-prints* (*Preprint* 1601.00947)

[83] Roberts B M, Blewitt G, Dailey C, Murphy M, Pospelov M, Rollings A, Sherman J, Williams W and Derevianko A 2017 *Nature Communications* **8** 1195 (*Preprint* 1704.06844)

[84] Bergé J 2017 ISLAND: the Inverse Square Law And Newtonian Dynamics Space Explorer *Proceedings of the 52nd Rencontres de Moriond in Gravitation* vol 52 p 191 (*Preprint* 1809.00698)

[85] Viswanathan V, Fienga A, Minazzoli O, Bernus L, Laskar J and Gastineau M 2018 *Monthly Notices of the Royal Astronomical Society* **476** 1877–1888 (*Preprint* 1710.09167)

[86] Banik I and Kroupa P 2019 *Monthly Notices of the Royal Astronomical Society* **487** 2665–2672 (*Preprint* 1907.00006)

[87] Bergé J, Baudis L, Brax P, Chiow S w, Christophe B, Doré O, Fayet P, Hees A, Jetzer P, Lämmerzahl C, List M, Métris G, Pernot-Borràs M, Read J, Reynaud S, Rhodes J, Rievers B, Rodrigues M, Sumner T, Uzan J P and Yu N 2019 *arXiv e-prints* arXiv:1909.00834 (*Preprint* 1909.00834)

[88] Jain B and VanderPlas J 2011 *Journal of Cosmology and Astroparticle Physics* **2011** 032 (*Preprint* 1106.0065)

[89] Cabré A, Vikram V, Zhao G B, Jain B and Koyama K 2012 *Journal of Cosmology and Astroparticle Physics* **2012** 034 (*Preprint* 1204.6046)

[90] Davis A C, Lim E A, Sakstein J and Shaw D J 2012 *Physical Review D* **85** 123006 (*Preprint* 1102.5278)

[91] Garbari S, Liu C, Read J I and Lake G 2012 *Monthly Notices of the Royal Astronomical Society* **425** 1445–1458 (*Preprint* 1206.0015)

[92] Smith M C, Whiteoak S H and Evans N W 2012 *Astrophysical Journal* **746** 181 (*Preprint* 1111.6920)

[93] Jain B, Vikram V and Sakstein J 2013 *Astrophysical Journal* **779** 39 (*Preprint* 1204.6044)

[94] Bovy J and Rix H W 2013 *Astrophysical Journal* **779** 115 (*Preprint* 1309.0809)

[95] Sakstein J 2013 *Physical Review D* **88** 124013 (*Preprint* 1309.0495)

[96] Vikram V, Cabré A, Jain B and Vand erPlas J T 2013 *Journal of Cosmology and Astroparticle Physics* **2013** 020 (*Preprint* 1303.0295)

[97] Bienaymé O, Famaey B, Siebert A, Freeman K C, Gibson B K, Gilmore G, Grebel E K, Bland-Hawthorn J, Kordopatis G, Munari U, Navarro J F, Parker Q, Reid W, Seabroke G M, Siviero A, Steinmetz M, Watson F, Wyse R F G and Zwitter T 2014 *Astronomy and Astrophysics* **571** A92 (*Preprint* 1406.6896)

[98] Hees A, Do T, Ghez A M, Martinez G D, Naoz S, Becklin E E, Boehle A, Chappell S, Chu D, Dehghanfar A, Kosmo K, Lu J R, Matthews K, Morris M R, Sakai S, Schödel R and Witzel G 2017 *Physical Review Letters* **118** 211101 (*Preprint* 1705.07902)

[99] De Laurentis M, De Martino I and Lazkoz R 2018 *European Physical Journal C* **78** 916 (*Preprint* 1811.00046)

[100] Desmond H, Ferreira P G, Lavaux G and Jasche J 2018 *Physical Review D* **98** 064015 (*Preprint* 1807.01482)

[101] Desmond H, Ferreira P G, Lavaux G and Jasche J 2018 *Physical Review D* **98** 083010 (*Preprint* 1807.11742)

[102] Buch J, Chau (John Leung S and Fan J 2019 *Journal of Cosmology and Astroparticle Physics* **2019** 026 (*Preprint* 1808.05603)

[103] Evans N W, O'Hare C A J and McCabe C 2019 *Phys. Rev.* **D99** 023012 (*Preprint* 1810.11468)

[104] Schmidt F, Vikhlinin A and Hu W 2009 *Physical Review D* **80** 083505 (*Preprint* 0908.2457)

[105] Gannouji R, Moraes B, Mota D F, Polarski D, Tsujikawa S and Winther H A 2010 *Physical Review D* **82** 124006 (*Preprint* 1010.3769)

[106] Schmidt F 2010 *Physical Review D* **81** 103002 (*Preprint* 1003.0409)

[107] Jain B and Khoury J 2010 *Annals of Physics* **325** 1479–1516 (*Preprint* 1004.3294)

[108] Ferraro S, Schmidt F and Hu W 2011 *Physical Review D* **83** 063503 (*Preprint* 1011.0992)

[109] Laureijs R, Amiaux J, Arduini S, Augueres J L, Brinchmann J, Cole R, Cropper M, Dabin C, Duvet L, Ealet A, Garilli B, Gondoin P, Guzzo L, Hoar J, Hoekstra H, Holmes R, Kitching T, Maciaszek T, Mellier Y, Pasian F, Percival W, Rhodes J, Saavedra Criado G, Sauvage M, Scaramella R, Valenziano L, Warren S, Bender R, Castander F, Cimatti A, Le Fèvre O, Kurki-Suonio H, Levi M, Lilje P, Meylan G, Nichol R, Pedersen K, Popa V, Rebolo Lopez R, Rix H W, Rottgering H, Zeilinger W, Grupp F, Hudelot P, Massey R, Meneghetti M, Miller L, Paltani S, Paulin-Henriksson S, Pires S, Saxton C, Schrabback T, Seidel G, Walsh J, Aghanim N, Amendola L, Bartlett J, Baccigalupi C, Beaulieu J P, Benabed K, Cuby J G, Elbaz D, Fosalba P, Gavazzi G, Helmi A, Hook I, Irwin M, Kneib J P, Kunz M, Mannucci F, Moscardini L, Tao C, Teyssier R, Weller J, Zamorani G, Zapatero Osorio M R, Boulade O, Foumond J J, Di Giorgio A, Guttridge P, James A, Kemp M, Martignac J, Spencer A, Walton D, Blümchen T, Bonoli C, Bortoletto F, Cerna C, Corcione L, Fabron C, Jahnke K, Ligori S, Madrid F, Martin L, Morgante G, Pamplona T, Prieto E, Riva M, Toledo R, Trifoglio M, Zerbi F, Abdalla F, Douspis M, Grenet C, Borgani S, Bouwens R, Courbin F, Delouis J M, Dubath P, Fontana A, Frailis M, Grazian A, Koppenhöfer J, Mansutti O, Melchior M, Mignoli M, Mohr J, Neissner C, Noddle K, Poncet M, Scodeggio M, Serrano S, Shane N, Starck J L, Surace C, Taylor A, Verdoes-Kleijn G, Vuerli C, Williams O R, Zacchei A, Altieri B, Escudero Sanz I, Kohley R, Oosterbroek T, Astier P, Bacon D, Bardelli S, Baugh C, Bellagamba F, Benoist C, Bianchi D, Biviano A, Branchini E, Carbone C, Cardone V, Clements D, Colombi S, Conselice C, Cresci G, Deacon N, Dunlop J, Fedeli C, Fontanot F, Franzetti P, Giocoli C, Garcia-Bellido J, Gow J, Heavens A, Hewett P, Heymans C, Holland A, Huang Z, Ilbert O, Joachimi B, Jennins

E, Kerins E, Kiessling A, Kirk D, Kotak R, Krause O, Lahav O, van Leeuwen F, Lesgourgues J, Lombardi M, Magliocchetti M, Maguire K, Majerotto E, Maoli R, Marulli F, Maurogordato S, McCracken H, McLure R, Melchiorri A, Merson A, Moresco M, Nonino M, Norberg P, Peacock J, Pello R, Penny M, Pettorino V, Di Porto C, Pozzetti L, Quercellini C, Radovich M, Rassat A, Roche N, Ronayette S, Rossetti E, Sartoris B, Schneider P, Semboloni E, Serjeant S, Simpson F, Skordis C, Smadja G, Smartt S, Spano P, Spiro S, Sullivan M, Tilquin A, Trotta R, Verde L, Wang Y, Williger G, Zhao G, Zoubian J and Zucca E 2011 *arXiv e-prints* arXiv:1110.3193 (*Preprint* 1110.3193)

[110] Zhao G B, Li B and Koyama K 2011 *Physical Review Letters* **107** 071303 (*Preprint* 1105.0922)

[111] Brax P, Davis A C and Li B 2012 *Physics Letters B* **715** 38–43 (*Preprint* 1111.6613)

[112] Brax P, Davis A C, Li B and Winther H A 2012 *Physical Review D* **86** 044015 (*Preprint* 1203.4812)

[113] Lombriser L, Schmidt F, Baldauf T, Mand elbaum R, Seljak U and Smith R E 2012 *Physical Review D* **85** 102001 (*Preprint* 1111.2020)

[114] Lombriser L, Koyama K, Zhao G B and Li B 2012 *Physical Review D* **85** 124054 (*Preprint* 1203.5125)

[115] Amendola L, Appleby S, Bacon D, Baker T, Baldi M, Bartolo N, Blanchard A, Bonvin C, Borgani S, Branchini E, Burrage C, Camera S, Carbone C, Casarini L, Cropper M, de Rham C, Di Porto C, Ealet A, Ferreira P G, Finelli F, García-Bellido J, Giannantonio T, Guzzo L, Heavens A, Heisenberg L, Heymans C, Hoekstra H, Hollenstein L, Holmes R, Horst O, Jahnke K, Kitching T D, Koivisto T, Kunz M, La Vacca G, March M, Majerotto E, Markovic K, Marsh D, Marulli F, Massey R, Mellier Y, Mota D F, Nunes N J, Percival W, Pettorino V, Porciani C, Quercellini C, Read J, Rinaldi M, Sapone D, Scaramella R, Skordis C, Simpson F, Taylor A, Thomas S, Trotta R, Verde L, Vernizzi F, Vollmer A, Wang Y, Weller J and Zlosnik T 2013 *Living Reviews in Relativity* **16** 6 (*Preprint* 1206.1225)

[116] Brax P and Valageas P 2013 *Physical Review D* **88** 023527 (*Preprint* 1305.5647)

[117] Dawson K S, Schlegel D J, Ahn C P, Anderson S F, Aubourg É, Bailey S, Barkhouser R H, Bautista J E, Beifiori A, Berlind A A, Bhardwaj V, Bizyaev D, Blake C H, Blanton M R, Blomqvist M, Bolton A S, Borde A, Bovy J, Brandt W N, Brewington H, Brinkmann J, Brown P J, Brownstein J R, Bundy K, Busca N G, Carithers W, Carnero A R, Carr M A, Chen Y, Comparat J, Connolly N, Cope F, Croft R A C, Cuesta A J, da Costa L N, Davenport J R A, Delubac T, de Putter R, Dhital S, Ealet A, Ebelke G L, Eisenstein D J, Escoffier S, Fan X, Filiz Ak N, Finley H, Font-Ribera A, Génova-Santos R, Gunn J E, Guo H, Haggard D, Hall P B, Hamilton J C, Harris B, Harris D W, Ho S, Hogg D W, Holder D, Honscheid K, Huehnerhoff J, Jordan B, Jordan W P, Kauffmann G, Kazin E A, Kirkby D, Klaene M A, Kneib J P, Le Goff J M, Lee K G, Long D C, Loomis C P, Lundgren B, Lupton R H, Maia M A G, Makler M, Malanushenko E, Malanushenko V, Mandelbaum R, Manera M, Maraston C, Margala D, Masters K L, McBride C K, McDonald P, McGreer I D, McMahon R G, Mena O, Miralda-Escudé J, Montero-Dorta A D, Montesano F, Muna D, Myers A D, Naugle T, Nichol R C, Noterdaeme P, Nuza S E, Olmstead M D, Oravetz A, Oravetz D J, Owen R, Padmanabhan N, Palanque-Delabrouille N, Pan K, Parejko J K, Pâris I, Percival W J, Pérez-Fournon I, Pérez-Ràfols I, Petitjean P, Pfaffenberger R, Pforr J, Pieri M M, Prada F, Price-Whelan A M, Raddick M J, Rebolo R, Rich J, Richards G T, Rockosi C M, Roe N A, Ross A J, Ross N P, Rossi G, Rubiño-Martin J A, Samushia L, Sánchez A G, Sayres C, Schmidt S J, Schneider D P, Scóccola C G, Seo H J, Shelden A, Sheldon E, Shen Y, Shu Y, Slosar A, Smee S A, Snedden S A, Stauffer F, Steele O, Strauss M A, Streblyanska A, Suzuki N, Swanson M E C, Tal T, Tanaka M, Thomas D, Tinker J L, Tojeiro R, Tremonti C A, Vargas Magaña M, Verde L, Viel M, Wake D A, Watson M, Weaver B A, Weinberg D H, Weiner B J, West A A, White M, Wood-Vasey W M, Yeche C, Zehavi I, Zhao G B and Zheng Z 2013 *Astronomical Journal* **145** 10 (*Preprint* 1208.0022)

[118] Simpson F, Heymans C, Parkinson D, Blake C, Kilbinger M, Benjamin J, Erben T, Hildebrandt H, Hoekstra H, Kitching T D, Mellier Y, Miller L, Van Waerbeke L, Coupon J, Fu L, Harnois-Déraps J, Hudson M J, Kuijken K, Rowe B, Schrabback T, Semboloni E, Vafaei S and Velander M 2013 *Monthly Notices of the Royal Astronomical Society* **429** 2249–2263 (*Preprint* 1212.3339)

[119] Van Waerbeke L, Benjamin J, Erben T, Heymans C, Hildebrandt H, Hoekstra H, Kitching T D, Mellier Y, Miller L, Coupon J, Harnois-Déraps J, Fu L, Hudson M, Kilbinger M, Kuijken K, Rowe B, Schrabback T, Semboloni E, Vafaei S, van Uitert E and Velander M 2013 *Monthly Notices of the Royal Astronomical Society* **433** 3373–3388 (*Preprint* 1303.1806)

[120] Beutler F, Saito S, Seo H J, Brinkmann J, Dawson K S, Eisenstein D J, Font-Ribera A, Ho S, McBride C K, Montesano F, Percival W J, Ross A J, Ross N P, Samushia L, Schlegel D J, Sánchez A G, Tinker J L and Weaver B A 2014 *Monthly Notices of the Royal Astronomical Society* **443** 1065–1089 (*Preprint* 1312.4611)

[121] Lombriser L 2014 *Annalen der Physik* **264** 259–282 (*Preprint* 1403.4268)

[122] Cataneo M, Rapetti D, Schmidt F, Mantz A B, Allen S W, Applegate D E, Kelly P L, von der Linden A and Morris R G 2015 *Physical Review D* **92** 044009 (*Preprint* 1412.0133)

[123] Harnois-Déraps J, Munshi D, Valageas P, van Waerbeke L, Brax P, Coles P and Rizzo L 2015 *Monthly Notices of the Royal Astronomical Society* **454** 2722–2735 (*Preprint* 1506.06313)

[124] Lombriser L, Simpson F and Mead A 2015 *Physical Review Letters* **114** 251101 (*Preprint* 1501.04961)

[125] Wilcox H, Bacon D, Nichol R C, Rooney P J, Terukina A, Romer A K, Koyama K, Zhao G B, Hood R, Mann R G, Hilton M, Manolopoulou M, Sahlén M, Collins C A, Liddle A R, Mayers J A, Mehrtens N, Miller C J, Stott J P and Viana P T P 2015 *Monthly Notices of the Royal Astronomical Society* **452** 1171–1183 (*Preprint* 1504.03937)

[126] Planck Collaboration, Ade P A R, Aghanim N, Arnaud M, Ashdown M, Aumont J, Baccigalupi C, Banday A J, Barreiro R B, Bartlett J G and et al 2016 *Astronomy and Astrophysics* **594** A13 (*Preprint* 1502.01589)

[127] Dark Energy Survey Collaboration, Abbott T, Abdalla F B, Aleksić J, Allam S, Amara A, Bacon D, Balbinot E, Banerji M, Bechtol K, Benoit-Lévy A, Bernstein G M, Bertin E, Blazek J, Bonnett C, Bridle S, Brooks D, Brunner R J, Buckley-Geer E, Burke D L, Caminha G B, Capozzi D, Carlsen J, Carnero-Rosell A, Carollo M, Carrasco-Kind M, Carretero J, Castander F J, Clerkin L, Collett T, Conselice C, Crocce M, Cunha C E, D'Andrea C B, da Costa L N, Davis T M, Desai S, Diehl H T, Dietrich J P, Dodelson S, Doel P, Drlica-Wagner A, Estrada J, Etherington J, Evrard A E, Fabbri J, Finley D A, Flaugher B, Foley R J, Fosalba P, Frieman J, García-Bellido J, Gaztanaga E, Gerdes D W, Giannantonio T, Goldstein D A, Gruen D, Gruendl

R A, Guarnieri P, Gutierrez G, Hartley W, Honscheid K, Jain B, James D J, Jeltema T, Jouvel S, Kessler R, King A, Kirk D, Kron R, Kuehn K, Kuropatkin N, Lahav O, Li T S, Lima M, Lin H, Maia M A G, Makler M, Manera M, Maraston C, Marshall J L, Martini P, McMahon R G, Melchior P, Merson A, Miller C J, Miquel R, Mohr J J, Morice-Atkinson X, Naidoo K, Neilsen E, Nichol R C, Nord B, Ogando R, Ostrovski F, Palmese A, Papadopoulos A, Peiris H V, Peoples J, Percival W J, Plazas A A, Reed S L, Refregier A, Romer A K, Roodman A, Ross A, Rozo E, Rykoff E S, Sadeh I, Sako M, Sánchez C, Sanchez E, Santiago B, Scarpine V, Schubnell M, Sevilla-Noarbe I, Sheldon E, Smith M, Smith R C, Soares-Santos M, Sobreira F, Soumagnac M, Suchyta E, Sullivan M, Swanson M, Tarle G, Thaler J, Thomas D, Thomas R C, Tucker D, Vieira J D, Vikram V, Walker A R, Wechsler R H, Weller J, Wester W, Whiteway L, Wilcox H, Yanny B, Zhang Y and Zuntz J 2016 *Monthly Notices of the Royal Astronomical Society* **460** 1270–1299 (*Preprint* 1601.00329)

[128] Abbott T M C, Abdalla F B, Alarcon A, Aleksić J, Allam S, Allen S, Amara A, Annis J, Asorey J, Avila S, Bacon D, Balbinot E, Banerji M, Banik N, Barkhouse W, Baumer M, Baxter E, Bechtol K, Becker M R, Benoit-Lévy A, Benson B A, Bernstein G M, Bertin E, Blazek J, Bridle S L, Brooks D, Brout D, Buckley-Geer E, Burke D L, Busha M T, Campos A, Capozzi D, Carnero Rosell A, Carrasco Kind M, Carretero J, Castander F J, Cawthon R, Chang C, Chen N, Childress M, Choi A, Conselice C, Crittenden R, Crocce M, Cunha C E, D'Andrea C B, da Costa L N, Das R, Davis T M, Davis C, De Vicente J, DePoy D L, DeRose J, Desai S, Diehl H T, Dietrich J P, Dodelson S, Doel P, Drlica-Wagner A, Eifler T F, Elliott A E, Elsner F, Elvin-Poole J, Estrada J, Evrard A E, Fang Y, Fernandez E, Ferté A, Finley D A, Flaugher B, Fosalba P, Friedrich O, Frieman J, García-Bellido J, Garcia-Fernandez M, Gatti M, Gaztanaga E, Gerdes D W, Giannantonio T, Gill M S S, Glazebrook K, Goldstein D A, Gruen D, Gruendl R A, Gschwend J, Gutierrez G, Hamilton S, Hartley W G, Hinton S R, Honscheid K, Hoyle B, Huterer D, Jain B, James D J, Jarvis M, Jeltema T, Johnson M D, Johnson M W G, Kacprzak T, Kent S, Kim A G, King A, Kirk D, Kokron N, Kovacs A, Krause E, Krawiec C, Kremin A, Kuehn K, Kuhlmann S, Kuropatkin N, Lacasa F, Lahav O, Li T S, Liddle A R, Lidman C, Lima M, Lin H, MacCrann N, Maia M A G, Makler M, Manera M, March M, Marshall J L, Martini P, McMahon R G, Melchior P, Menanteau F, Miquel R, Miranda V, Mudd D, Muir J, Möller A, Neilsen E, Nichol R C, Nord B, Nugent P, Ogando R L C, Palmese A, Peacock J, Peiris H V, Peoples J, Percival W J, Petravick D, Plazas A A, Porredon A, Prat J, Pujol A, Rau M M, Refregier A, Ricker P M, Roe N, Rollins R P, Romer A K, Roodman A, Rosenfeld R, Ross A J, Rozo E, Rykoff E S, Sako M, Salvador A I, Samuroff S, Sánchez C, Sanchez E, Santiago B, Scarpine V, Schindler R, Scolnic D, Secco L F, Serrano S, Sevilla-Noarbe I, Sheldon E, Smith R C, Smith M, Smith J, Soares-Santos M, Sobreira F, Suchyta E, Tarle G, Thomas D, Troxel M A, Tucker D L, Tucker B E, Uddin S A, Varga T N, Vielzeuf P, Vikram V, Vivas A K, Walker A R, Wang M, Wechsler R H, Weller J, Wester W, Wolf R C, Yanny B, Yuan F, Zenteno A, Zhang B, Zhang Y, Zuntz J and Dark Energy Survey Collaboration 2018 *Physical Review D* **98** 043526 (*Preprint* 1708.01530)

[129] Bonvin C and Fleury P 2018 *Journal of Cosmology and Astroparticle Physics* **2018** 061 (*Preprint* 1803.02771)

[130] Ishak M 2019 *Living Reviews in Relativity* **22** 1 (*Preprint* 1806.10122)

[131] Joyce A, Lombriser L and Schmidt F 2016 *Annual Review of Nuclear and Particle Science* **66** 95–122 (*Preprint* 1601.06133)

[132] Baker T, Psaltis D and Skordis C 2015 *Astrophysical Journal* **802** 63 (*Preprint* 1412.3455)

[133] Rudd D H, Zentner A R and Kravtsov A V 2008 *Astrophysical Journal* **672** 19–32 (*Preprint* astro-ph/0703741)

[134] Semboloni E, Hoekstra H, Schaye J, van Daalen M P and McCarthy I G 2011 *Monthly Notices of the Royal Astronomical Society* **417** 2020–2035 (*Preprint* 1105.1075)

[135] Fleury P, Dupuy H and Uzan J P 2013 *Physical Review D* **87** 123526 (*Preprint* 1302.5308)

[136] Zhang L, Rix H W, van de Ven G, Bovy J, Liu C and Zhao G 2013 *Atrophysical Journal* **772** 108 (*Preprint* 1209.0256)

[137] Read J I 2014 *Journal of Physics G Nuclear Physics* **41** 063101 (*Preprint* 1404.1938)

[138] McKee C F, Parravano A and Hollenbach D J 2015 *Astrophysical Journal* **814** 13 (*Preprint* 1509.05334)

[139] Brown M E 2012 *Annual Review of Earth and Planetary Sciences* **40** 467–494 (*Preprint* 1112.2764)

[140] Bergé J, Brax P, Pernot-Borràs M and Uzan J P 2018 *Classical and Quantum Gravity* **35** 234001 (*Preprint* 1808.00340)

[141] Everitt C W F, Debra D B, Parkinson B W, Turneaure J P, Conklin J W, Heifetz M I, Keiser G M, Silbergleit A S, Holmes T, Kolodziejczak J, Al-Meshari M, Mester J C, Muhlfelder B, Solomonik V G, Stahl K, Worden Jr P W, Bencze W, Buchman S, Clarke B, Al-Jadaan A, Al-Jibreen H, Li J, Lipa J A, Lockhart J M, Al-Suwaidan B, Taber M and Wang S 2011 *Physical Review Letters* **106** 221101 (*Preprint* 1105.3456)

[142] Ciufolini I, Moreno Monge B, Paolozzi A, Koenig R, Sindoni G, Michalak G and Pavlis E C 2013 *Classical and Quantum Gravity* **30** 235009 (*Preprint* 1310.2601)

[143] Iorio L, Ciufolini I and Pavlis E C 2002 *Classical and Quantum Gravity* **19** 4301–4309 (*Preprint* gr-qc/0103088)

[144] Lucchesi D M 2003 *Physics Letters A* **318** 234–240

[145] Lucchesi D M and Peron R 2010 *Physical Review Letters* **105** 231103 (*Preprint* 1106.2905)

[146] Lucchesi D M and Peron R 2014 *Phys. Rev. D* **89** 082002

[147] Li Z W, Yuan S F, Lu C and Xie Y 2014 *Research in Astronomy and Astrophysics* **14** 139-143

[148] Touboul P, Métris G, Rodrigues M, André Y, Baghi Q, Bergé J, Boulanger D, Bremer S, Carle P, Chhun R, Christophe B, Cipolla V, Damour T, Danto P, Dittus H, Fayet P, Foulon B, Gageant C, Guidotti P Y, Hagedorn D, Hardy E, Huynh P A, Inchauspe H, Kayser P, Lala S, Lämmerzahl C, Lebat V, Leseur P, Liorzou F, List M, Löffler F, Panet I, Pouilloux B, Prieur P, Rebray A, Reynaud S, Rievers B, Robert A, Selig H, Serron L, Sumner T, Tanguy N and Visser P 2017 *Physical Review Letters* **119** 231101 (*Preprint* 1712.01176)

[149] Touboul P, Métris G, Rodrigues M, André Y, Baghi Q, Bergé J, Boulanger D, Bremer S, Chhun R, Christophe B, Cipolla V, Damour T, Danto P, Dittus H, Fayet P, Foulon B, Guidotti P Y, Hardy E, Huynh P A, Lämmerzahl C, Lebat V, Liorzou F, List M, Panet I, Pires S, Pouilloux B, Prieur P, Reynaud S, Rievers B, Robert A, Selig H, Serron L, Sumner T and Visser P 2019 *Classical and Quantum Gravity* **36** 225006 (*Preprint* 1909.10598)

[150] Touboul P, Métris G, Rodrigues M, Bergé J, Robert A, Baghi Q, André Y, Bedouet J, Boulanger D, Bremer S, Carle P, Chhun R, Christophe B, Cipolla V, Damour T,

Danto P, Demange L, Dittus H, Dhuicque O, Fayet P, Foulon B, Guidotti P Y, Hagedorn D, Hardy E, Huynh P A, Kayser P, Lala S, Lämmerzahl C, Lebat V, Liorzou F m c, List M, Löffler F, Panet I, Pernot-Borràs M, Perraud L, Pires S, Pouilloux B, Prieur P, Rebray A, Reynaud S, Rievers B, Selig H, Serron L, Sumner T, Tanguy N, Torresi P and Visser P 2022 *Physical Review Letters* **129**(12) 121102

[151] Touboul P, Métris G, Rodrigues M, Bergé J, Robert A, Baghi Q, André Y, Bedouet J, Boulanger D, Bremer S, Carle P, Chhun R, Christophe B, Cipolla V, Damour T, Danto P, Demange L, Dittus H, Dhuicque O, Fayet P, Foulon B, Guidotti P Y, Hagedorn D, Hardy E, Huynh P A, Kayser P, Lala S, Lämmerzahl C, Lebat V, Liorzou F, List M, Löffler F, Panet I, Pernot-Borràs M, Perraud L, Pires S, Pouilloux B, Prieur P, Rebray A, Reynaud S, Rievers B, Selig H, Serron L, Sumner T, Tanguy N, Torresi P and Visser P 2022 *Classical and Quantum Gravity* **39** 204009

[152] Touboul P, Rodrigues M, Métris G, Chhun R, Robert A, Baghi Q, Hardy E, Bergé J, Boulanger D, Christophe B, Cipolla V, Foulon B, Guidotti P Y, Huynh P A, Lebat V, Liorzou F, Pouilloux B, Prieur P and Reynaud S 2022 *Classical and Quantum Gravity* **39** 204001 (*Preprint* 2012.06472)

[153] Liorzou F, Touboul P, Rodrigues M, Métris G, André Y, Bergé J, Boulanger D, Bremer S, Chhun R, Christophe B, Danto P, Foulon B, Hagedorn D, Hardy E, Huynh P A, Lämmerzahl C, Lebat V, List M, Löffler F, Rievers B, Robert A and Selig H 2022 *Classical and Quantum Gravity* **39** 204002 (*Preprint* 2012.11232)

[154] Robert A, Cipolla V, Prieur P, Touboul P, Métris G, Rodrigues M, André Y, Bergé J, Boulanger D, Chhun R, Christophe B, Guidotti P Y, Hardy E, Lebat V, Lienart T, Liorzou F and Pouilloux B 2022 *Classical and Quantum Gravity* **39** 204003 (*Preprint* 2012.06479)

[155] Rodrigues M, Touboul P, Métris G, Bedouet J, Bergé J, Carle P, Chhun R, Christophe B, Foulon B, Guidotti P Y, Lala S and Robert A 2022 *Classical and Quantum Gravity* **39** 204004 (*Preprint* 2201.10841)

[156] Chhun R, Hardy E, Rodrigues M, Touboul P, Métris G, Bergé J, Boulanger D, Christophe B, Danto P, Foulon B, Guidotti P Y, Huynh P A, Lebat V, Liorzou F and Robert A 2022 *Classical and Quantum Gravity* **39** 204005 (*Preprint* 2102.11087)

[157] Rodrigues M, Touboul P, Métris G, Robert A, Dhuicque O, Bergé J, André Y, Boulanger D, Chhun R, Christophe B, Cipolla V, Danto P, Foulon B, Guidotti P Y, Hardy E, Huynh P A, Lebat V, Liorzou F, Pouilloux B, Prieur P, Reynaud S and Torresi P 2022 *Classical and Quantum Gravity* **39** 204006 (*Preprint* 2112.10559)

[158] Bergé J, Baghi Q, Hardy E, Métris G, Robert A, Rodrigues M, Touboul P, Chhun R, Guidotti P Y, Pires S, Reynaud S, Serron L and Travert J M 2022 *Classical and Quantum Gravity* **39** 204007 (*Preprint* 2012.06484)

[159] Bergé J, Baghi Q, Robert A, Rodrigues M, Foulon B, Hardy E, Métris G, Pires S and Touboul P 2022 *Classical and Quantum Gravity* **39** 204008 (*Preprint* 2012.06485)

[160] Bergé J, Pernot-Borràs M, Uzan J P, Brax P, Chhun R, Métris G, Rodrigues M and Touboul P 2022 *Classical and Quantum Gravity* **39** 204010 (*Preprint* 2102.00022)

[161] Tino G M, Cacciapuoti L, Capozziello S, Lambiase G and Sorrentino F 2020 *Progress in Particle and Nuclear Physics* **112** 103772 (*Preprint* 2002.02907)

[162] Morisaki S, Fujita T, Michimura Y, Nakatsuka H and Obata I 2021 *Physical Review D* **103** L051702 (*Preprint* 2011.03589)

[163] Shaw E A, Ross M P, Hagedorn C A, Adelberger E G and Gundlach J H 2022 *Physical Review D* **105** 042007 (*Preprint* 2109.08822)

[164] Agrawal P, Kitajima N, Reece M, Sekiguchi T and Takahashi F 2020 *Physics Letters B* **801** 135136

[165] Abbott R, Abbott T D, Acernese F, Ackley K, Adams C, Adhikari N, Adhikari R X, Adya V B, Affeldt C, Agarwal D, Agathos M, Agatsuma K, Aggarwal N, Aguiar O D, Aiello L, Ain A, Ajith P, Akutsu T, Albanesi S, Allocca A, Altin P A, Amato A, Anand C, Anand S, Ananyeva A, Anderson S B, Anderson W G, Ando M, Andrade T, Andres N, Andrić T, Angelova S V, Ansoldi S, Antelis J M, Antier S, Appert S, Arai K, Arai K, Arai Y, Araki S, Araya A, Araya M C, Areeda J S, Arène M, Aritomi N, Arnaud N, Aronson S M, Arun K G, Asada H, Asali Y, Ashton G, Aso Y, Assiduo M, Aston S M, Astone P, Aubin F, Austin C, Babak S, Badaracco F, Bader M K M, Badger C, Bae S, Bae Y, Baer A M, Bagnasco S, Bai Y, Baiotti L, Baird J, Bajpai R, Ball M, Ballardin G, Ballmer S W, Balsamo A, Baltus G, Banagiri S, Bankar D, Barayoga J C, Barbieri C, Barish B C, Barker D, Barneo P, Barone F, Barr B, Barsotti L, Barsuglia M, Barta D, Bartlett J, Barton M A, Bartos I, Bassiri R, Basti A, Bawaj M, Bayley J C, Baylor A C, Bazzan M, Bécsy B, Bedakihale V M, Bejger M, Belahcene I, Benedetto V, Beniwal D, Bennett T F, Bentley J D, Benyaala M, Bergamin F, Berger B K, Bernuzzi S, Bersanetti D, Bertolini A, Betzwieser J, Beveridge D, Bhandare R, Bhardwaj U, Bhattacharjee D, Bhaumik S, Bilenko I A, Billingsley G, Bini S, Birney R, Birnholtz O, Biscans S, Bischi M, Biscoveanu S, Bisht A, Biswas B, Bitossi M, Bizouard M A, Blackburn J K, Blair C D, Blair D G, Blair R M, Bobba F, Bode N, Boer M, Bogaert G, Boldrini M, Bonavena L D, Bondu F, Bonilla E, Bonnand R, Booker P, Boom B A, Bork R, Boschi V, Bose N, Bose S, Bossilkov V, Boudart V, Bouffanais Y, Bozzi A, Bradaschia C, Brady P R, Bramley A, Branch A, Branchesi M, Brau J E, Breschi M, Briant T, Briggs J H, Brillet A, Brinkmann M, Brockill P, Brooks A F, Brooks J, Brown D D, Brunett S, Bruno G, Bruntz R, Bryant J, Bulik T, Bulten H J, Buonanno A, Buscicchio R, Buskulic D, Buy C, Byer R L, Cadonati L, Cagnoli G, Cahillane C, Bustillo J C, Callaghan J D, Callister T A, Calloni E, Cameron J, Camp J B, Canepa M, Canevarolo S, Cannavacciuolo M, Cannon K C, Cao H, Cao Z, Capocasa E, Capote E, Carapella G, Carbognani F, Carlin J B, Carney M F, Carpinelli M, Carrillo G, Carullo G, Carver T L, Diaz J C, Casentini C, Castaldi G, Caudill S, Cavaglià M, Cavalier F, Cavalieri R, Ceasar M, Cella G, Cerdá-Durán P, Cesarini E, Chaibi W, Chakravarti K, Subrahmanya S C, Champion E, Chan C H, Chan C, Chan C L, Chan K, Chan M, Chandra K, Chanial P, Chao S, Charlton P, Chase E A, Chassande-Mottin E, Chatterjee C, Chatterjee D, Chatterjee D, Chaturvedi M, Chaty S, Chen C, Chen H Y, Chen J, Chen K, Chen X, Chen Y B, Chen Y R, Chen Z, Cheng H, Cheong C K, Cheung H Y, Chia H Y, Chiadini F, Chiang C Y, Chiarini G, Chierici R, Chincarini A, Chiofalo M L, Chiummo A, Cho G, Cho H S, Choudhary R K, Choudhary S, Christensen N, Chu H, Chu Q, Chu Y K, Chua S, Chung K W, Ciani G, Ciecielag P, Cieślar M, Cifaldi M, Ciobanu A A, Ciolfi R, Cipriano F, Cirone A, Clara F, Clark E N, Clark J A, Clarke L, Clearwater P, Clesse S, Cleva F, Coccia E, Codazzo E, Cohadon P F, Cohen D E, Cohen L, Colleoni M, Collette C G, Colombo A, Colpi M, Compton C M, Constancio M, Conti L, Cooper S J, Corban P, Corbitt T R, Cordero-Carrión I, Corezzi S, Corley K R, Cornish N, Corre D, Corsi

T, McWilliams S T, Meacher D, Mehmet M, Mehta A K, Meijer Q, Melatos A, Melchor D A, Mendell G, Menendez-Vazquez A, Menoni C S, Mercer R A, Mereni L, Merfeld K, Merilh E L, Merritt J D, Merzougui M, Meshkov S, Messenger C, Messick C, Meyers P M, Meylahn F, Mhaske A, Miani A, Miao H, Michaloliakos I, Michel C, Michimura Y, Middleton H, Milano L, Miller A L, Miller A, Miller B, Millhouse M, Mills J C, Milotti E, Minazzoli O, Minenkov Y, Mio N, Mir L M, Miravet-Tenés M, Mishra C, Mishra T, Mistry T, Mitra S, Mitrofanov V P, Mitselmakher G, Mittleman R, Miyakawa O, Miyamoto A, Miyazaki Y, Miyo K, Miyoki S, Mo G, Moguel E, Mogushi K, Mohapatra S R P, Mohite S R, Molina I, Molina-Ruiz M, Mondin M, Montani M, Moore C J, Moraru D, Morawski F, More A, Moreno C, Moreno G, Mori Y, Morisaki S, Moriwaki Y, Mours B, Mow-Lowry C M, Mozzon S, Muciaccia F, Mukherjee A, Mukherjee D, Mukherjee S, Mukherjee S, Mukherjee S, Mukund N, Mullavey A, Munch J, Muñiz E A, Murray P G, Musenich R, Muusse S, Nadji S L, Nagano K, Nagano S, Nagar A, Nakamura K, Nakano H, Nakano M, Nakashima R, Nakayama Y, Napolano V, Nardecchia I, Narikawa T, Naticchioni L, Nayak B, Nayak R K, Negishi R, Neil B F, Neilson J, Nelemans G, Nelson T J N, Nery M, Neubauer P, Neunzert A, Ng K Y, Ng S W S, Nguyen C, Nguyen P, Nguyen T, Quynh L N, Ni W T, Nichols S A, Nishizawa A, Nissanke S, Nitoglia E, Nocera F, Norman M, North C, Nozaki S, Nuttall L K, Oberling J, O'Brien B D, Obuchi Y, O'Dell J, Oelker E, Ogaki W, Oganesyan G, Oh J J, Oh K, Oh S H, Ohashi M, Ohishi N, Ohkawa M, Ohme F, Ohta H, Okada M A, Okutani Y, Okutomi K, Olivetto C, Oohara K, Ooi C, Oram R, O'Reilly B, Ormiston R G, Ormsby N D, Ortega L F, O'Shaughnessy R, O'Shea E, Oshino S, Ossokine S, Osthelder C, Otabe S, Ottaway D J, Overmier H, Pace A E, Pagano G, Page M A, Pagliaroli G, Pai A, Pai S A, Palamos J R, Palashov O, Palomba C, Pan H, Pan K, Panda P K, Pang H, Pang P T H, Pankow C, Pannarale F, Pant B C, Panther F H, Paoletti F, Paoli A, Paolone A, Parisi A, Park H, Park J, Parker W, Pascucci D, Pasqualetti A, Passaquieti R, Passuello D, Patel M, Pathak M, Patricelli B, Patron A S, Patrone S, Paul S, Payne E, Pedraza M, Pegoraro M, Pele A, Arellano F E P, Penn S, Perego A, Pereira A, Pereira T, Perez C J, Périgois C, Perkins C C, Perreca A, Perriès S, Petermann J, Petterson D, Pfeiffer H P, Pham K A, Phukon K S, Piccinni O J, Pichot M, Piendibene M, Piergiovanni F, Pierini L, Pierro V, Pillant G, Pillas M, Pilo F, Pinard L, Pinto I M, Pinto M, Piotrzkowski K, Pirello M, Pitkin M D, Placidi E, Planas L, Plastino W, Pluchar C, Poggiani R, Polini E, Pong D Y T, Ponrathnam S, Popolizio P, Porter E K, Poulton R, Powell J, Pracchia M, Pradier T, Prajapati A K, Prasai K, Prasanna R, Pratten G, Principe M, Prodi G A, Prokhorov L, Prosposito P, Prudenzi L, Puecher A, Punturo M, Puosi F, Puppo P, Pürrer M, Qi H, Quetschke V, Quitzow-James R, Raab F J, Raaijmakers G, Radkins H, Radulesco N, Raffai P, Rail S X, Raja S, Rajan C, Ramirez K E, Ramirez T D, Ramos-Buades A, Rana J, Rapagnani P, Rapol U D, Ray A, Raymond V, Raza N, Razzano M, Read J, Rees L A, Regimbau T, Rei L, Reid S, Reid S W, Reitze D H, Relton P, Renzini A, Rettegno P, Rezac M, Ricci F, Richards D, Richardson J W, Richardson L, Riemenschneider G, Riles K, Rinaldi S, Rink K, Rizzo M, Robertson N A, Robie R, Robinet F, Rocchi A, Rodriguez S, Rolland L, Rollins J G, Romanelli M, Romano R, Romel C L, Romero-Rodríguez A, Romero-Shaw I M, Romie J H, Ronchini S, Rosa L, Rose C A, Rosińska D, Ross M P, Rowan S, Rowlinson S J, Roy S, Roy S, Roy S, Rozza D, Ruggi P, Ryan K, Sachdev S, Sadecki T, Sadiq J, Sago N, Saito S, Saito Y, Sakai K, Sakai Y, Sakellariadou M, Sakuno Y, Salafia O S, Salconi L, Saleem M, Salemi F, Samajdar A, Sanchez E J, Sanchez J H, Sanchez L E, Sanchis-Gual N, Sanders J R, Sanuy A, Saravanan T R, Sarin N, Sassolas B, Satari H, Sathyaprakash B S, Sato S, Sato T, Sauter O, Savage R L, Sawada T, Sawant D, Sawant H L, Sayah S, Schaetzl D, Scheel M, Scheuer J, Schiworski M, Schmidt P, Schmidt S, Schnabel R, Schneewind M, Schofield R M S, Schönbeck A, Schulte B W, Schutz B F, Schwartz E, Scott J, Scott S M, Seglar-Arroyo M, Sekiguchi T, Sekiguchi Y, Sellers D, Sengupta A S, Sentenac D, Seo E G, Sequino V, Sergeev A, Setyawati Y, Shaffer T, Shahriar M S, Shams B, Shao L, Sharma A, Sharma P, Shawhan P, Shcheblanov N S, Shibagaki S, Shikauchi M, Shimizu R, Shimoda T, Shimode K, Shinkai H, Shishido T, Shoda A, Shoemaker D H, Shoemaker D M, Shyamsundar S, Sieniawska M, Sigg D, Singer L P, Singh D, Singh N, Singha A, Sintes A M, Sipala V, Skliris V, Slagmolen B J J, Slaven-Blair T J, Smetana J, Smith J R, Smith R J E, Soldateschi J, Somala S N, Somiya K, Son E J, Soni K, Soni S, Sordini V, Sorrentino F, Sorrentino N, Sotani H, Soulard R, Souradeep T, Sowell E, Spagnuolo V, Spencer A P, Spera M, Srinivasan R, Srivastava A K, Srivastava V, Staats K, Stachie C, Steer D A, Steinlechner J, Steinlechner S, Stops D J, Stover M, Strain K A, Strang L C, Stratta G, Strunk A, Sturani R, Stuver A L, Sudhagar S, Sudhir V, Sugimoto R, Suh H G, Summerscales T Z, Sun H, Sun L, Sunil S, Sur A, Suresh J, Sutton P J, Suzuki T, Suzuki T, Swinkels B L, Szczepańczyk M J, Szewczyk P, Tacca M, Tagoshi H, Tait S C, Takahashi H, Takahashi R, Takamori A, Takano S, Takeda H, Takeda M, Talbot C J, Talbot C, Tanaka H, Tanaka K, Tanaka K, Tanaka T, Tanaka T, Tanasijczuk A J, Tanioka S, Tanner D B, Tao D, Tao L, Martin E N T S, Martín E N T S, Taranto C, Tasson J D, Telada S, Tenorio R, Terhune J E, Terkowski L, Thirugnanasambandam M P, Thomas M, Thomas P, Thompson J E, Thondapu S R, Thorne K A, Thrane E, Tiwari S, Tiwari S, Tiwari V, Toivonen A M, Toland K, Tolley A E, Tomaru T, Tomigami Y, Tomura T, Tonelli M, Torres-Forné A, Torrie C I, E Melo I T, Töyrä D, Trapananti A, Travasso F, Traylor G, Trevor M, Tringali M C, Tripathee A, Troiano L, Trovato A, Trozzo L, Trudeau R J, Tsai D S, Tsai D, Tsang K W, Tsang T, Tsao J S, Tse M, Tso R, Tsubono K, Tsuchida S, Tsukada L, Tsuna D, Tsutsui T, Tsuzuki T, Turbang K, Turconi M, Tuyenbayev D, Ubhi A S, Uchikata N, Uchiyama T, Udall R P, Ueda A, Uehara T, Ueno K, Ueshima G, Uraguchi F, Urban A L, Ushiba T, Utina A, Vahlbruch H, Vajente G, Vajpeyi A, Valdes G, Valentini M, Valsan V, van Bakel N, van Beuzekom M, van den Brand J F J, van den Broeck C, Vander-Hyde D C, van der Schaaf L, van Heijningen J V, Vanosky J, van Putten M H P M, van Remortel N, Vardaro M, Vargas A F, Varma V, Vasúth M, Vecchio A, Vedovato G, Veitch J, Veitch P J, Venneberg J, Venugopalan G, Verkindt D, Verma P, Verma Y, Veske D, Vetrano F, Viceré A, Vidyant S, Viets A D, Vijaykumar A, Villa-Ortega V, Vinet J Y, Virtuoso A, Vitale S, Vo T, Vocca H, von Reis E R G, von Wrangel J S A, Vorvick C, Vyatchanin S P, Wade L E, Wade M, Wagner K J, Walet R C, Walker M, Wallace G S, Wallace L, Walsh S, Wang J, Wang J Z, Wang W H, Ward R L, Warner J, Was M, Washimi T, Washington N Y, Watchi J, Weaver B, Webster S A, Weinert M, Weinstein A J, Weiss R, Weller C M, Wellmann F, Wen L, Weßels P, Wette K, Whelan J T, White D D, Whiting B F, Whittle C,

Wilken D, Williams D, Williams M J, Williamson A R, Willis J L, Willke B, Wilson D J, Winkler W, Wipf C C, Wlodarczyk T, Woan G, Woehler J, Wofford J K, Wong I C F, Wu C, Wu D S, Wu H, Wu S, Wysocki D M, Xiao L, Xu W R, Yamada T, Yamamoto H, Yamamoto K, Yamamoto K, Yamamoto T, Yamashita K, Yamazaki R, Yang F W, Yang L, Yang Y, Yang Y, Yang Z, Yap M J, Yeeles D W, Yelikar A B, Ying M, Yokogawa K, Yokoyama J, Yokozawa T, Yoo J, Yoshioka T, Yu H, Yu H, Yuzurihara H, Zadrożny A, Zanolin M, Zeidler S, Zelenova T, Zendri J P, Zevin M, Zhan M, Zhang H, Zhang J, Zhang L, Zhang T, Zhang Y, Zhao C, Zhao G, Zhao Y, Zhao Y, Zhou R, Zhou Z, Zhu X J, Zhu Z H, Zucker M E, Zweizig J, Ligo Scientific Collaboration, VIRGO Collaboration and Kagra Collaboration 2022 *Physical Review D* **105** 063030 (*Preprint* 2105.13085)

[166] Fedderke M A and Mathur A 2023 *Physical Review D* **107** 043004 (*Preprint* 2210.09324)

[167] Shergold J D 2021 *Journal of Cosmology and Astroparticle Physics* **2021** 052 (*Preprint* 2109.07482)

[168] Vacher L, Dias J D F, Schöneberg N, Martins C J A P, Vinzl S, Nesseris S, Cañas-Herrera G and Martinelli M 2022 *Physical Review D* **106** 083522 (*Preprint* 2207.03258)

[169] Martins C J A P and Prat Colomer M 2019 *Physics Letters B* **791** 230–235 (*Preprint* 1903.04310)

[170] Vilas Boas J M A, Magano D M N, Martins C J A P, Barbecho A and Serrano C 2020 *Astronomy and Astrophysics* **635** A80 (*Preprint* 2001.09129)

[171] Archidiacono M, Castorina E, Redigolo D and Salvioni E 2022 *Journal of Cosmology and Astroparticle Physics* **2022** 074 (*Preprint* 2204.08484)

[172] Akrami Y, Kallosh R, Linde A and Vardanyan V 2019 *Fortschritte der Physik* **67** 1800075 (*Preprint* 1808.09440)

[173] Martins C J A P and Vacher L 2019 *Physical Review D* **100** 123514 (*Preprint* 1911.10821)

[174] Ding G J and Feruglio F 2020 *Journal of High Energy Physics* **2020** 134 (*Preprint* 2003.13448)

[175] Stadnik Y V 2020 *Physical Review D* **102** 115016 (*Preprint* 2006.00185)

[176] Stadnik Y V 2021 *Physical Review A* **103** 062807 (*Preprint* 2010.01798)

[177] Davoudiasl H and Szafron R 2022 *arXiv e-prints* arXiv:2210.14959 (*Preprint* 2210.14959)

[178] Weinberg S 1972 *Gravitation and Cosmology: Principles and Applications of the General Theory of Relativity* (New York, NY: Wiley)

[179] Misner C W, Thorne K S and Wheeler J A 1973 *Gravitation*

[180] Wald R M 1984 *General Relativity* (Chicago, USA: Chicago Univ. Pr.)

[181] Carroll S M 2019 *Spacetime and Geometry* (Cambridge University Press) ISBN 978-0-8053-8732-2, 978-1-108-48839-6, 978-1-108-77555-7

[182] Peebles P J E and Ratra B 1988 *Astrophysical Journal Letters* **325** L17

[183] Weinberg S 1989 *Reviews of Modern Physics* **61** 1–23

[184] Zlatev I, Wang L and Steinhardt P J 1999 *Physical Review Letters* **82** 896–899 (*Preprint* astro-ph/9807002)

[185] Carroll S M 2001 *Living Reviews in Relativity* **4** 1 (*Preprint* astro-ph/0004075)

[186] Padmanabhan T 2003 *Physics Reports* **380** 235–320 (*Preprint* hep-th/0212290)

[187] Peebles P J and Ratra B 2003 *Reviews of Modern Physics* **75** 559–606 (*Preprint* astro-ph/0207347)

[188] Chiba T, Okabe T and Yamaguchi M 2000 *Physical Review D* **62** 023511 (*Preprint* astro-ph/9912463)

[189] Sahni V 2002 *Classical and Quantum Gravity* **19** 3435–3448 (*Preprint* astro-ph/0202076)

[190] Copeland E J, Sami M and Tsujikawa S 2006 *International Journal of Modern Physics D* **15** 1753–1935 (*Preprint* hep-th/0603057)

[191] Frieman J A, Turner M S and Huterer D 2008 *Annual Review of Astronomy and Astrophysics* **46** 385–432 (*Preprint* 0803.0982)

[192] Bamba K, Capozziello S, Nojiri S and Odintsov S D 2012 *Astrophysics and Space Science* **342** 155–228 (*Preprint* 1205.3421)

[193] Tsujikawa S 2013 *Classical and Quantum Gravity* **30** 214003 (*Preprint* 1304.1961)

[194] Fischbach E, Sudarsky D, Szafer A, Talmadge C and Aronson S H 1986 *Physical Review Letters* **56** 3–6

[195] Fayet P 1990 *Nuclear Physics B* **347** 743–768

[196] Fayet P 2017 *European Physical Journal C* **77** 53 (*Preprint* 1611.05357)

[197] Bergé J, Brax P, Métris G, Pernot-Borràs M, Touboul P and Uzan J P 2018 *Physical Review Letters* **120** 141101 (*Preprint* 1712.00483)

[198] Horndeski G W 1974 *International Journal of Theoretical Physics* **10** 363–384

[199] Brans C and Dicke R H 1961 *Physical Review* **124** 925–935

[200] Dicke R H 1962 *Physical Review* **125** 2163–2167

[201] Green M B, Schwarz J H and Witten E 1988 *Superstring Theory*

[202] Zwiebach B 2009 *A First Course in String Theory*

[203] Damour T and Donoghue J F 2010 *Physical Review D* **82** 084033 (*Preprint* 1007.2792)

[204] Damour T and Donoghue J F 2010 *Class. Quant. Grav.* **27** 202001 (*Preprint* 1007.2790)

[205] Hees A, Minazzoli O, Savalle E, Stadnik Y V and Wolf P 2018 *Physical Review D* **98** 064051 (*Preprint* 1807.04512)

[206] Antypas D, Tretiak O, Garcon A, Ozeri R, Perez G and Budker D 2019 *Physical Review Letters* **123** 141102 (*Preprint* 1905.02968)

[207] Kobayashi T, Takamizawa A, Akamatsu D, Kawasaki A, Nishiyama A, Hosaka K, Hisai Y, Wada M, Inaba H, Tanabe T and Yasuda M 2022 *Physical Review Letters* **129** 241301 (*Preprint* 2212.05721)

[208] Stadnik Y V 2022 *arXiv e-prints* arXiv:2206.10808 (*Preprint* 2206.10808)

[209] Banerjee A, Perez G, Safronova M, Savoray I and Shalit A 2022 *arXiv e-prints* arXiv:2211.05174 (*Preprint* 2211.05174)

[210] Brax P, van de Bruck C, Davis A C and Shaw D J 2008 *Physical Review D* **78** 104021 (*Preprint* 0806.3415)

[211] Brax P and Tamanini N 2016 *Physical Review D* **93** 103502 (*Preprint* 1512.07399)

[212] Burrage C and Sakstein J 2018 *Living Reviews in Relativity* **21** 1 (*Preprint* 1709.09071)

[213] Hinterbichler K and Khoury J 2010 *Phys. Rev. Lett.* **104** 231301 (*Preprint* 1001.4525)

[214] Burrage C, Copeland E J, Käding C and Millington P 2019 *Physical Review D* **99** 043539 (*Preprint* 1811.12301)

[215] Vainshtein A I 1972 *Physics Letters B* **39** 393–394

[216] Deffayet C, Dvali G, Gabadadze G and Vainshtein A 2002 *Physical Review D* **65** 044026 (*Preprint* hep-th/0106001)

[217] Arkani-Hamed N, Georgi H and Schwartz M D 2003 *Annals of Physics* **305** 96–118 (*Preprint* hep-th/0210184)

[218] Babichev E, Deffayet C and Ziour R 2009 *Int. J. Mod. Phys. D* **18** 2147–2154 (*Preprint* 0905.2943)

[219] Babichev E and Deffayet C 2013 *Classical and Quantum Gravity* **30** 184001 (*Preprint* 1304.7240)

[220] Damour T, Piazza F and Veneziano G 2002 *Physical Review D* **66** 046007 (*Preprint* hep-th/0205111)

[221] Ratra B and Peebles P J E 1988 *Physical Review D* **37** 3406–3427

[222] Fayet P 1996 *Classical and Quantum Gravity* **13** A19–A31

[223] Fayet P 2018 *Physical Review D* **97** 055039 (*Preprint* 1712.00856)
[224] Fayet P 2019 *Physical Review D* **99**(5) 055043
[225] Fayet P 1989 *Physics Letters B* **227** 127–132
[226] Eötvös R V 1890 *Math. Naturwiss. Berg. Ung. 8* S65–68
[227] Eötvös R V, Pekár D and Fekete E 1922 *Annalen der Physik* **373** 11–66
[228] Roll P G, Krotkov R and Dicke R H 1964 *Annals of Physics* **26** 442–517
[229] Dicke R H 1970 *Gravitation and the universe*
[230] Braginsky V and Panov V I 1971 *ZhEksp. Teor. Fiz. 61 873–1272* **61** 873–1272
[231] Su Y, Heckel B R, Adelberger E G, Gundlach J H, Harris M, Smith G L and Swanson H E 1994 *Phys. Rev. D* **50**(6) 3614–3636
[232] Baeßler S, Heckel B R, Adelberger E G, Gundlach J H, Schmidt U and Swanson H E 1999 *Phys. Rev. Lett.* **83**(18) 3585–3588
[233] Adelberger E G 2001 *Classical and Quantum Gravity* **18** 2397–2405
[234] Heckel B R, Adelberger E G, Cramer C E, Cook T S, Schlamminger S and Schmidt U 2008 *Physical Review D* **78** 092006 (*Preprint* 0808.2673)
[235] Worden P 1982 *Precision Engineering* **4** 139 – 144 ISSN 0141-6359
[236] Cavasinni V, Iacopini E, Polacco E and Stefanini G 1986 *Physics Letters A* **116** 157 – 161 ISSN 0375-9601
[237] Niebauer T M, McHugh M P and Faller J E 1987 *Physical Review Letters* **59** 609–612
[238] Kuroda K and Mio N 1989 *Physical Review Letters* **62** 1941–1944
[239] Kuroda K and Mio N 1990 *Physical Review D* **42** 3903–3907
[240] Carusotto S, Cavasinni V, Mordacci A, Perrone F, Polacco E, Iacopini E and Stefanini G 1992 *Physical Review Letters* **69**(12) 1722–1725
[241] Iafolla V, Nozzoli S, Lorenzini E C and Milyukov V 1998 *Review of Scientific Instruments* **69** 4146–4151
[242] Reasenberg R D, Patla B R, Phillips J D and Thapa R 2012 *Classical and Quantum Gravity* **29** 184013 (*Preprint* 1206.0028)
[243] Sakstein J 2018 *Physical Review D* **97** 064028 (*Preprint* 1710.03156)
[244] Everitt C W F, Damour T, Nordtvedt K and Reinhard R 2003 *Advances in Space Research* **32** 1297–1300
[245] Sumner T, Anderson J, Blaser J P, Cruise A M, Damour T, Dittus, Everitt C W F, Foulon B, Jafry Y R, Kent B J, Lockerbie N, Loeffler F, Mann G, Mester J, Pegrum C, Reinhardt R, Sandford M, Scheicher A, Speake C C, Torii R, Theil S, Touboul P, Vitale S, Vodel W and Worden P W 2007 *Advances in Space Research* **39** 254–258
[246] Overduin J, Everitt F, Worden P and Mester J 2012 *Classical and Quantum Gravity* **29** 184012 (*Preprint* 1401.4784)
[247] Nobili A M and Anselmi A 2018 *Physics Letters A* **382** 2205–2218 (*Preprint* 1709.02768)
[248] Nobili A M and Anselmi A 2018 *Physical Review D* **98**(4) 042002
[249] Cronin A D, Schmiedmayer J and Pritchard D E 2009 *Reviews of Modern Physics* **81** 1051–1129 (*Preprint* 0712.3703)
[250] Fray S, Diez C A, Hänsch T W and Weitz M 2004 *Physical Review Letters* **93**(24) 240404
[251] Bonnin A, Zahzam N, Bidel Y and Bresson A 2013 *Physical Review A* **88** 043615 (*Preprint* 1307.2734)
[252] Schlippert D, Hartwig J, Albers H, Richardson L L, Schubert C, Roura A, Schleich W P, Ertmer W and Rasel E M 2014 *Physical Review Letters* **112** 203002 (*Preprint* 1406.4979)
[253] Tarallo M G, Mazzoni T, Poli N, Sutyrin D V, Zhang X and Tino G M 2014 *Physical Review Letters* **113** 023005 (*Preprint* 1403.1161)
[254] Bonnin A, Zahzam N, Bidel Y and Bresson A 2015 *Physical Review A* **92** 023626 (*Preprint* 1506.06535)
[255] Duan X C, Deng X B, Zhou M K, Zhang K, Xu W J, Xiong F, Xu Y Y, Shao C G, Luo J and Hu Z K 2016 *Physical Review Letters* **117** 023001 (*Preprint* 1602.06377)
[256] Asenbaum P, Overstreet C, Kim M, Curti J and Kasevich M A 2020 *Physical Review Letters* **125** 191101 (*Preprint* 2005.11624)
[257] Tino G M, Sorrentino F, Aguilera D, Battelier B, Bertoldi A, Bodart Q, Bongs K, Bouyer P, Braxmaier C, Cacciapuoti L, Gaaloul N, Gürlebeck N, Hauth M, Herrmann S, Krutzik M, Kubelka A, Landragin A, Milke A, Peters A, Rasel E M, Rocco E, Schubert C, Schuldt T, Sengstock K and Wicht A 2013 *Nuclear Physics B Proceedings Supplements* **243** 203–217
[258] Aguilera D N, Ahlers H, Battelier B, Bawamia A, Bertoldi A, Bondarescu R, Bongs K, Bouyer P, Braxmaier C, Cacciapuoti L, Chaloner C, Chwalla M, Ertmer W, Franz M, Gaaloul N, Gehler M, Gerardi D, Gesa L, Gürlebeck N, Hartwig J, Hauth M, Hellmig O, Herr W, Herrmann S, Heske A, Hinton A, Ireland P, Jetzer P, Johann U, Krutzik M, Kubelka A, Lämmerzahl C, Land ragin A, Lloro I, Massonnet D, Mateos I, Milke A, Nofrarias M, Oswald M, Peters A, Posso-Trujillo K, Rasel E, Rocco E, Roura A, Rudolph J, Schleich W, Schubert C, Schuldt T, Seidel S, Sengstock K, Sopuerta C F, Sorrentino F, Summers D, Tino G M, Trenkel C, Uzunoglu N, von Klitzing W, Walser R, Wendrich T, Wenzlawski A, Weßels P, Wicht A, Wille E, Williams M, Windpassinger P and Zahzam N 2014 *Classical and Quantum Gravity* **31** 115010 (*Preprint* 1312.5980)
[259] Altschul B, Bailey Q G, Blanchet L, Bongs K, Bouyer P, Cacciapuoti L, Capozziello S, Gaaloul N, Giulini D, Hartwig J, Iess L, Jetzer P, Landragin A, Rasel E, Reynaud S, Schiller S, Schubert C, Sorrentino F, Sterr U, Tasson J D, Tino G M, Tuckey P and Wolf P 2015 *Advances in Space Research* **55** 501 – 524 ISSN 0273-1177
[260] Kellerbauer A, Amoretti M, Belov A S, Bonomi G, Boscolo I, Brusa R S, Büchner M, Byakov V M, Cabaret L, Canali C, Carraro C, Castelli F, Cialdi S, de Combarieu M, Comparat D, Consolati G, Djourelov N, Doser M, Drobychev G, Dupasquier A, Ferrari G, Forget P, Formaro L, Gervasini A, Giammarchi M G, Gninenko S N, Gribakin G, Hogan S D, Jacquey M, Lagomarsino V, Manuzio G, Mariazzi S, Matveev V A, Meier J O, Merkt F, Nedelec P, Oberthaler M K, Pari P, Prevedelli M, Quasso F, Rotondi A, Sillou D, Stepanov S V, Stroke H H, Testera G, Tino G M, Trénec G, Vairo A, Vigué J, Walters H, Warring U, Zavatarelli S, Zvezhinskij D S and AEGIS Proto-Collaboration 2008 *Nuclear Instruments and Methods in Physics Research B* **266** 351–356
[261] Alpha Collaboration, Amole C, Ashkezari M D, Baquero-Ruiz M, Bertsche W, Butler E, Capra A, Cesar C L, Charlton M, Eriksson S, Fajans J, Friesen T, Fujiwara M C, Gill D R, Gutierrez A, Hangst J S, Hardy W N, Hayden M E, Isaac C A, Jonsell S, Kurchaninov L, Little A, Madsen N, McKenna J T K, Menary S, Napoli S C, Nolan P, Olin A, Pusa P, Rasmussen C Ø, Robicheaux F, Sarid E, Silveira D M, So C, Thompson R I, van der Werf D P, Wurtele J S, Zhmoginov A I and Charman A E 2013 *Nature Communications* **4** 1785
[262] Aghion S, Ahlén O, Amsler C, Ariga A, Ariga T, Belov A S, Berggren K, Bonomi G, Bräunig P, Bremer J, Brusa R S, Cabaret L, Canali C, Caravita R, Castelli F, Cerchiari G, Cialdi S, Comparat D, Consolati G,

Derking H, di Domizio S, di Noto L, Doser M, Dudarev A, Ereditato A, Ferragut R, Fontana A, Genova P, Giammarchi M, Gligorova A, Gninenko S N, Haider S, Huse T, Jordan E, Jørgensen L V, Kaltenbacher T, Kawada J, Kellerbauer A, Kimura M, Knecht A, Krasnický D, Lagomarsino V, Lehner S, Magnani A, Malbrunot C, Mariazzi S, Matveev V A, Moia F, Nebbia G, Nédélec P, Oberthaler M K, Pacifico N, Petràček V, Pistillo C, Prelz F, Prevedelli M, Regenfus C, Riccardi C, Røhne O, Rotondi A, Sandaker H, Scampoli P, Storey J, Vasquez M A S, Špaček M, Testera G, Vaccarone R, Widmann E, Zavatarelli S and Zmeskal J 2014 *Nature Communications* **5** 4538

[263] Indelicato P, Chardin G, Grandemange P, Lunney D, Manea V, Badertscher A, Crivelli P, Curioni A, Marchionni A, Rossi B, Rubbia A, Nesvizhevsky V, Brook-Roberge D, Comini P, Debu P, Dupré P, Liszkay L, Mansoulié B, Pérez P, Rey J M, Reymond B, Ruiz N, Sacquin Y, Vallage B, Biraben F, Cladé P, Douillet A, Dufour G, Guellati S, Hilico L, Lambrecht A, Guérout R, Karr J P, Nez F, Reynaud S, Szabo C I, Tran V Q, Trapateau J, Mohri A, Yamazaki Y, Charlton M, Eriksson S, Madsen N, van der Werf D P, Kuroda N, Torii H, Nagashima Y, Schmidt-Kaler F, Walz J, Wolf S, Hervieux P A, Manfredi G, Voronin A, Froelich P, Wronka S and Staszczak M 2014 *Hyperfine Interactions* **228** 141

[264] Bertsche W A 2018 *Philosophical Transactions of the Royal Society of London Series A* **376** 20170265

[265] Khalidova O, Aghion S, Amsler C, Antonello M, Belov A, Bonomi G, Brusa R S, Caccia M, Camper A, Caravita R, Castelli F, Cerchiari G, Comparat D, Consolati G, Demetrio A, Noto L D, Doser M, Evans C, Fani M, Ferragut R, Fesel J, Fontana A, Gerber S, Giammarchi M, Gligorova A, Guatieri F, Hackstock P, Haider S, Hinterberger A, Holmestad H, Kellerbauer A, Krasnický D, Lagomarsino V, Lansonneur P, Lebrun P, Malbrunot C, Mariazzi S, Marton J, Matveev V, Müller S, Nebbia G, Nedelec P, Oberthaler M, Pagano D, Penasa L, Petracek V, Prelz F, Prevedelli M, Rienaecker B, Robert J, Røhne O, Rotondi A, Sandaker H, Santoro R, Smestad L, Sorrentino F, Testera G, Tietje I, Vujanovic M, Widmann E, Yzombard P, Zimmer C, Zmeskal J and Zurlo N 2019 The AEgIS experiment: towards antimatter gravity measurements *Journal of Physics Conference Series* (*Journal of Physics Conference Series* vol 1390) p 012104

[266] Pagano D, Aghion S, Amsler C, Bonomi G, Brusa R S, Caccia M, Caravita R, Castelli F, Cerchiari G, Comparat D, Consolati G, Demetrio A, Noto L D, Doser M, Evans A, Fani M, Ferragut R, Fesel J, Fontana A, Gerber S, Giammarchi M, Gligorova A, Guatieri F, Haider S, Hinterberger A, Holmestad H, Kellerbauer A, Khalidova O, Krasnický D, Lagomarsino V, Lansonneur P, Lebrun P, Malbrunot C, Mariazzi S, Marton J, Matveev V, Mazzotta Z, Müller S R, Nebbia G, Nedelec P, Oberthaler M, Pacifico N, Penasa L, Petracek V, Prelz F, Prevedelli M, Ravelli L, Rienaecker B, Robert J, Røhne O M, Rotondi A, Sandaker H, Santoro R, Smestad L, Sorrentino F, Testera G, Tietje I C, Widmann E, Yzombard P, Zimmer C, Zmeskal J and Zurlo N 2020 Gravity and antimatter: the AEgIS experiment at CERN *Journal of Physics Conference Series* (*Journal of Physics Conference Series* vol 1342) p 012016

[267] Charlton M, Eriksson S and Shore G M 2020 *arXiv e-prints* arXiv:2002.09348 (*Preprint* 2002.09348)

[268] Rousselle O, Cladé P, Guellati-Khelifa S, Guérout R and Reynaud S 2022 *New Journal of Physics* **24** 033045 (*Preprint* 2111.02815)

[269] Nordtvedt K 1968 *Physical Review* **170** 1186–1187

[270] Hofmann F and Müller J 2018 *Classical and Quantum Gravity* **35** 035015

[271] Merkowitz S M 2010 *Living Reviews in Relativity* **13** 7

[272] Lucchesi D M, Anselmo L, Bassan M, Pardini C, Peron R, Pucacco G and Visco M 2015 *Classical and Quantum Gravity* **32** 155012

[273] Nobili A M, Comandi G L, Bramanti D, Doravari S, Lucchesi D M and Maccarrone F 2008 *General Relativity and Gravitation* **40** 1533–1554

[274] Armano M, Audley H, Auger G, Baird J T, Bassan M, Binetruy P, Born M, Bortoluzzi D, Brandt N, Caleno M, Carbone L, Cavalleri A, Cesarini A, Ciani G, Congedo G, Cruise A M, Danzmann K, de Deus Silva M, De Rosa R, Diaz-Aguiló M, Di Fiore L, Diepholz I, Dixon G, Dolesi R, Dunbar N, Ferraioli L, Ferroni V, Fichter W, Fitzsimons E D, Flatscher R, Freschi M, García Marín A F, García Marirrodriga C, Gerndt R, Gesa L, Gibert F, Giardini D, Giusteri R, Guzmán F, Grado A, Grimani C, Grynagier A, Grzymisch J, Harrison I, Heinzel G, Hewitson M, Hollington D, Hoyland D, Hueller M, Inchauspé H, Jennrich O, Jetzer P, Johann U, Johlander B, Karnesis N, Kaune B, Korsakova N, Killow C J, Lobo J A, Lloro I, Liu L, López-Zaragoza J P, Maarschalkerweerd R, Mance D, Martín V, Martin-Polo L, Martino J, Martin-Porqueras F, Madden S, Mateos I, McNamara P W, Mendes J, Mendes L, Monsky A, Nicolodi D, Nofrarias M, Paczkowski S, Perreur-Lloyd M, Petiteau A, Pivato P, Plagnol E, Prat P, Ragnit U, Raïs B, Ramos-Castro J, Reiche J, Robertson D I, Rozemeijer H, Rivas F, Russano G, Sanjuán J, Sarra P, Schleicher A, Shaul D, Slutsky J, Sopuerta C F, Stanga R, Steier F, Sumner T, Texier D, Thorpe J I, Trenkel C, Tröbs M, Tu H B, Vetrugno D, Vitale S, Wand V, Wanner G, Ward H, Warren C, Wass P J, Wealthy D, Weber W J, Wissel L, Wittchen A, Zambotti A, Zanoni C, Ziegler T and Zweifel P 2016 *Physical Review Letters* **116** 231101

[275] Armano M, Audley H, Baird J, Binetruy P, Born M, Bortoluzzi D, Castelli E, Cavalleri A, Cesarini A, Cruise A M, Danzmann K, de Deus Silva M, Diepholz I, Dixon G, Dolesi R, Ferraioli L, Ferroni V, Fitzsimons E D, Freschi M, Gesa L, Gibert F, Giardini D, Giusteri R, Grimani C, Grzymisch J, Harrison I, Heinzel G, Hewitson M, Hollington D, Hoyland D, Hueller M, Inchauspé H, Jennrich O, Jetzer P, Karnesis N, Kaune B, Korsakova N, Killow C J, Lobo J A, Lloro I, Liu L, López-Zaragoza J P, Maarschalkerweerd R, Mance D, Meshksar N, Martín V, Martin-Polo L, Martino J, Martin-Porqueras F, Mateos I, McNamara P W, Mendes J, Mendes L, Nofrarias M, Paczkowski S, Perreur-Lloyd M, Petiteau A, Pivato P, Plagnol E, Ramos-Castro J, Reiche J, Robertson D I, Rivas F, Russano G, Slutsky J, Sopuerta C F, Sumner T, Texier D, Thorpe J I, Vetrugno D, Vitale S, Wanner G, Ward H, Wass P J, Weber W J, Wissel L, Wittchen A and Zweifel P 2018 *Physical Review Letters* **120** 061101

[276] Sumner T J, Shaul D N A, Schulte M O, Waschke S, Hollington D and Araújo H 2009 *Classical and Quantum Gravity* **26** 094006

[277] Nobili A M, Shao M, Pegna R, Zavattini G, Turyshev S G, Lucchesi D M, De Michele A, Doravari S, Comandi G L, Saravanan T R, Palmonari F, Catastini G and Anselmi A 2012 *Classical and Quantum Gravity* **29** 184011

[278] Touboul P, Foulon B and Willemenot E 1999 *Acta Astronautica* **45** 605–617

[279] Boudon Y, Barlier F, Bernard A, Juillerat R, Mainguy A M and Walch J J 1978 *Recherche Aérospatiale* **1978-6**

[280] Nati M, Bernard A, Foulon B and Touboul P 1994

ASTRE, a highly performant accelerometer for the low frequency range of the microgravity environment *24th Symposium on space environmental control systems, Friedrichshafen Germany, 1994.*

[281] Touboul P, Foulon B and LeClerc G 1998 STAR, The Accelerometer of the Geodesic Mission CHAMP *Proceedings of the 49th IAF Congress, Melbourne, Australia* vol 1998 pp IAF–98–B.3.07

[282] Reigber C, Lühr H and Schwintzer P 2002 *Advances in Space Research* **30** 129–134

[283] Tapley B D, Bettadpur S, Watkins M and Reigber C 2004 *Geophysical Research Letters* **31** L09607

[284] Marque J P, Christophe B and Foulon B 2010 Accelerometers of the GOCE Mission: Return of Experience from One Year of In-Orbit *ESA Living Planet Symposium* (*ESA Special Publication* vol 686) p 57

[285] Rummel R, Yi W and Stummer C 2011 *Journal of Geodesy* **85** 777–790

[286] Kornfeld R P, Arnold B W, Gross M A, Dahya N T, Klipstein W M, Gath P F and Bettadpur S 2019 *Journal of Spacecraft and Rockets* **56** 931–951

[287] Prieur P, Lienart T, Rodrigues M, Touboul P, Denver T, Jorgensen J, Bang A and Metris G 2017 Microscope mission: on-orbit assessment of the drag-free and attitude control system *ISTS-2017-d-038/ISSFD-2017-038 1-10, 26th Int Symp Space Flight Dynamics*

[288] Baghi Q 2016 *Optimisation de l'analyse de données de la mission spatiale MICROSCOPE pour le test du principe d'équivalence et d'autres applications* Ph.D. thesis Observatoire de Paris

[289] Touboul P, Métris G, Rodrigues M, Bergé J, Boulanger D, Chhun R, Christophe B, Cipolla V, Damour T, Dittus H, Fayet P, Foulon B, Guidotti P Y, Hardy E, Huynh P A, Lämmerzahl C, Lebat V, Liorzou F, List M, Pouilloux B, Prieur P, Reynaud S, Rievers B, Robert A, Serron L, Sumner T and Visser P in prep *Class. Quant. Grav.*

[290] Métris G, Xu J and Wytrzyszczak I 1998 *Celestial Mechanics and Dynamical Astronomy* **71** 137–151

[291] Mayer-Gurr T, Eicker A and Ilk K H 2006 *Proc. First Symp. Int. Grav. Field Ser.*

[292] Nofrarias i Serra M 2007 *Thermal Diagnostics in the LISA Technology Package Experiment* Ph.D. thesis Departament de Física Fonamental. Universitat de Barcelona

[293] Carbone L, Cavalleri A, Ciani G, Dolesi R, Hueller M, Tombolato D, Vitale S and Weber W J 2007 *Physical Review D* **76** 102003 (*Preprint* 0706.4402)

[294] Saulson P R 1990 *Physical Review D* **42** 2437–2445

[295] Willemenot E and Touboul P 2000 *Review of Scientific Instruments* **71** 302–309

[296] Touboul P 2009 *Space Science Reviews* **148** 455–474

[297] Hardy É, Levy A, Métris G, Rodrigues M and Touboul P 2013 *Space Science Reviews* **180** 177–191 (*Preprint* 1707.08024)

[298] Hardy É, Levy A, Rodrigues M, Touboul P and Métris G 2013 *Advances in Space Research* **52** 1634–1646 (*Preprint* 1707.07630)

[299] Bergé J, Touboul P, Rodrigues M and Liorzou F 2017 MICROSCOPE: five months after launch *Journal of Physics Conference Series* (*Journal of Physics Conference Series* vol 840) p 012028

[300] Foulon B, Rodrigues M, Metris G, Touboul P, Christophe B, Baghi Q and Panet I 2018 On-Orbit Gradiometry results with the scientific instrument of the French Space Mission MICROSCOPE *AGU Fall Meeting Abstracts* vol 2018 pp G13C–0530

[301] Rievers B, List M, Wöske F and Bremer S 2021 Update on the evaluation of the MICROSCOPE aeronomy experiment *43rd COSPAR Scientific Assembly. Held 28 January - 4 February* vol 43 p 2116

[302] Vitale S, Congedo G, Dolesi R, Ferroni V, Hueller M, Vetrugno D, Weber W J, Audley H, Danzmann K, Diepholz I, Hewitson M, Korsakova N, Ferraioli L, Gibert F, Karnesis N, Nofrarias M, Inchauspe H, Plagnol E, Jennrich O, McNamara P W, Armano M, Thorpe J I and Wass P 2014 *Physical Review D* **90** 042003 (*Preprint* 1404.4792)

[303] Bergé J, Massey R, Baghi Q and Touboul P 2019 *Monthly Notices of the Royal Astronomical Society* **486** 544–559 (*Preprint* 1903.05837)

[304] Baghi Q, Métris G, Bergé J, Christophe B, Touboul P and Rodrigues M 2015 *Phys. Rev. D* **91** 062003 (*Preprint* 1503.01470)

[305] Bergé J, Pires S, Baghi Q, Touboul P and Métris G 2015 *Phys. Rev. D* **92** 112006 (*Preprint* 1512.00492)

[306] Baghi Q, Métris G, Bergé J, Christophe B, Touboul P and Rodrigues M 2016 *Phys. Rev. D* **93** 122007 (*Preprint* 1608.08530)

[307] Pires S, Bergé J, Baghi Q, Touboul P and Métris G 2016 *Phys. Rev. D* **94** 123015 (*Preprint* 1612.05452)

[308] Pires S, Starck J L, Amara A, Teyssier R, Réfrégier A and Fadili J 2009 *Monthly Notices of the Royal Astronomical Society* **395** 1265–1279 (*Preprint* 0804.4068)

[309] Pires S, Mathur S, García R A, Ballot J, Stello D and Sato K 2015 *Astronomy and Astrophysics* **574** A18 (*Preprint* 1410.6088)

[310] Dhuicque O, Rodrigues M, Métris G and Touboul P 2021 *Advances in Space Research* **68** 1989–1997

[311] Smith G L, Hoyle C D, Gundlach J H, Adelberger E G, Heckel B R and Swanson H E 2000 *Physical Review D* **61** 022001

[312] Talmadge C, Berthias J P, Hellings R W and Standish E M 1988 *Phys. Rev. Lett.* **61** 1159–1162

[313] Yang S Q, Zhan B F, Wang Q L, Shao C G, Tu L C, Tan W H and Luo J 2012 *Physical Review Letters* **108** 081101

[314] Tan W H, Du A B, Dong W C, Yang S Q, Shao C G, Guan S G, Wang Q L, Zhan B F, Luo P S, Tu L C and Luo J 2020 *Physical Review Letters* **124** 051301

[315] Gasser J and Leutwyler H 1982 *Physics Reports* **87** 77–169

[316] Kalaydzhyan T and Yu N 2017 *Physical Review D* **96** 075007 (*Preprint* 1705.05833)

[317] Van Tilburg K, Leefer N, Bougas L and Budker D 2015 *Phys. Rev. Lett.* **115** 011802 (*Preprint* 1503.06886)

[318] Hees A, Guéna J, Abgrall M, Bize S and Wolf P 2016 *Physical Review Letters* **117** 061301 (*Preprint* 1604.08514)

[319] Savalle E, Hees A, Frank F, Cantin E, Pottie P E, Roberts B M, Cros L, McAllister B T and Wolf P 2021 *Physical Review Letters* **126** 051301 (*Preprint* 2006.07055)

[320] Tretiak O, Zhang X, Figueroa N L, Antypas D, Brogna A, Banerjee A, Perez G and Budker D 2022 *Physical Review Letters* **129** 031301 (*Preprint* 2201.02042)

[321] Oswald R, Nevsky A, Vogt V, Schiller S, Figueroa N L, Zhang K, Tretiak O, Antypas D, Budker D, Banerjee A and Perez G 2022 *Physica Review Letters* **129** 031302 (*Preprint* 2111.06883)

[322] Zhang X, Banerjee A, Leyser M, Perez G, Schiller S, Budker D and Antypas D 2022 *arXiv e-prints* arXiv:2212.04413 (*Preprint* 2212.04413)

[323] Zhao W, Gao D, Wang J and Zhan M 2022 *General Relativity and Gravitation* **54** 41 (*Preprint* 2102.02391)

[324] Ahlers H, Badurina L, Bassi A, Battelier B, Beaufils Q, Bongs K, Bouyer P, Braxmaier C, Buchmueller O, Carlesso M, Charron E, Chiofalo M L, Corgier R, Donadi S, Droz F, Ecoffet R, Ellis J, Estève F, Gaaloul N, Gerardi D, Giese E, Grosse J, Hees A, Hensel T, Herr W, Jetzer P, Kleinsteinberg G, Klempt C, Lecomte S, Lopes L, Loriani S, Métris G, Martin T,

Martín V, Müller G, Nofrarias M, Pereira Dos Santos F, Rasel E M, Robert A, Saks N, Salter M, Schlippert D, Schubert C, Schuldt T, Sopuerta C F, Struckmann C, Tino G M, Valenzuela T, von Klitzing W, Wörner L, Wolf P, Yu N and Zelan M 2022 *arXiv e-prints* arXiv:2211.15412 (*Preprint* 2211.15412)

[325] Kennedy C J, Oelker E, Robinson J M, Bothwell T, Kedar D, Milner W R, Marti G E, Derevianko A and Ye J 2020 *Physical Review Letters* **125** 201302 (*Preprint* 2008.08773)

[326] Boulder Atomic Clock Optical Network Bacon Collaboration, Beloy K, Bodine M I, Bothwell T, Brewer S M, Bromley S L, Chen J S, Deschênes J D, Diddams S A, Fasano R J, Fortier T M, Hassan Y S, Hume D B, Kedar D, Kennedy C J, Khader I, Koepke A, Leibrandt D R, Leopardi H, Ludlow A D, McGrew W F, Milner W R, Newbury N R, Nicolodi D, Oelker E, Parker T E, Robinson J M, Romisch S, Schäffer S A, Sherman J A, Sinclair L C, Sonderhouse L, Swann W C, Yao J, Ye J and Zhang X 2021 *Nature* **591** 564–569

[327] Vermeulen S M, Relton P, Grote H, Raymond V, Affeldt C, Bergamin F, Bisht A, Brinkmann M, Danzmann K, Doravari S, Kringel V, Lough J, Lück H, Mehmet M, Mukund N, Nadji S, Schreiber E, Sorazu B, Strain K A, Vahlbruch H, Weinert M, Willke B and Wittel H 2021 *Nature* **600** 424–428 (*Preprint* 2103.03783)

[328] Aiello L, Richardson J W, Vermeulen S M, Grote H, Hogan C, Kwon O and Stoughton C 2022 *Physical Review Letters* **128** 121101 (*Preprint* 2108.04746)

[329] Riess A G, Rodney S A, Scolnic D M, Shafer D L, Strolger L G, Ferguson H C, Postman M, Graur O, Maoz D, Jha S W, Mobasher B, Casertano S, Hayden B, Molino A, Hjorth J, Garnavich P M, Jones D O, Kirshner R P, Koekemoer A M, Grogin N A, Brammer G, Hemmati S, Dickinson M, Challis P M, Wolff S, Clubb K I, Filippenko A V, Nayyeri H, U V, Koo D C, Faber S M, Kocevski D, Bradley L and Coe D 2018 *Astrophysical Journal* **853** 126 (*Preprint* 1710.00844)

[330] Farooq O, Ranjeet Madiyar F, Crandall S and Ratra B 2017 *Astrophysical Journal* **835** 26 (*Preprint* 1607.03537)

[331] Webb J K, King J A, Murphy M T, Flambaum V V, Carswell R F and Bainbridge M B 2011 *Physical Review Letters* **107** 191101 (*Preprint* 1008.3907)

[332] Martins C J A P 2017 *Reports on Progress in Physics* **80** 126902 (*Preprint* 1709.02923)

[333] Murphy M T and Cooksey K L 2017 *Monthly Notices of the Royal Astronomical Society* **471** 4930–4945 (*Preprint* 1708.00014)

[334] Martins C J A P, Vielzeuf P E, Martinelli M, Calabrese E and Pandolfi S 2015 *Physics Letters B* **743** 377–382 (*Preprint* 1503.05068)

[335] Pernot-Borràs M, Bergé J, Brax P and Uzan J P 2019 *Physical Review D* **100** 084006 (*Preprint* 1907.10546)

[336] Brax P, Burrage C and Davis A C 2018 *International Journal of Modern Physics D* **27** 1848009-206

[337] Jaffe M, Haslinger P, Xu V, Hamilton P, Upadhye A, Elder B, Khoury J and Müller H 2017 *Nature Physics* **13** 938–942 (*Preprint* 1612.05171)

[338] Upadhye A 2012 *Physical Review D* **86** 102003 (*Preprint* 1209.0211)

[339] Decca R S, López D, Fischbach E, Klimchitskaya G L, Krause D E and Mostepanenko V M 2007 *Physical Review D* **75** 077101 (*Preprint* hep-ph/0703290)

[340] Jaeckel J and Roy S 2010 *Physical Review D* **82** 125020 (*Preprint* 1008.3536)

[341] Brax P and Burrage C 2011 *Physical Review D* **83** 035020 (*Preprint* 1010.5108)

[342] Pernot-Borràs M, Bergé J, Brax P and Uzan J P 2020 *Physical Review D* **101** 124056 (*Preprint* 2004.08403)

[343] Pernot-Borràs M, Bergé J, Brax P, Uzan J P, Métris G, Rodrigues M and Touboul P 2021 *Physical Review D* **103** 064070 (*Preprint* 2102.00023)

[344] Hamilton P, Jaffe M, Haslinger P, Simmons Q, Müller H and Khoury J 2015 *Science* **349** 849–851 (*Preprint* 1502.03888)

[345] Will C M 2018 *Theory and Experiment in Gravitational Physics* 2nd ed (Cambridge University Press)

[346] Kostelecký V A and Samuel S 1989 *Phys. Rev. D* **39**(2) 683–685

[347] Kostelecký V A and Potting R 1995 *Phys. Rev. D* **51**(7) 3923–3935

[348] Colladay D and Kostelecký V A 1997 *Phys. Rev. D* **55**(11) 6760–6774

[349] Colladay D and Kostelecký V A 1998 *Phys. Rev. D* **58**(11) 116002

[350] Kostelecký V A and Tasson J D 2011 *Phys. Rev. D* **83**(1) 016013

[351] Kostelecký V A and Russell N 2011 *Rev. Mod. Phys.* **83**(1) 11–31

[352] Pihan le Bars H, Guerlin C, Hees A, Peaucelle R, Tasson J D, Bailey Q G, Mo G, Delva P, Meynadier F, Touboul P, Métris G, Rodrigues M, Bergé J and Wolf P 2019 *Physical Review Letters* **123** 231102

[353] Tasson J D 2012 *Phys. Rev. D* **86**(12) 124021

[354] Hees A, Bailey Q G, Le Poncin-Lafitte C, Bourgoin A, Rivoldini A, Lamine B, Meynadier F, Guerlin C and Wolf P 2015 *Phys. Rev. D* **92**(6) 064049

[355] Bourgoin A, Hees A, Bouquillon S, Le Poncin-Lafitte C, Francou G and Angonin M C 2016 *Phys. Rev. Lett.* **117**(24) 241301

[356] Flowers N A, Goodge C and Tasson J D 2017 *Phys. Rev. Lett.* **119**(20) 201101

[357] Kostelecký V A and Tasson J D 2009 *Phys. Rev. Lett.* **102**(1) 010402

[358] Rosi G 2016 *Journal of Physics B Atomic Molecular Physics* **49** 202002

[359] Abrykosov P, Pail R, Gruber T, Zahzam N, Bresson A, Hardy E, Christophe B, Bidel Y, Carraz O and Siemes C 2019 *Advances in Space Research* **63** 3235–3248

[360] Lambrecht A, Neto P A M and Reynaud S 2006 *New Journal of Physics* **8** 243 (*Preprint* quant-ph/0611103)

[361] Fischbach E, Krause D E, McDuffie M H and Mueterthies M J 2021 *arXiv e-prints* arXiv:2105.03264 (*Preprint* 2105.03264)

[362] Fischbach E, Gruenwald J T, Krause D E, McDuffie M H, Mueterthies M J and Scarlett C Y 2021 *Physics Letters A* **399** 127300 (*Preprint* 2012.02862)

[363] Battelier B, Bergé J, Bertoldi A, Blanchet L, Bongs K, Bouyer P, Braxmaier C, Calonico D, Fayet P, Gaaloul N, Guerlin C, Hees A, Jetzer P, Lämmerzahl C, Lecomte S, Le Poncin-Lafitte C, Loriani S, Métris G, Nofrarias M, Rasel E, Reynaud S, Rodrigues M, Rothacher M, Roura A, Salomon C, Schiller S, Schleich W P, Schubert C, Sopuerta C F, Sorrentino F, Sumner T J, Tino G M, Tuckey P, Klitzing W v, Wörner L, Wolf P and Zelan M 2021 *Experimental Astronomy* **51** 1695–1736 (*Preprint* 1908.11785)

[364] Speake C C 1996 *Classical and Quantum Gravity* **13** A291–A297

[365] Alonso I, Alpigiani C, Altschul B, Araujo H, Arduini G, Arlt J, Badurina L, Balaz A, Bandarupally S, Barone B C B M, Barsanti M, Bass S, Bassi A, Battelier B, Baynham C F A, Beaufils Q, Belic A, Berge J, Bernabeu J, Bertoldi A, Bingham R, Bize S, Blas D, Bongs K, Bouyer P, Braitenberg C, Brand C, Braxmaier C, Bresson A, Buchmueller O, Budker D, Bugalho L, Burdin S, Callegari L C S, Calmet X, Calonico D, Canuel B, Caramete L I, Carraz O, Cassettari D, Chakraborty P, Chattopadhyay S, Chauhan U, Chen

X, Chen Y A, Chiofalo M L, Coleman J, Corgier R, Cotter J P, Cruise A M, Cui Y, Davies G, De Roeck A, Demarteau M, Derevianko A, Di Clemente M, Djordjevic G S, Donadi S, Dore O, Dornan P, Doser M, Drougakis G, Dunningham J, Easo S, Eby J, Elertas G, Ellis J, Evans D, Examilioti P, Fadeev P, Fanı M, Fassi F, Fattori M, Fedderke M A, Felea D, Feng C H, Ferreras J, Flack R, Flambaum V V, Forsberg R, Fromhold M, Gaaloul N, Garraway B M, Georgousi M, Geraci A, Gibble K, Gibson V, Gill P, Giudice G F, Goldwin J, Gould O, Grachov O, Graham P W, Grasso D, Griffin P F, Guerlin C, Gundogan M, Gupta R K, Haehnelt M, Hanımeli E T, Hawkins L, Hees A, Henderson V A, Herr W, Herrmann S, Hird T, Hobson R, Hock V, Hogan J M, Holst B, Holynski M, Israelsson U, Jeglic P, Jetzer P, Juzeliunas G, Kaltenbaek R, Kamenik J F, Kehagias A, Kirova T, Kiss-Toth M, Koke S, Kolkowitz S, Kornakov G, Kovachy T, Krutzik M, Kumar M, Kumar P, Lammerzahl C, Landsberg G, Le Poncin-Lafitte C, Leibrandt D R, Leveque T, Lewicki M, Li R, Lipniacka A, Liu C L M, Lopez-Gonzalez J L, Loriani S, Louko J, Gaetano Luciano G, Lundblad N, Maddox S, Mahmoud M A, Maleknejad A, March-Russell J, Massonnet D, McCabe C, Meister M, Meznarsic T, Micalizio S, Migliaccio F, Millington P, Milosevic M, Mitchell J, Morley G W, Muller J, Murphy E, Mustecaplıoglu O E, OShea V, Oi D K L, Olson J, Pal D, Papazoglou D G, Pasatembou E, Paternostro M, Pawlowski K, Pelucchi E, Pereira dos Santos F, Peters A, Pikovski I, Pilaftsis A, Pinto A, Prevedelli M, Puthiya-Veettil V, Quenby J, Rafelski J, Rasel E M, Ravensbergen C, Reguzzoni M, Richaud A, Riou I, Rothacher M, Roura A, Ruschhaupt A, Sabulsky D O, Safronova M, Saltas I D, Salvi L, Sameed M, Saurabh P, Schaffer S, Schiller S, Schilling M, Schkolnik V, Schlippert D, Schmidt P O, Schnatz H, Schneider J, Schneider U, Schreck F, Schubert C, Shayeghi A, Sherrill N, Shipsey I, Signorini C, Singh R, Singh Y, Skordis C, Smerzi A, Sopuerta C F, Sorrentino F, Sphicas P, Stadnik Y V, Stefanescu P, Tarallo M G, Tentindo S, Tino G M, Tinsley J N, Tornatore V, Treutlein P, Trombettoni A, Tsai Y D, Tuckey P, Uchida M A, Valenzuela T, Van Den Bossche M, Vaskonen V, Verma G, Vetrano F, Vogt C, von Klitzing W, Waller P, Walser R, Williams E W J, Windpassinger P, Wittrock U, Wolf P, Woltmann M, Worner L, Xuereb A, Yahia M, Yazgan E, Yu N, Zahzam N, Zambrini Cruzeiro E, Zhan M, Zou X, Zupan J and Zupanic E 2022 *arXiv e-prints* arXiv:2201.07789 (*Preprint* 2201.07789)

[366] Chiow S w, Williams J, Yu N and Müller H 2017 *Physical Review A* **95** 021603 (*Preprint* 1612.02053)

[367] Bertoldi A, Bongs K, Bouyer P, Buchmueller O, Canuel B, Caramete L I, Chiofalo M L, Coleman J, De Roeck A, Ellis J, Graham P W, Haehnelt M G, Hees A, Hogan J, von Klitzing W, Krutzik M, Lewicki M, McCabe C, Peters A, Rasel E, Roura A, Sabulsky D, Schiller S, Schubert C, Signorini C, Sorrentino F, Singh Y, Tino G M, Vaskonen V and Zhan M S 2021 *Experimental Astronomy* **51** 1417–1426

[368] Tino G M, Bassi A, Bianco G, Bongs K, Bouyer P, Cacciapuoti L, Capozziello S, Chen X, Chiofalo M L, Derevianko A, Ertmer W, Gaaloul N, Gill P, Graham P W, Hogan J M, Iess L, Kasevich M A, Katori H, Klempt C, Lu X, Ma L S, Müller H, Newbury N R, Oates C W, Peters A, Poli N, Rasel E M, Rosi G, Roura A, Salomon C, Schiller S, Schleich W, Schlippert D, Schreck F, Schubert C, Sorrentino F, Sterr U, Thomsen J W, Vallone G, Vetrano F, Villoresi P, von Klitzing W, Wilkowski D, Wolf P, Ye J, Yu N and Zhan M 2019 *European Physical Journal D* **73** 228 (*Preprint* 1907.03867)

[369] Barontini G, Blackburn L, Boyer V, Butuc-Mayer F, Calmet X, Crespo Lopez-Urrutia J R, Curtis E A, Darquie B, Dunningham J, Fitch N J, Forgan E M, Georgiou K, Gill P, Godun R M, Goldwin J, Guarrera V, Harwood A, Hill I R, Hendricks R J, Jeong M, Johnson M Y H, Keller M, Kozhiparambil Sajith L P, Kuipers F, Margolis H S, Mayo C, Newman P, Parsons A O, Prokhorov L, Robertson B I, Rodewald J, Safronova M S, Sauer B E, Schioppo M, Sherrill N, Stadnik Y V, Szymaniec K, Tarbutt M R, Thompson R C, Tofful A, Tunesi J, Vecchio A, Wang Y and Worm S 2021 *arXiv e-prints* arXiv:2112.10618 (*Preprint* 2112.10618)

[370] Savalle E, Guerlin C, Delva P, Meynadier F, le Poncin-Lafitte C and Wolf P 2019 *Classical and Quantum Gravity* **36** 245004 (*Preprint* 1907.12320)

[371] Roura A 2020 *Physical Review X* **10** 021014

[372] Dimopoulos S, Graham P W, Hogan J M, Kasevich M A and Rajendran S 2008 *Physical Review D* **78** 122002 (*Preprint* 0806.2125)

[373] Gao D F, Wang J and Zhan M S 2018 *Communications in Theoretical Physics* **69** 37 (*Preprint* 1711.03690)

[374] Geiger R, Landragin A, Merlet S and Pereira Dos Santos F 2020 *AVS Quantum Science* **2** 024702 (*Preprint* 2003.12516)

[375] Tino G M 2021 *Quantum Science and Technology* **6** 024014 (*Preprint* 2009.01484)

[376] Belenchia A, Carlesso M, Bayraktar Ö, Dequal D, Derkach I, Gasbarri G, Herr W, Li Y L, Rademacher M, Sidhu J, Oi D K L, Seidel S T, Kaltenbaek R, Marquardt C, Ulbricht H, Usenko V C, Wörner L, Xuereb A, Paternostro M and Bassi A 2022 *Physics Reports* **951** 1–70 (*Preprint* 2108.01435)

[377] da Fonseca V, Barreiro T, Nunes N J, Cristiani S, Cupani G, D'Odorico V, Génova Santos R, Leite A C O, Marques C M J, Martins C J A P, Milaković D, Molaro P, Murphy M T, Schmidt T M, Abreu M, Adibekyan V, Cabral A, Di Marcantonio P, González Hernández J I, Palle E, Pepe F A, Rebolo R, Santos N C, Sousa S G, Sozzetti A, Suárez Mascareño A and Zapatero Osorio M R 2022 *arXiv e-prints* arXiv:2204.02930 (*Preprint* 2204.02930)

[378] Manley J, Chowdhury M D, Grin D, Singh S and Wilson D J 2021 *Physics Review Letters* **126** 061301 (*Preprint* 2007.04899)

[379] Agrawal P, Bauer M, Beacham J, Berlin A, Boyarsky A, Cebrian S, Cid-Vidal X, d'Enterria D, De Roeck A, Drewes M, Echenard B, Giannotti M, Giudice G F, Gninenko S, Gori S, Goudzovski E, Heeck J, Hernandez P, Hostert M, Irastorza I G, Izmaylov A, Jaeckel J, Kahlhoefer F, Knapen S, Krnjaic G, Lanfranchi G, Monroe J, Outschoorn V I M, Lopez-Pavon J, Pascoli S, Pospelov M, Redigolo D, Ringwald A, Ruchayskiy O, Ruderman J, Russell H, Salfeld-Nebgen J, Schuster P, Shaposhnikov M, Shchutska L, Shelton J, Soreq Y, Stadnik Y, Swallow J, Tobioka K and Tsai Y D 2021 *European Physical Journal C* **81** 1015 (*Preprint* 2102.12143)

[380] Antypas D, Banerjee A, Bartram C, Baryakhtar M, Betz J, Bollinger J J, Boutan C, Bowring D, Budker D, Carney D, Carosi G, Chaudhuri S, Cheong S, Chou A, Chowdhury M D, Co R T, Crespo López-Urrutia J R, Demarteau M, DePorzio N, Derbin A V, Deshpande T, Chowdhury M D, Di Luzio L, Diaz-Morcillo A, Doyle J M, Drlica-Wagner A, Droster A, Du N, Döbrich B, Eby J, Essig R, Farren G S, Figueroa N L, Fry J T, Gardner S, Geraci A A, Ghalsasi A, Ghosh S, Giannotti M, Gimeno B, Griffin S M, Grin D, Grin D, Grote

H, Gundlach J H, Guzzetti M, Hanneke D, Harnik R, Henning R, Irsic V, Jackson H, Kimball D F J, Jaeckel J, Kagan M, Kedar D, Khatiwada R, Knirck S, Kolkowitz S, Kovachy T, Kuenstner S E, Lasner Z, Leder A F, Lehnert R, Leibrandt D R, Lentz E, Lewis S M, Liu Z, Manley J, Maruyama R H, Millar A J, Muratova V N, Musoke N, Nagaitsev S, Noroozian O, O'Hare C A J, Ouellet J L, Pappas K M W, Peik E, Perez G, Phipps A, Rapidis N M, Robinson J M, Robles V H, Rogers K K, Rudolph J, Rybka G, Safdari M, Safdari M, Safronova M S, Salemi C P, Schmidt P O, Schumm T, Schwartzman A, Shu J, Simanovskaia M, Singh J, Singh S, Smith M S, Snow W M, Stadnik Y V, Sun C, Sushkov A O, Tait T M P, Takhistov V, Tanner D B, Temples D J, Thirolf P G, Thomas J H, Tobar M E, Tretiak O, Tsai Y D, Tyson J A, Vandegar M, Vermeulen S, Visinelli L, Vitagliano E, Wang Z, Wilson D J, Winslow L, Withington S, Wooten M, Yang J, Ye J, Young B A, Yu F, Zaheer M H, Zelevinsky T, Zhao Y and Zhou K 2022 *arXiv e-prints* arXiv:2203.14915 (*Preprint* 2203.14915)

[381] Dvali G, Kühnel F and Zantedeschi M 2021 *Physical Review D* **104** 123507 (*Preprint* 2108.09471)

[382] Umeh O, Koyama K and Crittenden R 2021 *Journal of Cosmology and Astroparticle Physics* **2021** 049 (*Preprint* 2011.05876)

[383] Shao L, Wex N and Kramer M 2018 *Physical Review Letters* **120** 241104 (*Preprint* 1805.08408)

[384] Roy R, Abdikamalov A B, Ayzenberg D, Bambi C, Riaz S and Tripathi A 2021 *Physical Review D* **104** 044001 (*Preprint* 2103.08978)

[385] GRAVITY Collaboration, Abuter R, Amorim A, Anugu N, Bauböck M, Benisty M, Berger J P, Blind N, Bonnet H, Brandner W, Buron A, Collin C, Chapron F, Clénet Y, Coudé Du Foresto V, de Zeeuw P T, Deen C, Delplancke-Ströbele F, Dembet R, Dexter J, Duvert G, Eckart A, Eisenhauer F, Finger G, Förster Schreiber N M, Fédou P, Garcia P, Garcia Lopez R, Gao F, Gendron E, Genzel R, Gillessen S, Gordo P, Habibi M, Haubois X, Haug M, Haußmann F, Henning T, Hippler S, Horrobin M, Hubert Z, Hubin N, Jimenez Rosales A, Jochum L, Jocou K, Kaufer A, Kellner S, Kendrew S, Kervella P, Kok Y, Kulas M, Lacour S, Lapeyrère V, Lazareff B, Le Bouquin J B, Léna P, Lippa M, Lenzen R, Mérand A, Müler E, Neumann U, Ott T, Palanca L, Paumard T, Pasquini L, Perraut K, Perrin G, Pfuhl O, Plewa P M, Rabien S, Ramírez A, Ramos J, Rau C, Rodríguez-Coira G, Rohloff R R, Rousset G, Sanchez-Bermudez J, Scheithauer S, Schöller M, Schuler N, Spyromilio J, Straub O, Straubmeier C, Sturm E, Tacconi L J, Tristram K R W, Vincent F, von Fellenberg S, Wank I, Waisberg I, Widmann F, Wieprecht E, Wiest M, Wiezorrek E, Woillez J, Yazici S, Ziegler D and Zins G 2018 *Astronomy and Astrophysics* **615** L15 (*Preprint* 1807.09409)

[386] Amorim A, Bauböck M, Berger J P, Brandner W, Clénet Y, Coudé Du Foresto V, de Zeeuw P T, Dexter J, Duvert G, Ebert M, Eckart A, Eisenhauer F, Förster Schreiber N M, Garcia P, Gao F, Gendron E, Genzel R, Gillessen S, Habibi M, Haubois X, Henning T, Hippler S, Horrobin M, Hubert Z, Jiménez Rosales A, Jocou L, Kervella P, Lacour S, Lapeyrère V, Le Bouquin J B, Léna P, Ott T, Paumard T, Perraut K, Perrin G, Pfuhl O, Rabien S, Rodríguez-Coira G, Rousset G, Scheithauer S, Sternberg A, Straub O, Straubmeier C, Sturm E, Tacconi L J, Vincent F, von Fellenberg S, Waisberg I, Widmann F, Wieprecht E, Wiezorrek E, Yazici S and Gravity Collaboration 2019 *Physical Review Letters* **122** 101102 (*Preprint* 1902.04193)

[387] Do T, Hees A, Ghez A, Martinez G D, Chu D S, Jia S, Sakai S, Lu J R, Gautam A K, O'Neil K K, Becklin E E, Morris M R, Matthews K, Nishiyama S, Campbell R, Chappell S, Chen Z, Ciurlo A, Dehghanfar A, Gallego-Cano E, Kerzendorf W E, Lyke J E, Naoz S, Saida H, Schödel R, Takahashi M, Takamori Y, Witzel G and Wizinowich P 2019 *Science* **365** 664–668 (*Preprint* 1907.10731)

[388] Hees A, Do T, Roberts B M, Ghez A M, Nishiyama S, Bentley R O, Gautam A K, Jia S, Kara T, Lu J R, Saida H, Sakai S, Takahashi M and Takamori Y 2020 *Physical Review Letters* **124** 081101 (*Preprint* 2002.11567)

[389] Williams J, Chiow S w, Yu N and Müller H 2016 *New Journal of Physics* **18** 025018 (*Preprint* 1510.07780)

[390] Zhou L, Yan S T, Ji Y H, He C, Jiang J J, Hou Z, Xu R D, Wang Q, Li Z X, Gao D F, Liu M, Ni W T, Wang J and Zhan M S 2022 *Frontiers in Physics* **10** 1039119

[391] Barrett B, Condon G, Chichet L, Antoni-Micollier L, Arguel R, Rabault M, Pelluet C, Jarlaud V, Landragin A, Bouyer P and Battelier B 2022 *AVS Quantum Science* **4** 014401 (*Preprint* 2110.13273)

[392] Armano M, Audley H, Baird J, Binetruy P, Born M, Bortoluzzi D, Castelli E, Cavalleri A, Cesarini A, Cruise A M, Danzmann K, de Deus Silva M, Diepholz I, Dixon G, Dolesi R, Ferraioli L, Ferroni V, Fitzsimons E D, Freschi M, Gesa L, Gibert F, Giardini D, Giusteri R, Grimani C, Grzymisch J, Harrison I, Hartig M S, Heinzel G, Hewitson M, Hollington D, Hoyland D, Hueller M, Inchauspé H, Jennrich O, Jetzer P, Karnesis N, Kaune B, Korsakova N, Killow C J, Lobo J A, Liu L, López-Zaragoza J P, Maarschalkerweerd R, Mance D, Meshksar N, Martín V, Martin-Polo L, Martino J, Martin-Porqueras F, McNamara P W, Mendes J, Mendes L, Nofrarias M, Paczkowski S, Perreur-Lloyd M, Petiteau A, Pivato P, Plagnol E, Ramos-Castro J, Reiche J, Robertson D I, Rivas F, Russano G, Slutsky J, Sopuerta C F, Sumner T, Texier D, Thorpe J I, Trenkel C, Vetrugno D, Vitale S, Wanner G, Ward H, Wass P J, Weber W J, Wissel L, Wittchen A, Zweifel P and LISA Pathfinder Collaboration 2019 *Physical Review D* **100** 062003

[393] Pierce A, Riles K and Zhao Y 2018 *Physical Review Letters* **121** 061102 (*Preprint* 1801.10161)

[394] Morisaki S and Suyama T 2019 *Physical Review D* **100** 123512 (*Preprint* 1811.05003)

[395] Grote H and Stadnik Y V 2019 *Physical Review Research* **1** 033187 (*Preprint* 1906.06193)

[396] Viola L and Onofrio R 1997 *Physical Review D* **55** 455–462 (*Preprint* quant-ph/9612039)

[397] Geiger R and Trupke M 2018 *Physical Review Letters* **120** 043602 (*Preprint* 1801.08604)

[398] Emelyanov V A 2022 *European Physical Journal C* **82** 318 (*Preprint* 2110.10056)